Relatório Final de Atividades - Bolsistas CAPES- Pós-Doutorado e PVNS

Pergunta	Resposta
Nome Completo do Bolsista	Jerônimo Pereira de França
CPF	07674491854
Nº de Matrícula ou crachá	7810934-5/0002
E-mail	jeronimopf@gmail.com
Campus	São Paulo
Programa de Pós-Graduação	CIRURGIA TRANSLACIONAL
Nome do Projeto	Ação de biocompostos isolados de Mussismilia braziliensis, Morinda citrifolia e Garcinia mangostana no controle da proliferação celular e indução de apoptose em células cultivadas de Melanoma Metastático Humano: um estudo celular e molecular.
Número do Parecer FINAL do Projeto no Comitê de Ética em Pesquisa da UNIFESP	0758/2011
Coordenador (a) do Programa de Pós-Graduação	MIGUEL SABINO NETO
Nome do (a) Supervisor (a) do Projeto de Pós-Doutorado	Profa. Dra. Lydia Masako Ferreira
Nome do (a) da Diretoria Acadêmica do Campus	Prof.Dr. Luiz Leduíno de Salles Neto
E-mail do (a) Supervisor (a)	lydia.dcir@epm.br
Modalidade da Bolsa	Pós-Doutorado
Agência de Fomento	CAPES
Programa CAPES	PNPD - Programa Nacional de Pós-Doutorado - Edital 2011 - Cota Institucional
Período a que se refere o relatório - De:	out/13
Período a que se refere o relatório - À:	Jan/18
1. Atividades que foram realizadas no período a que se refere este	Atividades que foram realizadas no período a que se refere este Relatório, quanto ao seu conteúdo científico: Atividades: 1) Obtenção do tumor, extração, cultivo e subcultivo de células de melanoma e

Relatório, quanto ao seu conteúdo científico	melanoma humano (tecido adjacente ao tumor) e de linhagens (B16-F10). Já foram utilizadas células provenientes de 06 pacientes. Caracterização das células de melanoma por imunohistoquímica e imunofluorescência foi feita utilizando proteína S-100 e HMB-45 (Human Melanoma Black), marcadores frequentemente utilizados para diagnóstico do melanoma; 2) Preparo, frações isoladas do muco do coral da espécie Mussismilia braziliensis, obtidos por drenagem da superfície do coral, sem promover quebra na sua estrutura; 3) Determinação da citotoxicidade celular após o tratamento com extrato do muco do coral Mussismilia braziliensis, himatanthus lancifolius, Euphorbia tirucalli (látex etanolico e aquoso), Sinadenium grantii, utilizando o teste do 3-(4,5-Dimethyl-2-thiazoly)-2,5-diphenyl-2H tetrazolium bromide (MTT) e determinação da atividade antioxidante pelo método de captura do radical DPPH (2,2 difenil-1-picril—hidrazil), utilizando o ácido ascórbico (Vitamina C) como controle positivo; 4) Análise por citometria de fluxo por citometria de fluxo de células em necrose e apoptose. Foi identificado por citometria a ativação da caspase 3, confirmando a ação apoptótica do extrato e esta sendo feita a identificação das vias (caspase 8, 9, 12) e sobrevivência celular (p16, p21 e p53). 5) Ensaios citoquímica e imunicitoquímica por microscopia de fluorescência confocal com as células de melanomacom estudos morfológicos do núcleo, citoesqueleto, membrana. Já foram obtidos duas frações do extrato bruto obtido do coral; 6) Após a identificação e fracionamento em tubos de ensaio por HPLC/espectroscopia de massa, os biocompostos estão sendo analisados quanto a sua atividade biológica e identificados quanto a sua massa e estrutura. Houve participação em simpósios, congressos e foram feitos análise estatísticas dos dados e geram cerca de 5 publicações cientificas, com 01 artigo submetido e outro sendo finalizado a escrita.
2.Resultados alcançados. Descrição e recapitulação sintética dos resultados obtidos, ressaltando o alcance e as consequências do estudo	Conseguimos determinar as atividades biológicas de plantas e corais, conforme proposto no Projeto. Com desenvolvimento do Projeto foi possível a formação de recursos humanos com a participação de alunos de mestrado, doutorado, pós-doutorado e principalmente de alunos de iniciação científica. Resultados foram promissores, adequando os resultados alcançados e favorecendo o interesse de frações hidrofílicas e hidrofóbicas dos extratos que permitem a busca de biocompostos e com as caracterizações para os próximos ensaios nos interessaremos em patentes. A integração e envolvimentos dos pesquisadores e do supervisor do Projeto permitiu a execução do trabalho com a possibilidade da continuidade de execução dos trabalhos e possibilidade de integração de vários outros discentes e profissionais. A pesquisa permitiu a

	descoberta de atividades microbiológicas dos extratos. **O5 artigos completos publicados em revista de impacto na área de medicina III**: ALMEIDA, B.C. ; KLEINE, J.P.F.O. ; CAMARGO-KOSUGI, C.M. ; LISBOA, M.R. ; FRANÇA, C.N.; FRANÇA, J.P. ; SILVA, I.D.C.G. . Analysis of polymorphisms in codons 11, 72 and 248 of TP53 in Brazilian women with breast cancer. GENETICS AND MOLECULAR RESEARCH, v. 15, p. 1-10, 2016. FERNANDES, ANA CAROLINA MORAIS; FRANÇA, J. P. ; GAIBA, Silvana; ALOISE, ANTONIO CARLOS ; OLIVEIRA, ANDREA FERNANDES DE; MORAES, ANDREA APARECIDA DE FÁTIMA SOUZA ; FRANÇA, L. P.; FERREIRA, Lydia Masako . Development of experimental in vitro burn model. Acta Cirúrgica Brasileira (Online) , v. 29, p. 15-20, 2014. CANDIDA, THAMYRIS ; FRANÇA, J. P. ; CHAVES, ALBA LUCILVÂNIA FONSECA ; LOPES, FERNANDA ANDRADE RODRIGUES ; GAIBA, Silvana ; SACRAMENTO, CELIO KERSUL DO ;FERREIRA, Lydia Masako ; FRANÇA, L. P. Evaluation of antitumoral and antimicrobial activity of Morinda Icitrifolia L. grown in Southeast Brazil. Acta Cirúrgica Brasileira (Online) , v. 29, p. 10-14, 2014. SUARTZ, CAIO VINICIUS ; GAIBA, Silvana ; FRANÇA, J. P. ; ALOISE, ANTONIO CARLOS ; FERREIRA, Lydia Masako . Adipose-derived stem cells (ADSC) in the viability of random skin flap in rats. Acta Cirúrgica Brasileira (Online) , v. 29, p. 6-9, 2014. CUNHA, BRUNA LAIS ALMEIDA ; FRANÇA, JERÔNIMO PEREIRA DE ; MORAES, ANDREA APARECIDA DE FÁTIMA SOUZA ; CHAVES, ALBA LUCILVÂNIA FONSECA ; GAIBA, Silvana ; FONTANA, RENATO ; SACRAMENTO, CELIO KERSUL DO ; FERREIRA, Lydia Masako ; FRANÇA, Lucimar Pereira de . Evaluation of antimicrobial and antitumoral activity of Garcinia mangostana L. (mangosteen) grown in Southeast Brazil. Acta Cirúrgica Brasileira (Online) , v. 29, p. 21-28, 2014. HOCHMAN, BERNARDO; TUCCI-VIEGAS, VANINA M.; MONTEIRO, PAOLA K. P.; FRANÇA, JERÔNIMO P.; GAIBA, Silvana; FERREIRA, LYDIA M. The action of CGRP and SP on cultured skin fibroblasts. Central European Journal of Biology , v. 9, p. 717-726, 2014.
3.Trabalhos adicionais. Trabalhos científicos apresentados, publicados ou	Resumos Divulagação e/o publicados em Congresso: Gaiba, Silvana ; FRANÇA, J. P.; FRANÇA, FERREIRA, Lydia Masako; Lucimar Pereira de; F Avaliação do

submetidos à publicação ou que resultaram de patente apresentados,resultantes da bolsa concedida.	potencial antitumoral do extrato da folha e lattex (aquoso e etanólico) de Himatanthus drasticus e Sinadenium Grantii e euphorbia tirucalli em células tumorais B16-F10 e MCF7. 2014. Resultados parciais apresentando In: XIV Congresso Internacional de Cirurgia Experimental - SOBRADPEC e I Fórum de Pesquisa em Cirurgia Translacional, 2014, São Paulo. XIV Congresso Internacional de Cirurgia Experimental - SOBRADPEC e I Fórum de Pesquisa em Cirurgia Translacional, 2014. v. 1. SUARTZ, C. V. ; Gaiba, Silvana; FRANÇA, Jerônimo Pereira de ; Aloise, Antonio Carlos; FERREIRA, Lydia Masako. Adipose-derived stem cells (ADSC) in the viability of random skin flap in rats. In: XIV Congresso Internacional de Cirurgia Experimental - SOBRADPEC e I Forum de Pesquisa em Cirurgia Translacional, 2014, São Paulo. XIV Congresso Internacional de Cirurgia Experimental - SOBRADPEC e I Forum de Pesquisa em Cirurgia Translacional, 2014. v. 1. p. 39-40. Artigo Completo Submetido: Manuscript ID: marinedrugs (ISSN 1660-3397) -Type of manuscript) - 72040: Article Title: Antiproliferative and Cytotoxic Effect of Aqueous Extract from Mussismilia braziliensis Coral Mucus in Mouse Melanoma B16 F10 Cells. Authors: Fernanda Luiza Andrade de Azevedo, Lucimar Pereira de França, Silvana Gaiba, Andrea Aparecida Fátima Souza Moraes, Renato Fontana, Vanina Monique Tucci-Viegas, Lydia Masako Ferreira, Antonio de Miranda, Emiliano Nicolas Calderon, Jerônimo Pereira de França. Received: 2 December 2014 Trabalhos apresentados em Simpósio/Congresso: CANDIDA, T.; GAIBA, S.; FRANÇA, L. P.; MANGABEIRA, P.A.O.; CHAVES, A. L. F.; SACRAMENTO, C. K.; SILVA, L. A. M.; FERREIRA, L. M.; FRANÇA, J. P. Atividade antitumoral do extrato hidroAlcóolico da folha de Himatanthus drasticus em células tumorais de melanoma murino B16-F10. 2014. XII Semana Acadêmica da Medicina Veterinária e I Simpósio de Saúde Pública. SUARTZ, C. V.; Gaiba, Silvana; França, J.P.; FERREIRA, L. M. . Células-tronco do tecido adiposo na viabilidade do retalho cutâneo randômico dorsal em ratos. 2014. In: XIV Congresso Internacional de Cirurgia Experimental - SOBRADPEC e I Forum de Pesquisa em Cirurgia Translacional, 2014, São Paulo. XIV Congresso Internacional de Cirurgia Experimental - SOBRADPEC e I Forum de Pesquisa em Cirurgia Translacional, 2014.

	Prêmio - Melhor trabalho apresentado: CANDIDA, T.; GAIBA, S.; FRANÇA, L. P.; MANGABEIRA, P.A.O.; CHAVES, A. L. F.; SACRAMENTO, C. K.; SILVA, L. A. M.; FERREIRA, L. M.; FRANÇA, J. P. Atividade antitumoral do extrato hidroAlcóolico da folha de Himatanthus drasticus em células tumorais de melanoma murino B16-F10. 2014. XII Semana Acadêmica da Medicina Veterinária e I Simpósio de Saúde Pública.
4. Houve eventuais dificuldades encontradas para execução do Projeto?	Sim
5. Se "sim" para a resposta acima, aponte as dificuldades	Obtenção de culturas de melanócitos e de melanoma, subcultivo e congelamento. O rendimento do número de células viáveis é pequeno por amostra. Como o objetivo era utilizar amostras de cultivo até a 3ª passagem, foi necessário muito tempo de trabalho em cultivo da primária para produção de células suficientes para execução dos ensaios. O HPLC / espectrômetro de massa quebrou durante os ensaios de separação dos extratos. Foi necessário 03 meses de espera entre a nova coleta do extrato e realização de novos ensaios.
1. Atividades acadêmicas visando a melhoria e à inovação do ensino na Graduação, bem como sua integração com a Pós-Graduação. Detalhamento das atividades desenvolvidas (integração com a Graduação e a Pós-Graduação, seminários, jornadas, congressos, visitas, trabalho de campo, palestras, defesas de tese e dissertações).	Participação em Bancas: Doutorado: Programa de Pós-Graduação em Cirurgia Translacional, da UNIFESP/EPM, tem o prazer de convidá-lo(a) para integrar a Comissão da Banca de Tese de Doutorado, intitulada ¨CRIOPRESERVAÇÃO DE TECIDO ADIPOSO HUMANO E CARACTERIZAÇÃO IN VITRO E IN VIVO EM CAMUNDONGOS¨, do(a) aluno(a) Fabiana Cristina Zanata Fortoul, 16 de agosto de 2017. Doutorado: Programa de Pós-Graduação em Cirurgia Translacional da UNIFESP/EPM para integrar a Comissão da Banca de Tese de Doutorado, intitulada ¨AZT NA ATIVIDADE DA TELOMERASE, EXPRESSÃO DE P53 E APOPTOSE EM MELANOMA METASTÁTICO¨, do aluno Celestino Próspero de Souza Sobrinho, no dia 09 de outubro de 2017. Doutorado: banca de Allan Zimmermann. Células Tronco Mesenquimais Derivadas do Tecido Adiposo Autólogo na Técnica de Regeneração Óssea Guiada da Calvária de Coelhos. 2015. Tese (Doutorado em Cirurgia Plástica) - Universidade Federal de São Pau Doutorado: Participação em banca de ALEDSON VITOR FELIPE. Efeito do RNA interferente como modulador de resistência à epirrubicina sobre os níveis

de expressão do gene ABCB1 em linhagem de células AGS de câncer gástrico quimiorresistentes. 2014. Tese (Doutorado em Gastroenterologia) - Universidade Federal de São Paulo. FRANÇA, J. P.; Forones, N.M.; SILVA, J. L. V.; LOURENCO, L. G.; TOMA, L.

Mestrado: VEIGA, D. F.; Aloise, Antonio Carlos; FRANÇA, J. P.; Neto, J.D.S.. Participação em banca de Fernanda Sebba de Souza. Atividade Antimicrobiana in vivo e in vitro de dois antissépticos bucais. 2015. Dissertação (Mestrado em Mestrado Profissional em Ciências Aplicada a Saúde) - Universidade do Vale do Sapucaí.

Mestrado: VEIGA, D. F.; Mendonça, A.R.A.; Santos, I.D.A.O.; FRANÇA, J. P.. Participação em banca de Marina Moreira Costa. Laser InGaAlP (660nm) na Prevenção de Radiodermite em Pacientes com Câncer de Mama Submetidas a Radioterapia. 2015. Dissertação (Mestrado em Mestrado Profissional em Ciências Aplicada a Saúde) - Universidade do Vale do Sapucaí.

Mestrado: Teixeira, M.A,; LOYOLA, A. B. T.; FRANÇA, J. P.; Ferreira, L.M.. Participação em banca de Savia Perina Portilho Falci. Uso do Óleo de Maleleuca SP. como Agente Antimicrobiano em Feridas Contaminadas por Staphylococcus Aureus. 2015. Dissertação (Mestrado em Mestrado Profissional em Ciências Aplicada a Saúde) - Universidade do Vale do Sapucaí.

Mestrado: FRANÇA, J. P.; Ferreira, L.M.. Participação em banca de Marco Antonio Mattar. Avaliação da Pressão Contínua na Cultura Tridimensional de Fibroblastos Derivados do Ligamento Periodontal Humano. 2015. Dissertação (Mestrado em Cirurgia Plástica) - Universidade Federal de São Paulo.

Mestrado: FRANÇA, J. P.; Ferreira, L.M.. Participação em banca de Rafael de Mello e Oliveira. Reconstrução óssea aposicional com enxerto xenógeno associado à fração de células mononucleares da medula óssea na calvária de coelhos. 2014. Dissertação (Mestrado em Cirurgia Plástica) - Universidade Federal de São Paulo.

Mestrado: Disciplina de Cirurgia Plástica, venho convidá-lo para participar como membro ativo, da Banca de Tese de Mestrado, da aluna Delaine P. R. Miguel, intitulada ¨Fibroblastos periodontais humanos em meio de cultura suplementado com Il-1 Beta no modelo de força compressiva estática continua¨, que será realizada no dia 22/06/16

	Mestrado: Participação em banca de Rafael de Mello e Oliveira. Reconstrução óssea aposicional com enxerto xenógeno associado à fração de células mononucleares da medula óssea na calvária de coelhos. 2014. Dissertação (Mestrado em Cirurgia Plástica) - Universidade Federal de São Paulo. FRANÇA, J. P.; Ferreira, L.M. Cursos ministrados / Conferência Cultura de Melanócitos. 2014. FRANÇA, J. P.; (Apresentação de Trabalho/Conferência ou palestra). In: XIV Congresso Internacional de Cirurgia Experimental - SOBRADPEC e I Fórum de Pesquisa em Cirurgia Translacional, 2014, São Paulo. XIV Congresso Internacional de Cirurgia Experimental - SOBRADPEC e I Fórum de Pesquisa em Cirurgia Translacional, 2014. Cultura de Melanócitos e melanoma 2014. FRANÇA, J. Curso de curta duração ministrado Programa de Pesquisa em Cirurgia Translacional. Elisa e Citometria de Fluxo. 2014. FRANÇA, J. P.; Curso de curta duração ministrado Programa de Pesquisa em Cirurgia Translacional. Bioestatística utilizando o software Prism-3. 2014 FRANÇA, J. P.; Curso de curta duração ministrado Programa de Pesquisa em Cirurgia Translacional.
2. Resultados alcançados. Descrição e recapitulação sintética dos resultados obtidos, ressaltando o alcance e as consequências do estudo.	Conseguimos determinar as atividades biológicas de plantas e corais, conforme proposto no Projeto. Com desenvolvimento do Projeto foi possível a formação de recursos humanos com a participação de alunos de mestrado, doutorado, pós-doutorado e principalmente de alunos de iniciação científica. Resultados foram promissores, adequando os resultados alcançados e favorecendo o interesse de frações hidrofílicas e hidrofóbicas dos extratos que permitem a busca de biocompostos e com as caracterizações para os próximos ensaios nos interessaremos em patentes. A integração e envolvimentos dos pesquisadores e do supervisor do Projeto permitiu a execução do trabalho com a possibilidade da continuidade de execução dos trabalhos e possibilidade de integração de vários outros discentes e profissionais. A pesquisa permitiu a descoberta de atividades microbiológicas dos extratos. Há grande expectativa de obter produtos patenteáveis na finalização do Projeto. A evolução didática e pedagógica do pós-doutorando com satisfação, onde observamos adequada integração com o grupo de

	pesquisa e pós-graduação, que permitiu produzir palestras e cursos correlatos á linha de pesquisa ao qual o Programa de Pós-graduação está vinculado. A divulgação dos resultados do Projeto em congressos/simpósios nacionais e internacionais favorece e exibe a produção científica do mesmo. O pós-doutorando participou das atividades inerentes ao PPG de Pesquisa em Cirurgia Translacional com êxito e bom rendimento em pesquisa / ensino. Como exibido em resultados alcançados
1. Qual a frequência de realização de discussões científicas e técnicas com o (a) Supervisor (a), Coordenação do Programa de Pós-Graduação e Diretoria Acadêmica do Campus.	Semanal
2. Etapa cumprida no relatório apresentado. De acordo com o cronograma de atividades apresentado na concessão da bolsa, na escala de 1 a 5, assinale abaixo sobre a etapa de execução do Projeto.	4
Caso a etapa do Projeto esteja entre 1 e 2 até o momento, descreva abaixo motivo de não cumprimento do objeto	Não aplicável.
3. Em relação às expectativas da proposta inicial, os resultados obtidos estão:	Dentro do esperado
Caso não tenha resultados obtidos até o momento, descreva abaixo sua justificativa.	Não aplicável
4. A evolução do Projeto permite prever sua conclusão dentro do prazo previsto de acordo com o cronograma de atividades inicial?	Sim / finalizado
5. Se "não" ou "talvez" para a resposta acima, justifique sua resposta.	

1. Parecer do Relatório Técnico Científico apresentado pelo bolsista.	O laboratório de Cultura de Células da Supervisora Profa. Dra. Lydia Masako Ferreira conta com estrutura extremamente organizada, com equipamentos adequados tanto para cultivo de cultura células primários de melanócitos e melanomas, e ainda como de linhagem. Tivemos a colaboração da Profa. Helena B. Nader (Biologia Molecular) e do Prof. Ismael Guerreiro (ginecologia molecular). A equipe de atuação direta no desenvolvimento das atividades científicas, considerando os colaboradores, técnicos e discentes são de alta qualificação e dedicação, o que garante o desenvolvimento do Projeto. Tivemos toda a assistência durante o período de execução do Projeto.
2. Parecer do Relatório Didático e Pedagógico.	O bolsista participou das atividades técnico-cientificas com êxito, com publicações importantes definidas no andamento do projeto. Desenvolveu os objetivos de acordo com o cronograma proposto no Projeto. Há grande expectativa de obter produtos patenteáveis. A evolução didática e pedagógica do pós-doutorando foi ótima, onde observamos adequada integração com o grupo de pesquisa e pós-graduação, que permitiu produzir palestras, participação em bancas de mestrado e doutorado, aplicação de cursos correlatos á linha de pesquisa ao qual o Programa de Pós-graduação está vinculado. A divulgação dos resultados do Projeto em congressos/simpósios nacionais e internacionais favorece e exibe a produção científica do mesmo. O pós-doutorando participou das atividades inerentes ao PPG de Pesquisa em Cirurgia Translacional com êxito e bom rendimento em pesquisa / ensino. Como exibido em resultados alcançados
3. De acordo com os 2 pareceres descritos acima, consideramos que o bolsista em apreço tem meu parecer:	Favorável. Ao Projeto, a bolsa e ao Relatório parcial e final
Avaliação crítica com pontos positivos e negativos e considerações que se façam necessárias, quanto a assistência acadêmica, científica e de pesquisa.	O laboratório de Cultura de Células da Supervisora Profa. Dra. Lydia Masako Ferreira conta com estrutura extremamente organizada, com equipamentos adequados tanto para cultura células primários (melanócitos e melanoma) como de linhagem. A equipe de atuação direta no desenvolvimento das atividades científicas, considerando os colaboradores, técnicos e discentes são de alta qualificação e dedicação, o que garante o desenvolvimento do Projeto. Tive toda a assistência durante o período de execução do Projeto.
Com relação a assistência administrativa por parte dos colaboradores do Campus, Programa de Pós-Graduação e Pró-	Campus. Administrativamente satisfeito (a) Programa de Pós-Graduação. Administrativamente satisfeito (a) Pró-Reitoria de Pós-Graduação e Pesquisa. Administrativamente satisfeito (a)

Reitoria de Pós-Graduação e Pesquisa, o (a) Senhor (a) considera:	
Descreva em poucas linhas suas considerações com relação as respostas acima (independentemente de sua satisfação) para melhoras no atendimento no que diz respeito somente a sua participação e envolvimento como Pesquisador (a) nas áreas acima.	Tenho profunda admiração e gratidão pelo trabalho desenvolvido pelo Programa de Pós-graduação e Pró-reitoria de Pós-graduação e Pesquisa, tanto do ponto de vista administrativo com acadêmico. Não tenho nenhuma críticas.
Caso queira, anexe um arquivo como complemento deste Relatório. (Arquivos de até 5 mb cada)	

São Paulo, 29 de junho de 2011.
CEP 0758/11

IImo(a). Sr(a).
Pesquisador(a) IVAN DUNSHEE DE ABRANCHES OLIVEIRA SANTOS
Disciplina/Departamento: Cirurgia Plástica/Cirurgia da
Universidade Federal de São Paulo/Hospital São Paulo

Projeto de pesquisa intitulado: "Acao de biocompostos isolados de Mussismilia braziliensis, Morinda citrifolia e Garcinia mangostana no controle da proliferacao celular e inducao de apoptose em celulas cultivadas de Melanoma Metastatico Humano: um estudo celular e molecular".

Prezado(a) Pesquisador(a),

Cumprindo a resolução 196/96 do Conselho Nacional de Saúde, o projeto de pesquisa foi analisado por este Comitê de Ética em Pesquisa, o qual considerou pendente, baseando-se na(s) seguinte(s) consideração(ões):

- Deixar claro na metodologia: a biópsia de pele para obtenção das amostras será realizada durante cirurgia de rotina do serviço? Esclarecer

- O projeto é descrito como multicêntrico. Quais os centros participantes e apresentar carta de ciência destas ao CEP

- O TCLE deverá ser melhor descrito dos procedimentos que serão realizados com o paciente

As respostas a estas questões e comentários deverão ser encaminhadas em 2 vias, com o referido número de registro, no prazo máximo de 60 dias, conforme estabelecido na referida resolução. (Resolução 196 - Cap. VII. 13 b.)
Estamos à disposição para outros esclarecimentos no endereço: Rua Botucatu, 572 - 4º andar – conj. 41.

Atenciosamente,

Membro- Relator do Comitê de Ética em Pesquisa da
Universidade Federal de São Paulo/ Hospital São Paulo

Titulo do projeto:

Acao de biocompostos isolados de Mussismilia braziliensis, Morinda citrifolia e Garcinia mangostana no controle da proliferacao celular e inducao de apoptose em celulas cultivadas de Melanoma Metastatico Humano: um estudo celular e molecular.

Pesquisador: Ivan Dunshee de Abranches Oliveira Santos / idaos@terra.com.br

Currículo Lattes: http://lattes.cnpq.br/7940183627771947

Telefone: 1138875596

Fax: 1155764118

Disciplina: Cirurgia Plastica

Patrocinador: Ausente /

Pesq. Associados:

Dr. Jeronimo Pereira de Franca	jeronimopf@gmail.com	http://lattes.cnpq.br/4171296386053081
Prof. Dr. Ismael Dale Cotrim Guerreiro da Silva	ismael.dale@gmail.com	http://lattes.cnpq.br/7917312029683516
Dra. Lucimar Pereira de Franca	lucimarfrancap@gmail.com	http://lattes.cnpq.br/7761047342982840
Dra. Fernanda Lasakosvitsch Castanho	flcastanho@gmail.com	http://lattes.cnpq.br/1479969360605139
Profa. Dra. Lydia Masako Ferreira	lydia.dcir@epm.br	http://lattes.cnpq.br/1619822351741819

Orientador:

Coordenador de Curso: Prof. Dr. Miguel Sabino Neto
msabino@uol.com.br

Chefe da Disciplina: Prof. Dr. Ivan dunshee de Abranches Oliveira Santos
idaos@terra.com.br

Chefe do Departamento: Prof. Dr. Joao Nelson Rodrigues Branco

Objetivo acadêmico do estudo: Não envolve obtenção de título acadêmico

_____ _____

Assinatura do Investigador Principal **Assinatura do Chefe de Departamento ou Disciplina**

Estudo clínico observacional: Não se Aplica

Estudo clínico com intervenção terapêutica: Não randomizado

Estudo clínico com intervenção diagnóstica: Não randomizado

Característica do Estudo:

Desenvolvimento de novos formas terapêuticas: Fase I

Tipo de sujeito a ser incluído

- Paciente hospitalizado

Forma de recrutamento de voluntários

- Pelo próprio pesquisador

Meio de recrutamento: (Inserir o modelo escrito no campo abaixo)

- Contato pessoal

Outras características do estudo: assinalar 1 (um) ou mais itens:

Está credenciado no núcleo de proteção radiológica da UNIFESP:
(caso envolva material radioativo)

Nome do patologista responsável: Dr Gilles Landman
(caso envolva análise anatomo-patológica)

Escala do estudo: Multicêntrico Nacional

Avaliação do risco e desconforto da pesquisa ao paciente: Segundo critérios do pesquisador (probabilidade de que o indivíduo sofra algum dano ou desconforto como conseqüência imediata ou tardia do estudo)

Riscos: Intenso (ex. submissão a exames que necessitam de sedação ou anestesia)

Desconforto: Intenso (ex. submissão de exames que necessitam de sedação ou anestesia)

Procedimentos invasivos: Biópsia de tecidos

Forma de ressarcimento dos voluntários: (Detalhar esquema adotado)

Nao envolve ressarcimento

Duração esperada até o termino da pesquisa: 36

DESCRIÇÃO DO ESTUDO

Introdução:

Dentre os tumores estudados na população, o melanoma maligno tem chamado a atenção dos pesquisadores, pois, apesar de representar apenas 3% de todas a neoplasia cutâneas primárias, ele é responsável por 2/3 de todas as mortes relacionadas ao câncer de pele. A sua incidência vem aumentando significativamente em todo o mundo, mais rapidamente do que qualquer outro tipo de neoplasia maligna. Em estudos moleculares da ação de compostos antitumorais, dados recentes apontam inibidores da enzima DNA metiltransferase como um novo grupo de drogas antitumorais. Diferente das mudanças genéticas no câncer, as alterações epigenéticas como a metilação do DNA são potencialmente reversíveis e neste contexto as pesquisas têm voltado o interesse para a utilização de compostos bioativos na prevenção e

no tratamento de diversos tipos de câncer, principalmente pela baixa toxicidade apresentada por eles. O Brasil é um país de grandes dimensões, constituído por regiões famosas por sua biodiversidade distribuída em diferentes ecossistemas, tanto marinha quanto terrestre. O ecossistema marinho é um importante reservatório de produtos naturais bioativos com aplicações médicas. O coral da espécie Mussismilia braziliensis encontrado apenas no litoral do estado da Bahia apresenta uma literatura escassa em relação aos biocompostos presentes no muco com atividade antitumoral. Alguns metabólitos secundários presentes no muco dos corais são grandes aliados da indústria farmacêutica, pois têm demonstrado importantes efeitos terapêuticos para várias patologias humanas. Em relação ao ecossistema terrestre, surge a necessidade de conhecer melhor o potencial da flora nativa ou adaptada buscando formas de uso sustentável das espécies pouco conhecidas com o máximo aproveitamento e resíduo mínimo, preservando assim as reservas vegetais naturais. Trabalhos recentes indicam que extratos ou substâncias bioativas extraídas de plantas podem ter importantes efeitos sobre células tumorais, sendo uma alternativa para a descoberta de potentes agentes antitumorais.

Objetivos:

Avaliar a ação do extrato e produtos ativos do muco secretado pelo coral Mussismilia Brazilienses, bem como de polifenóis e bioativos purificados a partir de Morinda citrifolia e Garcinia mangostana no controle de crescimento das células de melanócitos e melanoma humano e no processo de indução de apoptose.

Material e Método:

EXTRAÇÃO E CULTIVO DE CÉLULAS DE MELANOMA HUMANO

CULTURA PRIMÁRIA

As células de melanoma serão obtidas de linfonodos metastáticos de seis pacientes, isoladas e cultivadas a partir de método descrito por RIKER e col., 1999, e modificado por Oliveira, A.F. e col. Acta Cirurgica Brasileira. 2005. Todos os procedimentos serão realizados em ambiente de fluxo laminar. O meio RPMI 1640 será utilizado após suplementação com soro fetal bovino (SFB) a 10%, L-glutamina 0,03%, penicilina 100 U/ml, estreptomicina 10 μg/ml, ciprofloxacina 10 μg/ml, anfotericina B 0,5 μg/ml para um total de 1 litro; o pH será ajustado em 7,4 (RPMI completo). O meio será esterilizado em filtro de 0,22 μm e armazenado a temperatura de -4°C. Para coleta das células, 10 ml do meio será transferido para um tubo cônico de 15 ml e mantido à temperatura ambiente. A punção aspirativa por agulha fina será realizada no intra-operatório de linfadenectomia de seis pacientes com melanoma metastático com intuito de colher células dos linfonodos acometidos para realização de cultura primária. Os pacientes serão informados sobre o método e objetivo do trabalho e assinaram termo de consentimento. Seringa de 10 ml acoplada a uma agulha 25 x 0,7 mm será utilizada para aspirar células dos linfonodos metastáticos; a agulha será introduzida no nódulo e mantida no interior do mesmo enquanto aplicamos uma pressão negativa contínua através da seringa. Antes de retirar a agulha, a pressão deve ser desfeita e o espécime coletado será colocado em tubo cônico de 15 ml com 10 ml de meio de cultura no seu interior. Esse material será levado num intervalo máximo de trinta minutos para o laboratório, onde será centrifugado durante cinco minutos com velocidade de 1300 rpm (358 G). As células serão ressuspensas com 10 ml de meio de cultura e novamente centrifugadas na mesma velocidade e intervalo de tempo, para retirar o máximo de impurezas. As células serão ressuspensas em 5 ml de meio de cultura e colocadas em uma garrafa de cultura de 25 cm², que será mantida numa estufa com temperatura de 37º C em 5% de CO². A troca do meio de cultura foi realizada a cada 2 dias. Após a primeira semana de cultivo, o meio RPMI 1640 sem ciprofloxacina será utilizado. Figura 1, mostra um frasco de cultura de melanomas (25 cm²) que atingiu uma confluência celular de 80%.

EXTRAÇÃO E CULTIVO DE CÉLULAS MELANÓCITOS HUMANO

Um fragmento de pele humana normal da região inguinal ou axilar de área aproximada de 3,0 cm de comprimento por 0,5 cm de largura será removido da margem da incisão realizada na pele e subcutâneo para acesso aos linfonodos situados nessas áreas; devido realização de retalhos cutâneos a partir das margens da incisão para viabilizar a remoção dos linfonodos em bloco, a irrigação do plexo subdérmico, responsável pela vascularização da pele desses retalhos, fica prejudicada, assim é realizado rotineiramente a retirada dessas bordas com a finalidade de revitalizar o tecido e promover uma boa cicatrização da pele no local da incisão. Este fragmento de pele Será incubada à 37ºC por 15 minutos com solução de Hank?s sem Ca++ e Mg++ (Gibco) contendo 0,25% de tripsina. Será acrescido 0,02% de EDTA e incubado por mais 10 minutos à 37ºC. A epiderme será dissociada utilizando uma tesoura de Iris curva formando uma suspensão de células epidérmicas que será centrifugada a 358 G. As células serão ressuspensas em 5 ml de meio de cultura Hu16 com mistura de Ham`s F12 (Gibco) e colocadas em uma garrafa de cultura de 25 cm², que será mantida numa estufa com temperatura de 37º C em 5% de CO². Será acrescido ao meio de cultura, suplementação com soro fetal bovino (SFB) a 10%, L-glutamina 0,03%, penicilina 100 U/ml, 10 μg/ml de ciprofloxacina, 0,5 μg/ml anfotericina B, 20 ng/mL bFGF (Sigma), 20 μg/ml de isobutilmetilxantina (sigma) para um total de 1 litro; o pH será

ajustado em 7,4. No meio de cultura será mantidas por três dias 100 μg/ml de geneticina para evitar o crescimento de fibroblastos e queratinócitos, como descrito por CHEN, Y.F. et al, 2001 e CHEN, Y.F. et al, 2004.

SUBCULTIVO DE CÉLULAS

As culturas de células serão tratadas com tripsina 0,2%, antes ou durante o estado de subconfluência. O meio será removido e as células lavadas com PBS NaCl (140mM), NaH2PO4 (2,6mM), Na2HPO4 (10mM) e EDTA (0,5mM) com 100U/ml de penicilina e 100mg/ml de estreptomicina, o qual será aspirado. Após lavagem com PBS adicionaremos 2,0 ml de tripsina em cada garrafa. As garrafas contendo as culturas de células serão transferidas para a estufa de CO2 o tempo suficiente para que as células se soltem da matriz da garrafa (1-4 minutos), conforme o grau de atividade enzimática. Durante este intervalo, monitoraremos o descolamento das células com o auxílio do microscópio invertido de contraste de fase. A suspensão de células será transferida para um tubo cônico, em RPMI completo e centrifugada durante 4 min a 358 g. A seguir, o sobrenadante será descartado e o sedimento ressuspenso em 2,5 ml de RPMI. Faz-se a contagem dessas células por meio da câmara de Neubauer. Para cada garrafa serão transferidas aproximadamente 103 células, onde adicionaremos o RPMI completo, homogeneizando e transferindo 2 ml dessa suspensão para cada placa de cultura. As células atingirão a confluência nestas placas dentro de 5 a 7 dias, com aproximadamente de 5x105 células por placa. As células do melanoma aderidas à superfície da garrafa começaram a se dividir em aproximadamente 2 dias. A primeira cultura de células será denominada passagem zero. Para os protocolos experimentais, utilizaram-se as mesmas da passagem 1-3.

CARACTERIZAÇÕES DE CÉLULAS DE MELANOMA POR IMUNOHISTOQUÍMICA

O conteúdo de uma garrafa de cultura será tripsinizado e subcultivado em duas garrafas de mesma área, seguindo o protocolo descrito para subcultivo (4.2.2.1). Nesse mesmo procedimento, uma alíquota das células será fixada em lâminas com microvials. O procedimento será realizado utilizando micropipetas e serão colocados 40 μl de polilisina em cada área da lâmina, que permanecerão em repouso durante 1 hora. Após esse intervalo, o excesso da polilisina será aspirado e logo em seguida colocado 20 μl da suspensão de células. Finalmente, após intervalo de 1 hora, o material será fixado com 20 μl de álcool absoluto. As lâminas serão armazenadas em frasco também com álcool absoluto e encaminhadas para o setor de Patologia. O diagnóstico da cultura será confirmado através da imuno-histoquímica utilizando a proteína S-100 e HMB-45 (Human Melanoma Black), marcadores freqüentemente utilizados para diagnóstico do melanoma. O HMB-45 é utilizado devido sua especificidade na detecção de células de melanoma, mas em relação à proteína S-100 é menos sensível. O procedimento técnico para caracterização das células do melanoma consistirá de hidratação com álcool, lavagem em água corrente, bloqueio da peroxidase endógena, incubação do anticorpo primário e da peroxidase, e a revelação da reação.

PLANTAS MEDICINAIS UTILIZADAS CONTRA O CÂNCER

Plantas utilizadas para o tratamento do câncer para este projeto, iniciando os experimentos e descrições com as seguintes espécies: Morinda citrifolia L. (Noni), Garcinia mangostana L. (Mangostão). No entanto, outras espécies poderão ser incluídas ao estudo. Obtidas do viveiro de plantas da Universidade Estadual de Santa Cruz - UESC onde serão coletadas pelas manhãs em áreas verdes e jardins do setor, no período de frutificação, e imediatamente processadas. As espécies serão depositadas no Herbarium de Botânica da UESC sob Número de Voucher definido, e apresentado no primeiro relatório ou publicação. Para as descrições morfológicas, os diferentes órgãos vegetais, indicados em literatura e utilizados nos testes in vitro serão, pós desidratação, incluídos em historesina, posteriormente, seccionados em micrótomo rotativo e montados em lâminas histológicas. As lâminas serão coradas com azul de toluidina O para análise em microscopia fotônica.

Para o estudo histoquímico serão realizados cortes manuais com uso de lâminas de barbear. Os cortes serão submetidos aos seguintes testes histoquímicos: Cloreto férrico, para detectar a presença de compostos fenólicos; DMACA e cafeína, para flavonóides; Dragendorf, para alcalóides; lugol, para amido; Sudam III, para lipídios e 2,4-dinitrophenylhydrazine, para terpenos. Outros testes poderão ser acrescentados caso ocorra a necessidade de elucidar a ocorrência de substâncias não identificadas.

O registro das características morfológicas e compostos químicos detectados serão realizados mediante fotografias em máquina digital acoplada ao microscópio fotônico.

PREPARAÇÃO DO EXTRATO DAS PLANTAS MEDICINAIS

Os frutos da planta Morinda citrifolia L. (Noni), Garcinia mangostana L. (Mangostão) serão coletados no município de salobrinho, estado da Bahia. As condições do solo, pluviosidade, temperatura média anual, e outras informações pertinentes as condições do cultivo serão determinadas e informadas na ocasião do primeiro relatório e futuras publicações do trabalho, assim como a identificação botânica e nº da exsicata depositada no herbarium. Os frutos serão picados, dessecados em estufa de circulação forçada de ar, durante 8 dias, a uma temperatura máxima de 45 °C (± 1). Após essa etapa, o material será triturado em moinho, tipo Willis, obtendo-se um pó que será

acondicionado em um frasco de vidro âmbar hermeticamente fechado e identificado, onde permanecerá até o momento do preparo dos extratos. Preparação dos extratos: O extrato etanólico será obtido através de maceração a frio, após quatro extrações sucessivas, sendo filtrado usando-se papel de filtro Whatman nº 1. Em seguida, concentrado em evaporador rotativo sob pressão reduzida, à temperatura entre 42 e 45 °C e, então, liofilizado. Utiliza-se em média 1,3 L de etanol para cada extração realizada. O extrato aquoso foi obtido através de cocção, ou seja, 50 g de pó da matéria vegetal para 500 mL de água destilada e, em seguida, deixou-se ferver por dois minutos e, após o resfriamento da temperatura ambiente, a solução obtida será filtrada, obtendo-se então uma solução a 10%. Determinação do peso seco: Será retirada uma alíquota de 1 mL de cada extrato, colocada em estufa de circulação forçada de ar, a uma temperatura de 45 °C (±1), até a obtenção de um peso constante, procedimento realizado em triplicata. A massa média obtida referente a 1 mL será relacionada ao respectivo volume total, obtendo-se então a massa total em mg/mL. Esse procedimento será realizado para o extrato aquoso com o objetivo de determinar o peso seco e, para o extrato etanólico, para avaliar o rendimento aproximado após a evaporação do etanol (BRITO, D.R.B. et. al., 2009).

PREPARAÇÃO DO EXTRATO DO MUCO DO CORAL PLANTAS MEDICINAIS

O muco do coral da espécie Mussismilia Braziliensis será obtido por drenagem da superfície do coral sem promover quebra na sua estrutura. Tal processo será feito com auxílio de uma cânula acoplada a um sistema de sucção a vácuo. As amostras serão armazenadas em tubos cônicos estéreis e mantidas em caixas de isopor com gelo seco por no máximo 1h. Tempo necessário para a coleta e transporte do material ao laboratório para os ensaios e preparação dos extratos. 1L de água do mar será pré-filtrada em sistema Millipore com filtro 8μm e em seguida de 0,2 μm e adicionada ao muco na proporção 1:1 para solubilizar por agitação magnética e posteriormente será liofilizada para realização dos ensaios (REIS, A.M.M., et al., 2009).

DETERMINAÇÃO DA ATIVIDADE CELULAR

Para determinação da atividade celular dos melanócitos e melanomas após o tratamento com polifenóis e bioativos isolados do muco do coral, da Morina citrofolia e da Garcinia será utilizada uma solução de 3-(4,5-Dimethyl-2-thiazoly)-2,5-diphenyl-2H tetrazolium bromide (MTT). Serão semeadas 1x103 células em cada poço de placas de cultura (96 poços) com 90 ?L de meio RPMI 1640 completo e mantidas em incubadora úmida a 37ºC e 5% de CO2 por 24 horas. O meio de cultura será removido e substituído por 100?L de solução de dimetilsulfóxido (DMSO) e após 10 minutos, as leituras de absorbância serão realizadas em equipamento de Elisa SpectraMax M2e E(Molecular Devices) em um comprimento de onda de 570nm.

ANÁLISE POR CITOMETRIA DE FLUXO DE CÉLULAS CULTIVADAS EM NECROSE E APOPTOSE

A técnica de citometria de fluxo com duas cores (FCM) será utilizada para detectar apoptose e necrose usando iodeto de propídeo (PI) e anexina-V marcada com isotiocianato de fluoresceína como descrito por van OOSTVELDT& e col., 1999. O método consiste em fazer a marcação do DNA celular pelo iodeto de propídeo e da fosfatidilserina com FITC - Anexina V, simultaneamente, utilizando 500mL de solução tampão acrescentando 10mL de solução de PI (50mg/mL) e 10mL de anexina-V-FITC. As células serão ressuspensas em 100mL de solução tampão contendo: PI e anexina-V-FITC e incubada por 10 min, protegida da luz em temperatura ambiente para a análise por citometria de fluxo.

IDENTIFICAÇÃO POR CITOMETRIA DE FLUXO DAS PROTEÍNAS ENVOLVIDAS NA APOPTOSE (CASPASE 3, 8, 9, 12) E/OU SOBREVIVÊNCIA CELULAR (P16, P21 E P53)

As células de melanócitos e melanoma cultivadas serão tripsinizadas e ressuspensas em Tyrode Normal ou PBS sem EDTA a 4ºC. Após centrifugação a 1000 rpm as células serão ressuspensas em formol a 2% por 15minutos. Após uma nova centrifugação as células serão ressuspensas e incubadas por 10 minutos em uma solução de Tyrode Normal ou PBS contendo glicina. Após este procedimento as células serão centrifugadas e ressuspensas em Tyrode ou PBS contendo albumina sérica bovina BSA (1%). As células serão incubadas com anticorpo primário contra a caspase-3, 12 ou P53 previamente diluídos em solução de Tyrode Normal ou PBS com BSA (1%) por 1 hora a 4°C. Posteriormente, as células serão centrifugadas a 1000rpm e incubadas com anticorpo secundário conjugado com FITC, diluídos 1:300 (4mg/ml). Após 30min de incubação procede-se a análise em um citômetro de fluxo, FACScalibur, Becton Dickinson, San Jose, CA, EUA. Serão analisadas 10.000 eventos por amostra, com fluxo não superior a 100 células / segundo. As células serão analisadas pela intensidade de fluorescência no canal de FL1 com excitação/emissão em 488, analisado em escala logarítmica utilizando o software Cell Quest da Becton Dickinson.

AVALIAÇÃO DA FRAGMENTAÇÃO DO DNA E/OU APOPTOSE POR TESTE DE TUNEL

A detecção e quantificação de apoptose será realizada utilizando-se o kit Roche®, baseado na marcação de quebras de fita de DNA pela técnica de marcação dos terminais de com dUTP (conjugada com FITC) mediada pela enzima deoxinucleotidil transferase terminal

(Terminal deoxynucleotidyl transferase mediated dUTP nick end labeling =TUNEL). Para a realização do teste de TUNEL, será seguida a metodologia descrita a seguir:

Após o tratamento das células com a droga, elas sofrerão o processo de fixação com a adição de solução de paraformaldeído 4% recém-preparado e incubação por 1 hora em temperatura ambiente. Após este período, as células serão lavadas com PBS. A seguir, as células serão permeabilizadas com solução Triton X-100 a 2o.C por dois minutos e novamente lavadas com PBS por duas vezes. Para controle positivo de apoptose, algumas lamínulas com células foram tratadas com deoxirribonuclease I 3U/ ?L por 20 minutos em temperatura ambiente.

Todas as lamínulas serão incubadas por sessenta minutos a 37ºC no escuro com 50?L de solução recém preparada de mistura de TUNEL (solução com a enzima deoxinucleotidil transferase e dUTP marcada com FITC), com exceção das lamínulas para o controle negativo que ficarão livre da solução de mistura de TUNEL.

Após o período de incubação, as células serão lavadas três vezes com PBS. As lamínulas então, transferidas para lâminas de vidro, intercaladas com 10 ?L de solução DAPI/antifade. A visualização será feita por Microscopia de fluorescência confocal.

CITOQUÍMICA E IMUNOCITOQUÍMICA PARA ANÁLISE POR MICROSCOPIA DE FLUORESCÊNCIA E MICROSCOPIA CONFOCAL

Para os ensaios de imunocitoquímica e detecções citoquímicas, as células melanoma serão subcultivadas sobre lamínula circular de 12 mm de diâmetro em uma concentração de 103 células/lamínula e mantidas em placa contendo 24 poços. As análises serão realizados com células cultivadas após 3 dias. As células serão lavadas 5 vezes em PBS sem EGTA (0,1M, pH 7,4) e então realizado o ensaio desejado. A seguir serão realizado os procedimentos utilizados para imunocitoquímica e citoquímica. As células serão semeadas em placas de 0,15 mm (Part # 04200415 clean Bioptechs, Inc.) e em solução Tyrode Normal. A marcação das células com sondas e corantes fluorescentes será feita de acordo com o método descrito por Bkaily e cols. 1995 e Decho e Kawaguchi, 1999. As células marcadas serão examinadas com o microscópio confocal CARL ZEISS modelo LSM 510, do laboratório de Microscopia Confocal da UNIFESP-EPM.

IMUNOCITOQUÍMICA E CITOQUÍMICA PARA MICROSCOPIA DE FLUORESCÊNCIA CONFOCAL: MARCAÇÃO DAS MITOCÔNDRIAS, NÚCLEO E FILAMENTOS DE ACTINA

Para o estudo morfológico, das células de melanoma humano isoladas de acordo com o método descrito no item 4.1, serão coletadas em placa de polietileno estéril com 24 poços e fixadas com 500 ?L de álcool etílico absoluto durante 15 minutos, à temperatura ambiente. Posteriormente, o sobrenadante será retirado e então, será adicionado solução de PBS (140,0 mM NaCl, 2,6 mM NaH2PO4.H2O, 10,0 mM Na2HPO4, 0,5 mM EDTA; pH 7,4) contendo BSA 0,1 % e glicina 1 M por 20 minutos. Em seguida, as ilhotas pancreáticas serão permeabilizadas com uma solução de PBS contendo BSA 0,1% e saponina 0,1 % por 15 minutos. Após este período, serão incubadas com Faloidina conjugado com Alexa Fluor 488 (Molecular Probes). Após 40 minutos de incubação, as células serão lavadas com solução de PBS contendo BSA 0,1% e em seguida, será adicionado o corante DAPI (marcador de DNA - Molecular Probes), onde as células serão incubadas durante 15 minutos protegidas da luz. Após o período de incubação, elas serão lavadas com solução de PBS contendo BSA 0,1 %. Posteriormente, as células serão marcadas com Mitotracker red (Molecular Probes), durante 1 minuto e então, serão lavadas com solução de PBS com BSA 0,1 %. Então serão coletadas com o auxílio da lupa binocular e transferidas para as lâminas, onde será adicionado o Fluormount G. Preparadas às lâminas, a visualização e a obtenção de imagens dar-se-á por meio do microscópio de fluorescência confocal, usando filtros apropriados aos fluoróforos utilizados.

ANÁLISE POR WESTERN BLOT

A separação das proteínas será feitas em gel para eletroforese de poliacrilamida em SDS de 4 a 20% (BIORAD) e exposta a eletroforese por 1,5h. As proteínas serão transferidas para uma membrana de nitrocelulose que será incubada com salina tampão Tris-HCl com 0,1% de Tween 20 (pH 7.4) contendo 3% contendo leite desnatado. Os anticorpos policlonais de coelho contra caspase 3, 8, 9, 12 e p16 e 53 permaneceram 4°C em overnight. As membranas serão lavadas três vezes por 05 minutos cada com salina tampão Tris-HCl contendo 0,1% de Tween 20. A imunoreatividade será detectada pelo aumento da quimioluminescência (ECL Kit Amersham Pharmacia Biotech) e visualizada pela autoradiografia. Os autoradiogramas serão analizados pela densitometria por software de analise de imagens, neste processo a densidade e a área de cada banda serão medidas. O valor total das caspase 3, 8, 9, 12 e p16 e 53 serão calculadas através da determinação da área e densidade de cada banda. Os valores de cada banda serão normalizados em relação ao controle (Qin et al., 2001).

ANÁLISE E SEPARAÇÃO DE FRAÇÕES, PEPTÍDIOS E PROTEÍNAS DO MUCO E EXTRATO PRODUZIDO PELO CORAL MUSSISMILIA BRAZILIENSIS POR ELETROFORESE 2-D

As amostras provenientes do Muco do CORAL Mussismilia braziliensis nos diferentes tratamentos, serão submetidas à precipitação de proteína, utilizando-se 20% TCA gelado. A solução ficará precipitando em gelo por 30 minutos. Após esse período passará por um processo

de centrifugação e lavagem com acetona ou etanol para remover o TCA residual. Posteriormente, será determinada a quantidade de proteínas, utilizando-se o 2D Quant kit (GE), de acordo com as instruções do fabricante.
A eletroforese bidimensional consiste em cinco etapas principais, que são: focalização isoelétrica (primeira dimensão, eletroforese desnaturante em gel de poliacrilamida (segunda dimensão); detecção das proteínas, digitalização e análise de imagem.
As fitas de gel (Immobiline Dry Strip) 13 cm pH 3-10 NL (GE Healthcare) serão corridas em aparelho IPGPhor (GE Healthcare). As fitas IPG serão colocadas no suporte e rehidratadas ?overnight? a 30 volts em tampão de rehidratação, (7M uréia, 2M thiouréia, 2% CHAPS, 0,5% tampão IPG e 100 mM DTT) contendo 400 μg de proteínas. A focalização será realizada utilizando-se um protocolo com múltiplas etapas (1h a 500V, 1h a 1000V e 6h a 8000V). Antes da segunda dimensão, cada uma das fitas será equilibrada por 15 minutos em 10 mL de um tampão contendo 50mM Tris-HCL, pH 8.8, 6 M uréia, 30% glicerol, 2% SDS, traços de azul de bromofenol, suplementado com 10 mg/mL de DTT. Após esta etapa, as fitas serão equilibradas por 15 minutos, no tampão descrito acima, porém substituindo-se o DTT por 25 mg/ml de iodoacetamida.
A eletroforese de segunda dimensão será realizada a 150V usando gel de poliacrilamida (12%) utilizando-se um sistema de tampão continuo do tipo Laemmli. Para a segunda dimensão, será utilizado o equipamento SE 600 Ruby (GE Healthcare).
VISUALIZAÇÃO DAS PROTEÍNAS E ANÁLISE DE IMAGENS
Os géis serão corados com o kit ?colloidal coomassie? (Novex), digitalizados em aparelho Imagescanner II (Ge) e as imagens obtidas serão analisadas através de software específico (Image Master 6 (GE). Os ?spots? correspondentes às proteínas serão quantificados após normatização volumétrica, aonde o volume de cada ?spot? será dividido pelo volume total de todos os ?spots? de acordo com critérios preconizados por Mahon e Dupree (2001).
IDENTIFICAÇÃO DE PROTEÍNAS POR ESPECTROMETRIA DE MASSAS
PREPARO DAS AMOSTRAS
Os spots correspondentes às proteínas serão excisados do gel, descorados em 200 μL NH4HCO3 em acetonitrila 50 %, o sobrenadante será descartado e os géis serão desidratados em 100 μL de acetonitrila 100 % por 5 minutos e secos no vácuo para retirar a acetonitrila por 10 minutos. Serão colocados 4 μL de tripsina 25 ng/μL, deixados a 4 ºC por 10 minutos para absorção da solução nos pedaços de gel, adicionado NH4HCO3 até cobrir e deixados a 37 ºC por 16 horas para ação da tripsina. O sobrenadante será coletado e passado para um novo tubo, os pedaços de gel que ficarem serão lavados duas vezes com 50 μL de acetonitrila 50 % contendo ácido fórmico 0,1 %, sendo agitados por 15 minutos no vórtex em cada lavagem, depois o sobrenadante será passado para o mesmo tubo que continha o sobrenadante da digestão. Os peptídeos assim obtidos serão concentradas em uma centrífuga a vácuo Concetrator 5301 (Eppendorf) até atingir entre 10 e 15 μL.
APLICAÇÃO DAS AMOSTRAS NO NANOESI-Q-TOF
Os peptídeos obtidos conforme descrito acima, serão submetidos à cromatografia de fase-reversa no nanoAcquity UPLC (WATERS) em duas colunas C18, sendo a primeira uma coluna trapping de 5 μm, 180 μm x 20 mm e a segunda de 1,7 μm 100 μm x 100 mm, sob um fluxo de 0,6 μL/min em uma corrida de 50 minutos, onde serão coletados 4 μL de cada amostra. Os peptídeos serão separados de acordo com um gradiente de acetonitrila, sendo 1 % até 1 minuto, de 1 a 40 minutos houve um gradiente linear de acetonitrila até chegar a 50 %, de 40 a 45 minutos essa concentração aumentará para 85 %, de 45 a 47 mantendo-se constante a 85 % e aos 48 minutos a concentração de acetonitrila diminuirá para 1 % permanecendo até os 50 minutos.
Os peptídeos separados serão ionizados em um capilar sob voltagem de 3000 V (Micromass Q-TOFmicro), fragmentados no modo positivo com seleção da intensidade relativa mínima de 10 counts, sendo analisados os 3 íons mais intensos por cada scan de 1 segundo, com energia de colisão variando entre 20 e 95 eV de acordo com a relação m/z dos peptídeos. Os espectros de MS/MS serão analisados no ProteinLynx Global Server 4.2 (WATERS), sendo comparados com o banco de dados do NCBI e/ou Swiss Prot, configurados para digestão tríptica, com 1 sítio de clivagem perdida, erro tolerante de 30 ppm e tolerância para erro de massa igual a 0,3 Da.
DETERMINAÇÃO DA METILAÇÃO DO DNA
A determinação do padrão de metilação do DNA será realizada utilizando-se o EpiTect HRM PCR Kit (Qiagen) de acordo com as especificações do fabricante. A detecção e quantificação de CpGs metiladas no DNA será realizada por meio de fluorescência. O corante flurescente presente no kit não interage com o DNA de fita simples (ssDNA), mas se liga ativamente a dsDNA. As reações serão realizadas no Rotor-Gene Q 2plex HRM System (Quiagen). O programa gera um gráfico onde está plotada a intensidade de fluorescência em função do número de ciclos de amplificação.
RT-PCR EM TEMPO REAL

O FastLane Cell SYBR Green Kit (Quiage) compreende 4 etapas: remoção de contaminantes extracelular, lise celular com a estabilização do RNA, a eliminação do DNA genômico, e a transcrição reversa. Células cultivadas serão brevemente lavadas com tampão FCW para remover o meio de cultura, material extracelular liberado por células vivas, e material intracelular liberado por qualquer células lisadas. A remoção desses materiais é importante, pois eles podem interferir com a quantificação por real-time RT-PCR. Após a lavagem com tampão FCW, as células cultivadas serão então lisadas por 5 minutos, utilizando tampão FCP. Este tampão também estabiliza a RNA celular e bloqueia a ação de inibidores de transcriptase reversa. O lisado é brevemente incubado em tampão gDNA Wipeout a 42 ° C por 5 minutos para efetivamente eliminar a contaminação do DNA genômico.
Para as reações de PCR em Tempo Real serão utilizados os primers disponíveis comercialmente (Qiagen). As reações serão realizadas no Rotor-Gene Q 2plex HRM System (Quiagen). O programa gera um gráfico onde está plotada a intensidade de fluorescência em função do número de ciclos de amplificação. Um limiar (threshold) é definido manualmente, onde a intensidade de fluorescência é estatisticamente diferente da fluorescência de fundo (background) e a curva encontra-se na fase logarítmica de amplificação. O ciclo da reação no qual a fluorescência da amostra intercepta o threshold é chamado Ct (Cycle Threshold). Assim, a comparação entre a expressão gênica de diferentes amostras é realizada através da comparação entre os Cts. Amostras com Cts menores apresentam maior quantidade do gene alvo no cDNA template inicial na reação.
APRESENTAÇÃO DOS DADOS E ANÁLISE ESTATÍSTICA
A concentração intracelular de proteínas específicas e outros parâmetros experimentais serão representados como valores médios ou como porcentagem de aumento relativo ao controle, sendo analisados pelo programa computacional ?GraphPad Prism 3? (GraphPad Software, San Diego, CA, USA). Os valores serão expressos como média ± erro padrão. Será utilizada a análise estatística pelo teste de ANOVA seguido pelo teste de Newman-Keuls para múltiplas comparações. A significância estatística será dada por $p<0,05$.

Critérios de inclusão e exclusão:

CRITERIOS DE INCLUSAO
- Pacientes com idade acima de 18 anos e abaixo de 65 anos
- Pacientes que concordaram em participar da pesquisa e assinaram o termo de consentimento livre e esclarecido
- Pacientes com condições cognitiva e psiquiátricas para assinar o termo de consentimento livre e esclarecido ou com responsavel legal que responda e assine o termo de consentimento livre e esclarecido
- Pacientes com diagnostico anatomopatológico de melanoma cutâneo
- Pacientes com metástase de melanoma nos linfonodos axilares ou inguinais (estádio III)

CRITERIOS DE EXCLUSAO
- Pacientes com idade abaixo de 18 anos e acima de 65 anos
- Não concordar em participar da pesquisa
- Não concordar em submeter-se a procedimento operatório
- Pacientes sem condições cognitiva e psiquiátricas para assinar o termo de consentimento livre e esclarecido ou sem responsavel legal

Justificativa para realização do estudo/hipoteses a serem testadas

A incidência do melanoma vem aumentando em todo o mundo e está estreitamente relacionada às pessoas de pele branca e com excessiva exposição ao sol (SIGALOTI et al., 2010). Quando diagnosticados nos estádios iniciais, possuem um bom prognóstico quanto à sua cura (FAURI et al., 2010). Dentre os tumores estudados na população, o melanoma maligno tem chamado a atenção dos pesquisadores, pois, apesar de representar apenas 3% de todas a neoplasia cutâneas primárias, ele é responsável por 2/3 de todas as mortes relacionadas ao câncer de pele (CAPIZZI & DONOHUE, 1994). A sua incidência vem aumentando significativamente em todo o mundo, mais rapidamente do que qualquer outro tipo de neoplasia maligna. Segundo dados do Instituto Nacional do Câncer (INCA), 1.303 morreram, sendo 749 homens e 554 mulheres e para o ano de 2010 a estimativa de novos casos era de 5.930, sendo 2960 homens e 2.970 mulheres, (http://www.inca.gov.br/estimativa/2008).
O ecossistema marinho é um importante reservatório de produtos naturais bioativos com aplicações médicas. Em particular o coral da espécie Mussismilia braziliensis encontrado apenas no litoral do estado da Bahia apresenta uma literatura escassa em relação aos biocompostos presentes no muco com atividade antitumoral. Alguns metabólitos secundários presentes no muco dos corais são grandes aliados da indústria farmacêutica, pois têm demonstrado importantes efeitos terapêuticos para muitas patologias humanas (LIANG et al., 2008). Trabalhos recentes indicam que extratos ou substâncias bioativas extraídas do muco de corais e plantas podem ter importantes

efeitos sobre células tumorais, sendo uma alternativa para a descoberta de potentes agentes antitumorais (DING et al., 1999; JATKAR et al., 2010; LIANG et al., 2008). Quanto aos estudos moleculares da ação de compostos antitumorais, dados recentes apontam inibidores da enzima DNA metiltransferase como um novo grupo de candidatos a drogas antitumorais (BRUECKNER B et al, 2007). Diferente das mudanças genéticas no câncer, as alterações epigenéticas como a metilação do DNA são potencialmente reversíveis e dentro deste contexto as pesquisas têm voltado o interesse para a utilização de compostos bioativos na prevenção e no tratamento de diversos tipos de cânceres, por apresentarem baixa toxicidade. Por outro lado, será necessário inicialmente avaliar a morfologia e histoquímica das plantas que constituirão os estudos de base para caracterização das espécies e indicação dos compostos químicos presentes nas mesmas que atuarão no tratamento do câncer. Diante desse cenário, esse projeto tem por objetivo avaliar o potencial antitumoral de extratos produzidos pelo muco do coral da espécie Mussismilia braziliensis, bem como avaliar o efeito de polifenóis e bioativos purificados a partir de Morinda citrifolia e Garcinia mangostana no padrão de metilação de genes supressores de tumor como p53, p21 e p16, na expressão desses genes e dos codificadores de caspases (3, 8, 9 e 12) em células do melanoma metastático humano, considerando a resposta para a inibição da proliferação celular e indução das vias de apoptose.

Descrição da Infra-estrutura dos locais onde se processarão todas as etapas do estudo:

EXTRAÇÃO E CULTIVO DE CÉLULAS DE MELANOMA HUMANO PRIMÁRIO; EXTRAÇÃO E CULTIVO DE CÉLULAS MELANÓCITOS HUMANO; CARACTERIZAÇÕES DE CÉLULAS DE MELANOMA POR IMUNOHISTOQUÍMICA SERÁ REALIZADO NO LABORATORIO DA DISCIPLINA DE CIRURGIA PLASTICA DO DEPARTAMENTO DE CIRUGIA-UNIFESP

PREPARAÇÃO DO EXTRATO DAS PLANTAS MEDICINAIS E PREPARAÇÃO DO EXTRATO DO MUCO DO CORAL PLANTAS MEDICINAIS NO LABORATORIO DA UNIVERSIDADE ESTADUAL DE SANTA CRUZ- UESC- BAHIA

DETERMINAÇÃO DA ATIVIDADE CELULAR; IDENTIFICAÇÃO POR CITOMETRIA DE FLUXO DAS PROTEÍNAS ENVOLVIDAS NA APOPTOSE (CASPASE 3, 8, 9, 12) E/OU SOBREVIVÊNCIA CELULAR (P16, P21 E P53); AVALIAÇÃO DA FRAGMENTAÇÃO DO DNA E/OU APOPTOSE POR TESTE DE TUNEL; IDENTIFICAÇÃO DE PROTEÍNAS POR ESPECTROMETRIA DE MASSAS; RT-PCR EM TEMPO REAL NO LABORATORIO DE BIOLOGIA MOLECULAR DA DISCIPLINA DE GINECOLOGIA E OBSTETRICIA DO DEPARTAMENTO DE MEDICINA - UNIFESP

CITOQUÍMICA E IMUNOCITOQUÍMICA PARA ANÁLISE POR MICROSCOPIA DE FLUORESCÊNCIA E MICROSCOPIA CONFOCAL NO MULTIUSUARIO - UNIFESP

Referências Bibliográficas:

· ADACHI, T., SCHAMEL, W.W., KIM, K.M., WATANABE, T., BECKER, B., NIELSEN, P.J. and Reth, M. Embo j. 15:1534-1541, 1996.
· BANDYOPADHYAY D, MISHRA A, MEDRANO EE: Overexpression of histone deacetylase 1 confers resistance to sodium butyrate-mediated apoptosis in melanoma cells through a p53-mediated pathway. Cancer Res. 64:7706-7710, 2004
· BASLER GC, FADER DJ, YAHANDA A, SONDAK VK, JOHNSON TM. The utility of fine needle aspiration in the diagnosis of melanoma metastatic to lymph nodes. J Am Acad Dermatol.; 36:403-8 (1997).
· Bissonnette R.P; Echeverri, F.; Mahboubi A.; Green D.R. Nature. 1992; 359:552-4.
· BKAILY,G. GROSS-LOUIS,N.NAIK,R.JAALOUK,D.POTHIER,P. Mol. Cell Biochem., 154:113-121, (1995).
· BRECKENRIDJE, D.G., STOJANOVIC, M., MARCELLUS, R.C. E SHORE, G.C. The journal of cell biology. V. 160, number 7, 2003.
· BRITO, D.R.B.; FERNANDES, R.M.; FERNANDES, M.Z.L.C.M.; FERREIRA, M.D.S.; ROLIM, F. R. L.; AND FILHO, M.L.S. Anthelmintic activity of aqueous and ethanolic extracts of Morinda citrifolia fruit on Ascaridia galli. Rev. Bras. Parasitol. Vet., Jaboticabal, v. 18, n. 4, p. 32-36. 2009.
· BRUECKNER B, KUCK D, LYKO F. DNA methyltransferase inhibitors for cancer therapy. Cancer J. Jan-Feb;13(1):17-22, 2007.
· BUDIHARDJO, I.H., OLIVER, M., LUTTER, X., LUO E X. WANG. Annu Ver Cell Dev Biol. 15:269-290,1999.
· CAMPISI, J. Senescent cells, tumor suppression, and organismal aging: good citizens, bad neighbors. Cell 120, 513-522, 2005
· CAPIZZI PJ, DONOHUE JH. - Metastatic melanoma of the gastrointestinal tract: a review of the literature. Compr Ther. 20(1): 20-23, (1994).
· CASTRO, AP. et al. Bacterial Community Associated with Healthy and Diseased Reef Coral Mussismilia hispida from Eastern Brazil.

Microb Ecol. 59: 658-667 (2010).
· CASTRO, AP., ARAÚJO,S.D., REIS, A.M.M., MOURA, R.L.,FRANCINI-FILHO, R.B.,PAPPAS, G., RODRIGUES, TB., THOMPSON, FL, KRÜGER, RH. Bacterial Community Associated with Healthy and Diseased Reef Coral Mussismilia hispida from Eastern Brazil. Microb Ecol. 59:658-667, (2010).
· CHAN-BLANCO Y., VAILLANT F., PEREZ A. M., REYNES, M. BRILLOUET J., BRAT P. J. Foot Comp. Anal. 19:645-654, 2006.
· CHEN YF, YANG PY, HUNG CM, et al. Transplantation of autologous cultured melanocytes for treatment of large segmental vitiligo. J Am Acad Dermatol. 2001; 44:543-5.
· COLLINS, CJ, AND SEDIVY, JM. Involvement of the INK4a ? Arf gene locus in senescence. Aging Cell. 2, 145-150, 2003
· CONKEY,M.C.; ORRENIUS, D.J.S. New York: Cold Spring Harlon, 1992: 227-46.
· DAVIS CD, MILNER JA. Diet and cancer prevention. In: Temple NJ, Wilson T, Jacobs DV, Eds. Nutritional Health: Strategies for disease prevention. Humana Press, pp151-171, 2006
· DAVIS CD, MILNER JA. Diet and cancer prevention. In: TEMPLE NJ, WILSON T, JACOBS DV, Eds. Nutritional Health: Strategies for disease prevention. Humana Press, pp151-171, 2006
· DAVIS, C. D. Exp Biol Med.; 232:176-183, (2007).
· DAVIS, CD. Nutritional Interactions: Credentialing of Molecular Targets for Cancer Prevention. Exp Biol Med. 232:176-183, 2007
· DECHO, A. W. E KAWAGUCHI, T. Biotechniques, 27:1246-1252, (1999).
· DENG, Y., LIN, Y. E WU,X. Genes dev.16:33-45, 2002.
· DEWEY, W.C.; LING,C.C.; MEYN, R.E. International Journal of Radiation Oncolology Biology Physics 33: 781-96, (1995).
· DING,JL.,FUNG, FMY., NG, GWS and CHOU, L.M.Novel Bioactivities from a Coral, Galaxea fascicularis: DNase-like Activity and Apoptotic Activity Against a Multiple-Drug-Resistant Leukemia Cell Line. Mar. Biotechnol. 1, 328-336, (1999).
· EIZIRIK, D.L. Endocrinology 145 (11): 5087-5096, (2004).
· ENGLUND, K. ET AL. Journal of Clinical Endocrinology and Metabolism, Vol. 83, No. 11, 1998
· FADOK, V.A.; HENSON, P.M. Current Biology 13: R655-R657, (2003).
· FAN et al. Chinese agricultural Chem. Soc., 5: 540-551, 1997.
· FAURI CALEFI, JÁ., DIEHL, ED.,CARTELLI, A., BAKOS,L.,EDELWEISS, MIA. A proteína p16 e o melanoma cutâneo. Revista da AMRIGS, Porto Alegre, 54 (1): 81-91, jan.-mar. (2010).
· FRESHNEY RI. Culture of tumor tissue. In:Culture of animal cells. 3ed. Wiley-Liss Inc;. p 449-56, (1994).
· FULDA, S., WICK,W., WELLER, M. E DEBATIN, K.M. Nat. Med. 8:808-815, 2002.
· FUNG, FMY; DING, JL. A novel antitumour compound from the mucus of a coral, Galaxea fascicularis, inhibits topoisomerase I and II. Toxicon, Vol: 36, nº 7, pag: 1053-1058 (1998).
· GERNER RE, KITAMURA H, MOORE GE. Studies of tumor cells lines derived from patients with malignant melanoma. Oncology. 31:31-43, (1975).
· GRIVICICH, I; REGNER, A; ROCHA, AB. Morte celular por apoptose. Rev Bras de Cancerologia. 53 (3): 335-343 (2007).
· HABERLAND M, MONTGOMERY RL, OLSON EN. The many roles of histone deacetylases in development and physiology: implications for disease and therapy. Nat Rev Genet. 10(January (1)):32-42, 2009
· HO, C. K.; Huang, Y. L.; Chen, C. C. Planta Med. 2002, 68, 975.
· http://www.inca.gov.br/estimativa/2010/estimativa20091201. BRASIL. Ministério da Saúde. Instituto Nacional de Câncer. Estimativa 2010: incidência de câncer no Brasil. Rio de Janeiro, 2009.Acesso 15. Abril. (2011).
· http://www2.inca.gov.br/wps/wcm/connect/tiposdecancer/site/home/pele melanoma/definicao acesso em maio 2011).
· HUNOT, S.; FLAVELL, R.A. Science. 292 (5518): 865-866, (2001).
· ISSA JP, KANTARJIAN HM. Targeting DNA methylation. Clin Cancer Res. 15 (June (12)):3938-46, 2009
· JAENISCH R, BIRD A. Epigenetic regulation of gene expression: how the genome integrates intrinsic and environmental signals. Nat Genet. March (33 Suppl):245-54, 2003
· JATKAR, AA., BROWN, BE., BYTHELL, J.C.,GUPPY, R., MORRIS, NJ., PEARSONS, JP. Coral Mucus: The Properties of Its Constituent Mucins. School of Biology and School of Biomedical Sciences and Institute. Biomacromolecules, 11, 883-888, 2010.
· JOHNSTON, I. S and F. ROHWER. Microbial landscapes on the outer tissue surfaces of the reef-building coral Porites compressa. Coral Reefs 26:375-383,(2007).

· KERR JFR, SEARLE J. VIRCHOWS. Arch (Cell Pathol) .1973; 13:87-102.
· KERR, JF, WINTERFORD, CM; HARMON, BV. Cancer 73 (8): 2013-2026, (1994).
· KEUM YS, JEONG WS, KONG AN. Chemoprevention by isothiocyanates and their underlying molecular signaling mechanisms. Mutat Res 555: 191-202, 2004
· LACY, PE. and KOSTIANOVSKY, M. Diabetes. 16: 35-39, (1967).
· LAZAR, D.F.; SALTIEL, A.R. Nature reviews drug discovery 5 (4): 333-342, (2006).
· LI MX, LI NQ, GU ZN, ZHOU XH, SUN YL, WU YQ. Talanta. 1998 Aug;46(5):993-7.
· LIANG, CH. et al. Extracts from Cladiella australis, Clavularia viridis and Klyxum simplex (soft corals) are capable of inhibiting of Growth of Human Oral Squamous Cell Carcinoma Cells. Marine Drugs (6): 595-606 , (2008).
· LINK A, BALAGUER F, GOEL A. Cancer chemoprevention by dietary polyphenols: Promising role for epigenetics. Biochemical Pharmacology (80) 1771-1792, 2010
· LOCKSIN, R.A.; ZAKERI, Z. Nature Reviews Molecular Cell Biology 2 (7): 545-550, (2001).
· LYNDA CHIN, LEVI A. GARRAWAY and DAVID E. FISHER. Malignant melanoma: genetics and therapeutics in the genomic. Genes & Dev. 20: 2149-2182, (2006).
· MATSUMOTO, K.; Akao, Y.; Kobayashi, E.; Ohguchi, K.; Ito, T.; Tanaka, T.; Iinuma, M.; Nozawa, Y. J. Nat. Prod. 2003, 66, 1124.
· MATSUMOTO, K.; YUKIHIRO AKAO; HONG YI.; KENJI OHGUCHI.; TETSURO ITO.; TOSHIYUKI TANAKA; EMI KOBAYASHI.; Munekazu Iinumac and Yoshinori Nozawaa. Preferential target is mitochondria in alfa-mangostin-induced apoptosis in human leukemia HL60 cells. Bioorganic & Medicinal Chemistry. 12 (2004) 5799-5806.
· MCCONKEY, D.J.; JONDAL, M.; ORRENIUS, S. Seminars in Immunology 4 (6): 371-377, (1992).
· MERÉTIKA, A. H. C. PERONI, N. HANAZAKI, N. Acta bot. bras., 24: 386-394, 2010.
· MURPHY, K.M.; STREIPS, U.N.; LOCK, R.B. Oncogene 8144: 5991-5999, (1999).
· MURRAY MR, STOUT AP. The classification and diagnosis of human tumors by tissue culture methods. Text Rep Biol Med. 12:898-915, (1954).
· NAKAGAWA, Y.; IINUMA, M.; NAOE, T.; NOZAWA, Y. AND AKAO, Y. Characterized mechanism of a-mangostin-induced cell death: Caspase-independent apoptosis with release of endonuclease-G from mitochondria and increased miR-143 expression in human colorectal cancer DLD-1 cells. Bioorganic & Medicinal Chemistry 15 (2007) - 5620-5628.
· NASCIMENTO, V. E. ; MARTINS, A. B. G.; HOJO, R. H. Caracterização física e química de frutos de mamey. Revista Brasileira de Fruticultura, Jaboticabal - SP, v. 30, n. 4, p. 953- 957, Dezembro 2008.
· NYSTRÖM M, MUTANEN M. Diet and epigenetics in colon câncer. World J Gastroenterol January 21; 15(3): 257-263, 2009
· O´SHEA,J.D., HAY, M.F., GRAN, D.J. J Reprod Fertil 1978; 54:183-7.
· OJOPI, E.P.B., NETO, E.D. Genes e Câncer. Biotecnologia Ciência & Desenvolvimento; nº 27, (2002).
· OLIVEIRA PA, COLAÇO A, CHAVES R, GUEDES-PINTO H, LUIS F. DE-LA-CRUZ LFP, LOPES C. Chemical carcinagenesis. Anais da Academia Brasileira de Ciências.79 (4): 593-616, 2007
· Oliveira, AF., Gragnani A., OLIVEIRA FILHO, RS., ABRANCHES OLIVEIRA, ID., FRANÇA, SG., SIMÕES, MM., ENOKIHARA, S., FERREIRA, LM.Modelo experimental de cultura primária de melanoma metastático por punção aspirativa de agulha fina. Acta Cirúrgica Brasileira - Vol 20 (5) (2005).· OLIVEIRA, AF., SANTOS, IDAO., TUCUNDUVA, TCM., SANCHES LG., ; OLIVEIRA FILHO RS., ENOKIHARA MMSS., FERREIRA LM. Sentinel lymph node biopsy in cutaneous melanoma. Acta Cirurgica Brasileira. 22: 332-336 (2007).
· PAROLIN, M.B.; REASON, I.J.M. Arquivos de Gastroenterologia 38 (2): 138-144, (2001).
· POLSTER, B.M., KINNALLY, K.W., FISKUM, G. J Biol Chem 1:2001
· QIN, Z.H., WANG, Y., KIKLY, K.K., SAPP, E. KEGEL, K.B., ARONIM, N. E DIFIGLIA, M. J Biol Chem, Vol.276, N° 11, 2001
· REIS, A.MM. ARAÚJO JR, S.D.,MOURA, RL., FRANCINI-FILHO, RB.,PAPPAS JR, G. COLEHO, AMA., KRÜGER, R.H. AND THOMPSON, F.L.Bacterial diversity associated with the Brazilian endemic reef coral Mussismilia braziliensis. Brazil Journal of Applied Microbiology, (2009).
· RICCI, J.E., GOTTLIEV, R.A., GREEN, D.R. The journal of cell biology. v 160, number 1, 2003.
· RICHARDS HW, MEDRANO EE: Epigenetic marks in melanoma. Pigment Cell Melanoma Res. 22:14-29, 2009
· RIKER AI, PANELLI MC, KAMMULA US, WANG E, WUNDERLICH J, ABATI A, FETSCH P, ROSEMBERG SA e MARINCOLA FM. Development and characterization of melanoma cells lines established by fine-needle aspiration biopsy: advances in the monitoring of

patients with metastatic melanoma. Cancer Detect Prev.; 23(5):387-96, (1999).
· ROCCO, JW, SIDRANSKY, D. p16(MTS-1 ? CDKN2 ? INK4a) in cancer progression. Exp. Cell Res. 264, 42-55, 2001
· RUBINFELD, B., P. ROBBINS, M. EL-GAMIL, I. ALBERT, E. PORFIRI & P. POLAKIS. Stablization of beta-catenin by genetic defects in melanoma cell lines. Science (1997).
· SANTOS, H. B.; MODESTO-FILHO, J.; DINIZ, M. F. F. M.;VASCONCELOS, T. H. C.; PEREIRA, F. S. B.; RAMALHO, J. A.; DANTAS, J. G.; SANTOS E. B. Rev.. Brasil. de Farmacognosia, 18: 70-76, 2008.
· SCAFFIDI, C.S., FULDA, A.F, SRIVASAN, C., FRIESEN, F., LI, K.J., TOMASELLI, K.M., DEBATIN, P.H., KRAMMER, M.E. Embo j. 17:1675-1687,1998.
· SELLINS KS, COHEN J.J. J. Immunol 1987;139:3199-206.
· SHERR, CJ. The ink4a ? arf network in tumour suppression. Nat. Rev. Mol. Cell Biol. 2, 731-737, 2001
· SHIMIZU, S.I., KONISH, A., KODAMA, T., TSUJIMOTO, Y. Proc. Natl Acad Sci Usa 97(7): 3100-5, 2000.
· SIGALOTTI, L. et al. Epigenetics of human cutaneous melanoma: setting the stage for new therapeutic strategies. Journal of Translation Medicine. 8:56, (2010).
· SMITH, C.L. E YOULE, R.J. Dev. Cell 1:515-525, 2001.
· SURH YJ. Cancer chemoprevention with dietary phytochemicals. Nat Rev Câncer. 3:768-780, 2003
· SURH, Y. J. Nat. Rev. Cancer. 2003, 3,768.
· SUSIN, S.A., LORENZO, H.K. ZAMZAMI,N., MARZO, I., SNOW, B.E., BROTHERS, G.M., MANEION, J., JACOTOT, E., COSTANTIN, P., LOEFFLER,M., LAROCHETTE, N., GOODLETT, D.R., AEBERSOLD, R. SIDEROVSKI, D.P. PENNINGER, J.M., KROEMER, G. Nature. 397:441-6,1999.
· SVETOMIR N. MARKOVIC (MD, PhD). Malignant Melanoma in the 21st Century, Part 1: Epidemiology, Risk Factors, Screening, Prevention, and Diagnosis, (2000).
· TAPIERO, H.; TEW, KD.; BA, G.D.; MATHE, G. Biomedicine Pharmacotherapy 56 (4): 200-207, 2002.
· VAN OOSTVELDT, K.; DOSOGNE, H.; BURVENICH, C.; PAAPE, MJ, BROCHEZ, V.; VAN DEN E.E. Veterinary Immunology and Immunopathology 70 (1-2): 125-133, (1999).
· VIEIRA NETO, R.D. (Ed.) Frutíferas potenciais para os tabuleiros costeiros e baixadas litorâneas. Aracajú: Embrapa Tabuleiros Costeiros/Empresa de Desenvolvimento Agropecuário de Sergipe - Emdagro, 2002. 216p.
· WANG M. Y., WEST B., JENSEN C. J. NOWICHI D. SU, C. PALU, A. K. ANDERSON G. Acta Pharmacol. Sin. 23: 1127-1141, 2002.
· YIN, X.M., WANG,K., GROSS,A., ZHO, Y., ZINKEL, S., KLOCCKE, B., ROTH, K.A. E KORSMEYER, S.J. Nature. 400:886-891, 1999.

Parecer pessoal do(s) investigador(es) quanto aos riscos, desconfortos, vantagens, desvantagens e os métodos adotados para proteçãodo voluntário:

Os pacientes que serão incluidos no estudo necessitam da realização da cirurgia para retirada dos linfonodos metastaticos. O material para pesquisa sera coletado apos anestesia do pacientes, portanto o mesmo nao sera submetido a maior desconforto ou risco devido a coleta do material

Descrição sobre o uso e destinação dos dados e/ou material coletado ao final do estudo:

O material coletado e os resultados serao utilizados somente para divulgacao cientifica atraves de publicacao em revista cientifica e em congressos cientificos

Orçamento detalhado da Pesquisa (atendendo letra J do parágrafo VI.2 da resolução 196/96)

Amostra processada pela equipe:

Nº estimado de pacientes a serem triados:

Nº consultas

Exames laboratoriais

Enfermeiro do protocolo fará coleta:

Quantidade de coletas de amostra:

Diárias de internação:	**Real**	**Estimado**
Tempo em Enfermaria:		
Tempo em UTI:		
Tempo no Hospital:		

O estudo envolve a realiazação de exame laboratorial?

O estudo envolve a realização de exame por imagem?

O estudo envolve a realização de procedimento médico?

Custos

Material Consumo (Nacional)
Descrição do item: papel sulfite
Quantidade: 03 (500 folhas) Valor(unitário): 15 Total: R$ 45,00

Material Consumo (Nacional)
Descrição do item: cartucho tinta para impressora
Quantidade: 02 Valor(unitário): 100 Total: R$ 200,00

Material Consumo (Nacional)
Descrição do item: canetas
Quantidade: 02 caixas Valor(unitário): 10 Total: R$ 20,00

Total Geral: R$ 265,00

Adipose-derived stem cells (ADSC) in the viability of random skin flap in rats[1]

Caio Vinicius Suartz[I], Silvana Gaiba[II], Jerônimo Pereira de França[III], Antonio Carlos Aloise[II], Lydia Masako Ferreira[IV]

DOI: http://dx.doi.org/10.1590/S0102-86502014001400002

[I]Graduate Student, Department of Surgery Federal University of São Paulo, São Paulo, SP, Brazil. Technical procedures.
[II]PhD Plastic Surgery Division, Department of Surgery Federal University of Sao Paulo, São Paulo, SP, Brazil. Technical procedures, acquisition and interpretation of data, manuscript writing.
[III]PhD, Associate Professor, Department of Biological Sciences, Universidade Estadual de Santa Cruz, Ilhéus-BA, Brazil. Interpretation of data and critical revision.
[IV]Head and Full Professor, Plastic Surgery Division, UNIFESP, Researcher 1A-CNPq, Director Medicine III-CAPES, Sao Paulo-SP, Brazil. Scientific and intellectual content of the study, interpretation of data and critical revision.

ABSTRACT

Purpose: To evaluate the effects of the adipose-derived stem cells (ADSC) in the viability of random skin flap in rats.

Methods: Thirty five adult male Wistar rats (weight 250–300 g) were used. ADSC were isolated from adult male rats (n=5). ADSC were separated, cultured and then analyzed. A dorsal skin flap measuring 10x4 cm was raised and a plastic barrier was placed between the flap and its bed. After the surgical procedure, the animals were randomized into two groups (n=15 each group), group control and group ADSC. In all groups the procedures were performed immediately after the surgery. The percentage of flap necrosis was measured on the seventh postoperative day.

Results: The ADSC were able to replicate in our culture conditions. We also induced their adipogenic, osteogenic and chondrogenic differentiation, verifying their mesenchymal stem cells potentiality *in vitro.* The results were statistically significant showing that the ADSC decreased the area of necrosis ($p<0.05$).

Conclusion: The cells demonstrated adipogenic, osteogenic and chondrogenic differentiation potential *in vitro.* The administration of adipose-derived stem cells was effective to increase the viability of the random skin flaps in rats.

Key words: Surgical Flaps; Rats; Adult Stem Cells; Stem Cells; Adipose Tissue

Introduction

The stem cells are characterized by their undifferentiated state and their ability to not only generate new stem cells but also specialized cells with different functions. Stem cells can be embryonic or adult[1]. Stem cells derived from adipose tissue are the pluripotent type. In this case these cells can differentiate into osteocytes, chondrocytes, adipocytes, muscle cells, neural and angiogenic lineages[1,2].

The beginning of the study of stem cells occurred to the researchers Ernest McCulloch and James Till at the Ontario Cancer Institute in Toronto. Their research reported on the presence of self-renewing cells in bone marrow of mice, and these cells were postulated as regenerative stem cells[3,4].

In 2001 stem cells derived from adipose tissue (ADSC) were added to the group of adult stem, showing that they are able to differentiate into mesodermal cells (adipocytes, chondrocytes, osteocytes, and myocytes)[1].

Nowadays it is known that the ADSCs have the ability to form consistent cells as neurons[5], Oligodendrocytes[6], Schwann cells[7,8] and epidermal cell lineage[9].

The clinical use of this cell type may vary from angiogenesis and neurogenesis stimulation in spinal cord injury[10] to the suppression of the inflammatory response, oxidative stress, and apoptosis in rodent models of ischemia and reperfusion[11].

The partial necrosis of the skin flaps remains a significant problem in plastic surgery. Recent studies on addition of stem cells from adipose tissue in subcutaneous tissue of rats demonstrate increased vascularity and viability of skin flaps[12,13]. The aim of this study was to evaluate the effects of adipose-derived stem cells on the viability of random skin flap in rats.

Methods

This project was approved by the Ethics Committee of UNIFESP - CEUA N 251501. Animals (250g–300 g) were anesthetized with an intraperitoneal injection of 60 mg/kg of ketamine and 5 mg/kg xylazine. The dorsal random skin flap, measuring 10X4 cm, following experimental model proposed by[14] was raised from the deep fascia, including the superficial fascia, *panniculus carnosus*, subcutaneous tissue, and skin. After flap elevation, a plastic barrier (polyester/polyethylene), with the same dimensions (10X4 cm) was placed between the skin flap and its bed. The flap was then sutured back in place with simple 4-0 nylon sutures. Subsequently, $5X10^6$ ADSC in PBS (0.5 mL) were slowly injected into the caudal vein over 3 min using a insulin syringe in the group experimental. Control group of animals received only 0.5 mL of PBS.

Macroscopic analysis of necrosis percentages

The percentage of skin flap necrosis was measured on the seventh postoperative day, using the paper template method described by[15]. After anesthesia, each flap's limit between viable skin and necrosis was delineated with a pen. The viable tissue limit has been characterized by soft skin, pink, warm and haired, and necrotic tissue by stiff, dark cool, and hairless skin.

Isolation, culture and expansion of ADSC

ADSC were isolated from adult male Wistar rats (weight 250 – 300 g, n = 5). Rat adipose tissue from inguinal region was enzymatically dissociated for 30 min at 37 °C by 0.1 % (w/v) collagenase type I (Sigma-Aldrich). After centrifugation, the stromal cell pellet was resuspended in Dulbecco's Modified Eagle's Medium/Nutrient Mixture F-12 Ham (DMEM/F12) (Sigma-Aldrich) supplemented with 10% Fetal Bovine Serum (FBS) (Cultilab, Campinas-SP, Brazil), 100 U/ml penicillin (Sigma-Aldrich) and 0.1 mg/ml streptomycin (Sigma-Aldrich). The culture was maintained at 37ºC in humidified atmosphere of 95% O2 and 5% CO2 and passages with trypsin/EDTA (Gibco) when required. Cells at passage 3 or below were used for experimentation.

Differentiation assays

Differentiation assays was done according to the method described by Gaiba et al 2012. Osteogenic, adipogenic and chondrogenic differentiation were performed to ascertain multipotency of isolated cells. The cells cultured in differentiation media for 21 days. After that, the cultures were stained by a solution of Alizarin, Oil Red O and Toluidine Blue for osteogenic, adipogenic and chondrogenic differentiation, respectively. The fixed and dyed cells were observed using Nikon Ti-U optical microscope and photographed using the NIS-Elements - 3.2 Software (Nikon Instruments INC, New York).

Statistical analysis

The results are expressed as mean ± SD. Comparison between two means was performed by unpaired Student's t-test. All data were analyzed using GraphPad Prism 3.0 software. Statistically significance was accepted when $P<0.05$.

Results

Macroscopic analysis of necrosis percentages

The regions of survival and necrosis were clearly demarcated in every flap at 7th day post operation. Figure 1 presents means and distribution of data obtained for percentages of flap viability in the groups. The percentages of viability area (mean ± standard deviation) in the ADSC and control groups were (58.14 ± 4.460)% and (38.86 ± 5.021)%, respectively.

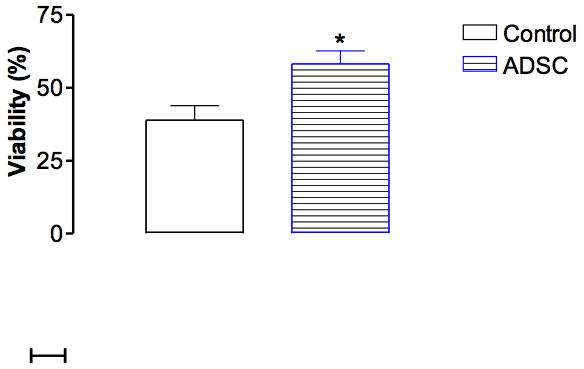

FIGURE 1 - Distribution of the percentage of viability area of the groups. These values were analyzed using unpaired Student's t test and statistical significance was obtained ($p < 0.05$).

Isolation, culture and expansion of ADSC

Upon applying multilineage differentiation (adipogenic, osteogeneic and chondrogenic) the cells showed accumulated intracellular lipid droplets as revealed by Oil Red O staining (Figure 2A) and displayed extracellular calcium precipitates, which were identified by Alizarin red staining (Figure 2B) and Chondrogenic differentiation demonstrated by Toluidin blue stain (Figure 2C). Indicates that these cells can differentiate into adipocytes, osteoblasts and chondroblasts.

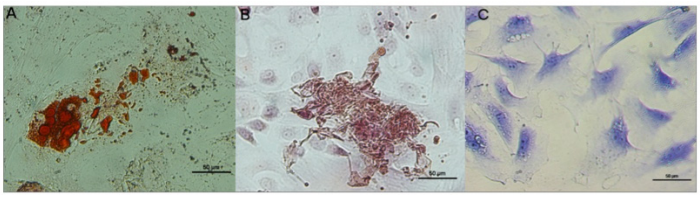

FIGURE 2 - Multilineage differentiation. ADSC are typical fibroblast-like cells with fusiform shape. (**A**) Adipogenic differentiation demonstrated by Oil Red O staining after 21 days (positive intracellular lipid droplets). (**B**) Osteogenic differentiation demonstrated by Alizarin red stain after 21 days induction (positive staining of calcium nodule formation). (**C**) Chondrogenic differentiation demonstrated by Toluidin blue stain 21 days induction.

Discussion

The use of ADSCs capable of differentiate into mesodermal cells is made since 2001[1]. Their applicability in experimental models is increasing and it is approaching clinical practice[16].

In plastic surgery this type of cell has also been studied and increasingly used, for example, to increase the success rate of viability in the grafts[17] and small defects in fat grafting[18]. Studies have been done in rats comparing qualitatively peritoneal and inguinal region tissues[18], however there are no studies that quantitatively compare the number of ADSC in these regions. Thus, interpreting the results we can infer that the number of stem cells in the inguinal region predominates over the peritoneal region (data not shown).

The peritoneal fat, have lower gain of adipose tissue mass compared to lower regions of the body, as the inguinal region, due to a protective mechanism that aims to reduce the metabolic consequences of weight gain[19]. The statistically significant results comparing both collected areas directs the ADSC extraction from the inguinal region, ensuring greater concentration of cells collected in comparision to the peritoneal region, which in turn can be useful in designing future studies aimed at testing the properties of ADSC, as done in this work, which envisaged its closest application to clinical practice.

Regarding the clinical applicability of stem cells, the cutaneous flap is a common and valuable procedure in plastic surgery, such as the repair of retractions of burns and reconstructions after oncologic resections. However, there are factors such as ischemia and necrosis, which may damage its development, justifying the need to investigate possibilities to reduce these risks and increase the viability of the flap[20-24].

Studies with models of grafts[25], and flaps[26] using the inguinal region ADSC showed increased viability of the necrotic area, however the route of administration of ADSC was subcutaneously. In the present study, the route of administration was intravenous, finding similar results to those mentioned, which show an increase in flap viability with the use of ADSC.

The statistically significant results regarding the use of ADSC from the inguinal region, decreasing skin flap necrosis, contribute to approximate the experimental use to clinical practice. However, further studies are needed to complement these results, such as the realization of immunohistochemical markers seeking whether there is an increased local vascularization of the flap and the presence of stem cells applied in the flap area.

Conclusion

The cells demonstrated adipogenic, osteogenic and chondrogenic differentiation potential *in vitro.* The administration of adipose-derived stem cells was effective to increase the viability of the random skin flaps in rats.

References

1. Zuk PA, Zhu M, Mizuno H, Huang J, Futrell JW, Katz AJ, Benhaim P, Lorenz HP, Hedrick MH. Multilineage cells from human adipose tissue: implications for cell-based therapies. Tissue Eng. 2001 Apr;7(2):211-28.
2. Planat-Benard V, Silvestre JS, Cousin B, André M, Nibbelink M, Tamarat R, Clergue M, Manneville C, Saillan-Barreau C, Duriez M, Tedgui A, Levy B, Pénicaud L, Casteilla L. Plasticity of human adipose lineage cells toward endothelial cells: physiological and therapeutic perspectives. Circulation. 2004 Feb 10;109(5):656-63.
3. Becker AJ, McCulloch EA, Till JE. Cytological demonstration of the clonal nature of spleen colonies derived from transplanted mouse marrow cells. Nature. 1963 Feb 2;197:452-4.
4. Zhang J, Shehabeldin A, da Cruz LA, Butler J, Somani AK, McGavin M, Kozieradzki I, dos Santos AO, Nagy A, Grinstein S, Penninger JM, Siminovitch KA. Antigen receptor-induced activation and cytoskeletal rearrangement are impaired in Wiskott-Aldrich syndrome protein-deficient lymphocytes. J Exp Med. 1999 Nov 1;190(9):1329-42.
5. Kang SK, Putnam LA, Ylostalo J, Popescu IR, Dufour J, Belousov A, Bunnell BA. Neurogenesis of Rhesus adipose stromal cells. J Cell Sci. 2004 Aug 15;117(Pt 18):4289-99.
6. Safford KM, Safford SD, Gimble JM, Shetty AK, Rice HE. Characterization of neuronal/glial differentiation of murine adipose-derived adult stromal cells. Exp Neurol. 2004 Jun;187(2):319-28.
7. Kingham PJ, Kalbermatten DF, Mahay D, Armstrong SJ, Wiberg M, Terenghi G. Adipose-derived stem cells differentiate into a Schwann cell phenotype and promote neurite outgrowth in vitro. Exp Neurol. 2007 Oct;207(2):267-74.
8. Xu Y, Liu L, Li Y, Zhou C, Xiong F, Liu Z, Gu R, Hou X, Zhang C. Myelin-forming ability of Schwann cell-like cells induced from rat adipose-derived stem cells in vitro. Brain Res. 2008 Nov 6;1239:49-55.
9. Trottier V, Marceau-Fortier G, Germain L, Vincent C, Fradette J. IFATS collection: Using human adipose-derived stem/stromal cells for the production of new skin substitutes. Stem Cells. 2008 Oct;26(10):2713-23.
10. Oh JS, Park IS, Kim KN, Yoon DH, Kim SH, Ha Y. Transplantation of an adipose stem cell cluster in a spinal cord injury. Neuroreport. 2012 Mar 28;23(5):277-82.
11. Reichenberger MA, Heimer S, Schaefer A, Lass U, Gebhard MM, Germann G, Leimer U, Köllensperger E, Mueller W. Adipose derived stem cells protect skin flaps against ischemia-reperfusion injury. Stem Cell Rev. 2012 Sept;8(3):854-62.
12. Yang M, Sheng L, Li H, Weng R, Li QF. Improvement of the skin flap survival with the bone marrow-derived mononuclear cells transplantation in a rat model. Microsurgery. 2010 May;30(4):275-81.
13. Lee DW, Jeon YR, Cho EJ, Kang JH, Lew DH. Optimal administration routes for adipose-derived stem cells therapy in ischaemic flaps. J Tissue Eng Regen Med. 2014 Aug;8(8):596-603.
14. MCFarlane RM, Deyoung G, Henry RA. The design of a pedicle flap in the rat to study necrosis and its prevention. Plast Reconstr Surg. 1965 Feb;35:177-82.
15. Sasaki GH, Pang CY. Hemodynamics and viability of acute neurovascular island skin flaps in rats. Plast Reconstr Surg. 1980 Feb;65(2):152-8.
16. Wei X, Yang X, Han ZP, Qu FF, Shao L, Shi YF. Mesenchymal stem cells: a new trend for cell therapy. Acta Pharmacol Sin. 2013 Jun;34(6):747-54.
17. Beahm EK, Walton RL, Patrick CW Jr. Progress in adipose tissue construct development. Clin Plast Surg. 2003 Oct;30(4):547-58.
18. DiGirolamo M, Fine JB, Tagra K, Rossmanith R. Qualitative regional differences in adipose tissue growth and cellularity in male Wistar rats fed ad libitum. Am J Physiol. 1998 May;274(5 Pt 2):R1460-7.
19. Tchoukalova YD, Koutsari C, Votruba SB, Tchkonia T, Giorgadze N, Thomou T, Kirkland JL, Jensen MD. Sex- and depot-dependent differences in adipogenesis in normal-weight humans. Obesity (Silver Spring). 2010 Oct;18(10):1875-80.
20. Harder Y, Amon M, Erni D, Menger MD. Evolution of ischemic tissue injury in a random pattern flap: a new mouse model using intravital microscopy. J Surg Res. 2004 Oct;121(2):197-205.
21. Abla LE, Gomes HC, Percario S, Ferreira LM. Acetylcysteine in random skin flap in rats. Acta Cir Bras. 2005 Mar-Apr;20(2):121-3.
22. Liebano RE, Abla LE, Ferreira LM. Effect of low-frequency transcutaneous electrical nerve stimulation (TENS) on the viability of ischemic skin flaps in the rat: an amplitude study. Wound Repair Regen. 2008 Jan-Feb;16(1):65-9.
23. Tacani PM, Liebano RE, Pinfildi CE, Gomes HC, Arias VE, Ferreira LM. Mechanical stimulation improves survival in random-pattern skin flaps in rats. Ultrasound Med Biol. 2010 Dec;36(12):2048-56.
24. Nishioka MA, Pinfildi CE, Sheliga TR, Arias VE, Gomes HC, Ferreira LM. LED (660 nm) and laser (670 nm) use on skin flap viability: angiogenesis and mast cells on transition line. Lasers Med Sci. 2012 Sept;27(5):1045-50.
25. Zografou A, Papadopoulos O, Tsigris C, Kavantzas N, Michalopoulos E, Chatzistamatiou T, Papassavas A, Stavropoulou-Gioka C, Dontas I, Perrea D. Autologous transplantation of adipose-derived stem cells enhances skin graft survival and wound healing in diabetic rats. Ann Plast Surg. 2013 Aug;71(2):225-32.
26. Yue Y, Zhang P, Liu D, Yang JF, Nie C, Yang D. Hypoxia preconditioning enhances the viability of ADSCs to increase the survival rate of ischemic skin flaps in rats. Aesthetic Plast Surg. 2013 Feb;37(1):159-70.

Correspondence:
Lydia Masako Ferreira
Disciplina de Cirurgia Plástica-UNIFESP
Rua Napoleão de Barros, 715/4º andar
04042-002 Sao Paulo - SP Brasil
Tel.: (55 11)5576-4118
Fax: (55 11)5571-6579
sandra.dcir@epm.br
silvanagaiba@gmail.com

Financial sources: CAPES, CNPq (nº 312356/2009-9)

[1]Research performed at Plastic Surgery Division, Federal University of Sao Paulo (UNIFESP), Brazil.

Analysis of polymorphisms in codons 11, 72 and 248 of *TP53* in Brazilian women with breast cancer

B.C. Almeida[1], J.P.F.O. Kleine[1], C.M. Camargo-Kosugi[1,2], M.R. Lisboa[1], C.N. França[3], J.P. França[4] and I.D.C.G. Silva[1]

[1]Laboratório de Ginecologia Molecular e Proteômica, Departamento de Ginecologia, Universidade Federal de São Paulo, São Paulo, SP, Brasil
[2]Centro de Pesquisa Translacional, Departamento de Otorrinolaringologia e Cirurgia de Cabeça e Pescoço, Universidade Federal de São Paulo, São Paulo, SP, Brasil
[3]Departamento de Lípides, Aterosclerose e Biologia Vascular, Universidade Federal de São Paulo, São Paulo, SP, Brasil
[4]Laboratório de Biofísica Celular e Molecular, Departamento de Ciências Biológicas, Universidade Estadual de Santa Cruz, Ilhéus, BA, Brasil

Corresponding author: B.C. Almeida
E-mail: bruc_10@hotmail.com

Genet. Mol. Res. 15 (1): gmr.15017055
Received June 23, 2015
Accepted October 26, 2015
Published February 19, 2016
DOI http://dx.doi.org/10.4238/gmr.15017055

ABSTRACT. The association between *TP*53 gene polymorphisms and breast cancer (BC) in Brazilian women is a controversial topic. In this cross-sectional study, we evaluated the association between clinical pathological variables and three polymorphisms (*TP53**11, *TP53**72, and *TP53**248) in BC patients and controls. Genomic DNA was extracted from the blood cells of 393 participants; the cancer-free control subjects were 26-72 years old (41 ± 11.03) and the BC patients were 28-80 years old (51 ± 10.70). We used standard polymerase chain reaction-restriction fragment length polymorphism and confirmed the results by genetic sequencing. In *TP53**11, there was 100% homozygous Glu distribution in both groups.

*TP53**72 showed genotypic distribution: in the control group, there was 16.10% homozygous Pro, and 42.44% heterozygous and 41.46% homozygous Arg; in the BC group, there was 15.43% homozygous Pro, and 42.55% heterozygous and 42.02% homozygous Arg. The relative frequency of each allele was 0.37% for Pro and 0.63% for Arg in the control group, and 0.37% for Pro and 0.63% for Arg in the BC group. The nuclear grade (P = 0.0084) and adapted histological grade (P = 0.0265) were associated with *TP53**72. The distribution of the codon 72 genotypes did not deviate from Hardy-Weinberg equilibrium in either group. In *TP53**248, there was 100% homozygous Arg distribution in both groups. In codon 72, the Arg allele is the most prevalent in Brazilian women. *TP53**72 may be associated with susceptibility to BC, although more studies are required to evaluate the profile of Brazilian women with BC.

Key words: Breast cancer; Restriction enzymes; TP53; p53 protein; SNP; Brazilian women

INTRODUCTION

Breast cancer (BC) is a non-cutaneous, multifactorial, heterogeneous disease. It has many subtypes with distinct biological features that are driven by numerous underlying molecular alterations, and can exhibit different potentials for recurrence and distant metastasis (Yersal and Barutca, 2014). Mutations of the *TP53* gene are the most common genetic alterations in BC, accounting for 30% of the cases. However, some of the molecular subtypes of BC have higher levels of alteration. Some types of alteration are clearly linked to higher frequency of substitutions, resulting in the production of p53 protein with potential new functions, such as p63 and p73 inactivation. Notably, molecular apocrine and basal-like tumors present a much higher frequency of complex mutations (deletions/insertions) that often lead to a lack of p53 protein (Bertheau et al., 2013).

The p53 protein plays an important role in cell-cycle regulation and maintenance of genome stability by preventing mutations (Stojnev et al., 2010), and the most prominent property of p53 as a protein is its action as a transcription factor (Levine and Oren, 2009). The response to stress occurs through the induction of p53, which essentially happens by post-translational modifications resulting in protein stabilization (by escape from proteasome-mediated degradation), and in conformational changes that increase the affinity of p53 for specific DNA sequences. This pathway regulates the transcription of target genes or interacts with heterologous factors to mediate negative regulation of cell-cycle progression and induction of apoptosis. Cell-cycle arrest is controlled by transcriptional modulation of p53-transactivated genes such as *CDKN1A* and *GADD45.* Induction of apoptosis involves both transcription-dependent and -independent mechanisms. Pro-apoptotic transcriptional targets of p53 include *PUMA*, *BAX*, and *FAS/CD95* (Méplan et al., 2000; de Moura Gallo et al., 2005). p53 also interacts with numerous cellular proteins, and these molecular interaction might contribute to the inhibitory role of p53 in tumorigenesis (Whibley et al., 2009).

TP53 mutations are found in all exons of the gene, but the mutation located at codon 11 in exon 2, which encodes the extreme N-terminus, and the mutation of the last codon of exon 11, which encodes the extreme C-terminus, account for only 0.1% of the 15,000 mutations identified. These regions contain important regulatory domains and sites of post-translational modification, which

play an important role in the control of p53 activity. The N-terminus of p53 contains the binding site for mdm2, the main regulator of p53 protein stability, and the C-terminus participates in the regulation of DNA-binding activity (Guimaraes and Hainaut, 2002). The critical region, in which many mutations are recognized, is called the "hotspot"; it has six codons and is detectable in almost all types of cancer (Stojnev et al., 2010). These residues are all located at the DNA-binding surface of the protein and play important roles either in protein-DNA contacts (codons 245, 248, and 273) or in the conformation of the protein (codons 175, 249, and 282) (Guimaraes and Hainaut, 2002; Stojnev et al., 2010). The most widely studied polymorphism in exon 4 is an amino acid residue change, proline/arginine (Pro/Arg), on the reverse strand located at codon 72. The prevalence of the Arg allele ranges from 40 to 80% in tumors (Pim and Banks, 2004). Several studies suggest that the polymorphism described above may have a functional impact. Moreover, it has been shown that the Arg and Pro p53 variants have different half-lives and transcriptional properties *in vitro*. Nevertheless, some researchers have suggested the possibility that the presence of the Arg allele might be linked with a higher susceptibility to cancers associated with human papillomavirus infections (Guimaraes and Hainaut, 2002;Akkiprik et al., 2009), and other cancer types such as lung, hepatocellular, colorectal, and bladder cancer. We used clinical pathological feature analysis to investigate the polymorphisms at codons 11, 72, and 248 by comparing women with BC with healthy women. The analysis of these three polymorphisms may be relevant to the development of BC once the mutations have occurred at important sites of the *TP53* gene. Moreover, identifications of these polymorphisms may be useful for predicting clinical variables in the relatives of the BC patient.

MATERIAL AND METHODS

Study population

The Research Ethics Committee of Universidade Federal de São Paulo UNIFESP/EPM under protocol No. 72.537 approved this study. Prior to commencement, all participants signed an informed consent form. This cross-sectional study included 188 women in whom BC had been surgically and histopathologically confirmed; there were 169 (89.89%) cases of invasive ductal carcinoma, nine cases of invasive lobular carcinoma (4.79%), five cases of *in situ* ductal carcinoma (2.66%); and five cases (2.66%) were not recognized.

Two hundred and five women with no previous history of cancer were assigned to a non-malignant control group. All the women came from the same population, ethnicity, and geographic region.

Genotype assay

Genomic DNA was extracted from the lymphocytes in peripheral blood samples using an Illustra™ blood genomicPrep Spin Kit (GE Healthcare, Piscataway, NJ, USA) according to the manufacturer instructions. The polymerase chain reaction-restriction fragment length polymorphism (PCR-RFLP) conditions used to amplify the fragments containing the *TP53* codons 11 (rs201382018), 72 (rs1042522), and 248 (rs11540652) have been described previously (Camargo-Kosugi et al., 2014), and were adapted in our laboratory.

Briefly, each PCR mixture (25 μL) contained 25 pM each primer, Polymerase Chain Reaction Master Mix - *Taq* DNA polymerase (pH 8.5), dATP, dGTP, dCTP, dTTP and $MgCl_2$

(Promega, Madison, WI, USA), and 50-100 ng genomic DNA, and the volume was completed with Nuclease-Free Water (Promega). The primers amplified fragments of 379 base pairs (bp) in the *TP53**11 codon, 279 bp in the *TP53**72 codon (Figure 1), and 236 bp in the *TP53**248 codon. The amplified PCR samples were analyzed on 2% agarose gel using ethidium bromide staining, followed by treatment of the amplified fragment with an appropriate restriction enzyme. The amplicons of *TP53**11, *TP53**72, and *TP53**248 were digested with *Taq*$^{\alpha}$I, *Bst*UI, and *Hpa*II restriction enzymes (New England BioLabs, Ipswich, MA, USA), respectively. Because the presence or absence of the restriction enzyme recognition site results in the formation of restriction fragments of different sizes, allele identification was achieved by 3% agarose gel electrophoresis analysis (Amersham Pharmacia Biotech model EPS1001, Piscataway, NJ, USA), observation was carried out under UV light, and the images were recorded using a Kodak Digital Science 1D system. The PCR conditions, primer sequences, enzyme digestion temperatures and durations, fragment sizes, and amino acid changes are described in Table 1.

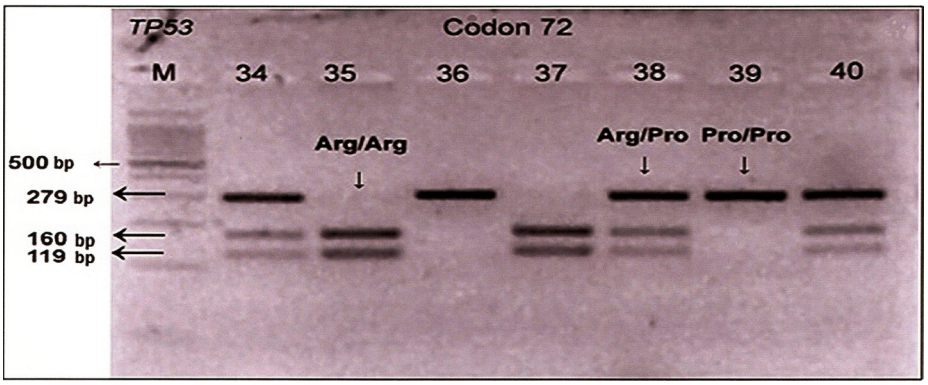

Figure 1. Polymerase chain reaction-restriction fragment length polymorphism (PCR-RFLP) in codon 72 polymorphism, detection of homozygous Pro (Pro/Pro), heterozygous (Pro/Arg), and homozygous Arg (Arg/Arg). *Lane M* = 100-bp ladder.

Table 1. Primers, restriction enzymes, and polymerase chain reaction (PCR) conditions.

Polymorphism (locations)	Primers sequences (5'→3')	Restriction enzyme	SNP sequences	Amino acid	DNA fragments
*TP53**11 rs201382018	F: 5'-CTTGGGTTGTGGTGAAACATTG-3' R: 5'-AGCGAAAATTCATGGGACTGAC-3'	*Taq*$^{\alpha}$I 65°C for 4 h	GAG CAG	Glu Gln	239+140 379
*TP53**72* rs1042522	F: 5'-TCCCCCTTGCCGTCCCAA-3' R: 5'-CGTGCAAGTCACAGACTT-3'	*Bst*UI 60°C for 4 h	CCC CGC	Pro Arg	279 160+119
*TP53**248 rs11540652	F: 5'-TAGGTTGGCTCTGACTGTACCA-3' R: 5'-TGTGATGAGAGGTGGATGGGTA-3'	*Hpa*II 37°C for 4 h	CGG CAG	Arg Gln	164+72 236

PCR conditions (codons 11, 72, and 248)

Initial denaturations (°C/min)	Denaturing (°C/s)	Annealing (°C/s)	Polymerization (°C/min)	Final extension (°C/min)
94/5	40 cycles			72/7
	94/45	58/45	72/1	

*Three fragments with 279, 160, and 119 bp indicates heterozygous (Pro/Arg) SNP = single-nucleotide polymorphism.

Direct sequencing of DNA fragment

Direct sequencing of double-stranded DNA fragments was performed using an Applied Biosystems 3500/3500xL Genetic Analyzer (Applied Biosystems | Hitachi, Foster City, CA, USA), as shown in Figure 2.

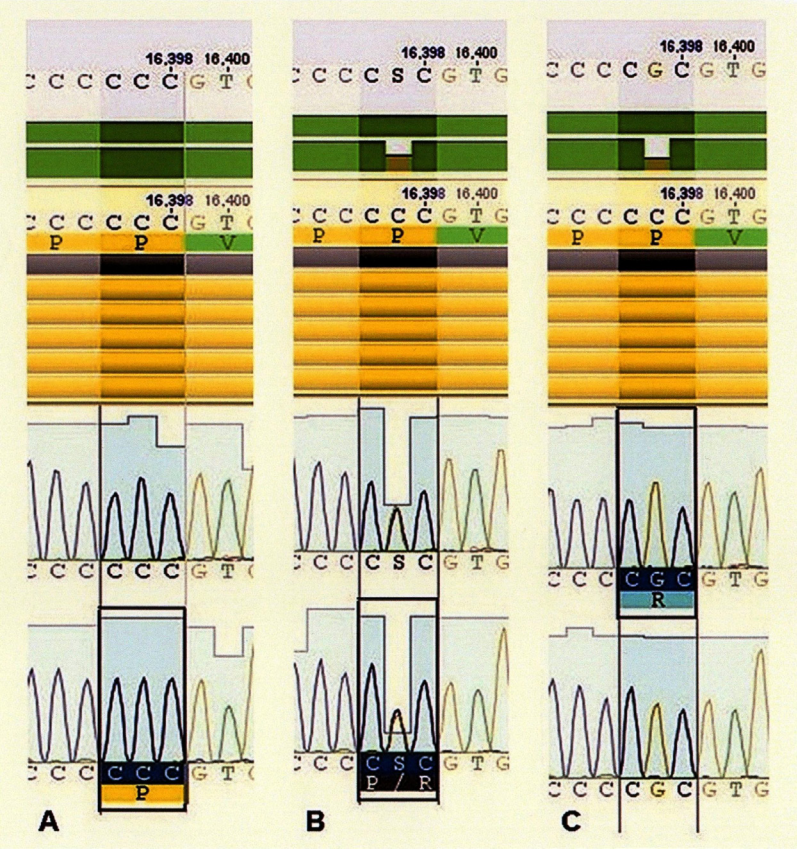

Figure 2. DNA sequencing of codon 72. **A.** Homozygous Pro. **B.** Heterozygous Pro/Arg. **C.** Homozygous Arg.

Statistical analysis

Analyses were performed using the SPSS (v20.0; Chicago, IL, USA) and the GraphPad Prism (v3.0; CA, USA) softwares. The χ^2 test was used to analyze categorical variables and the two-sided unpaired Student *t*-test was used to compare the continuous variable age. The strength of association between each *TP53* polymorphism and cancer risk was evaluated by pooled odds ratios with 95% confidence intervals. The association between independent variables and the development of breast cancer was determined using a logistic regression method. The association between the *TP53* polymorphism and clinical pathological characteristics of the BC was assessed using the χ^2 test. P-values less than 0.05 were considered statistically significant. Hardy-Weinberg equilibrium (HWE) was detected using a goodness-of-fit χ^2 test.

RESULTS

The analysis included 393 women. The cancer-free control subjects were 26-72 years old (mean age 41 ± 11.03) and the BC patients were 28-80 years old (mean age 51 ± 10.70). These values were corrected by logistic regression ($P < 0.0001$).

We did not detect *TP53* codon 11 or 248 polymorphisms in either controls or cases using PCR-RFLP, and we did not find any genetic variations; all samples were homozygous Glu and homozygous Arg for the two codons, respectively. The distribution of the codon 72 genotypes in control and patient groups did not deviate from the HWE. Genotype proportions in the control and case groups are presented in Table 2, with no significant statistical association of the Pro/Pro genotype with BC risk (P = 0.9823). The relative frequency of each allele was 0.37% for Pro and 0.63% for Arg in the control group, and 0.37% for Pro and 0.63% for Arg in the BC group (P = 0.8584). The Arg allele was the most frequent in both groups and showed a higher percentage in more than half of the samples.

Table 2. Distribution of *TP53**72 polymorphism genotypes among breast cancer and control groups.

N (%)		Pro/Pro	Pro/Arg	Arg/Arg	OR[a]	RR	95%CI	P*
Control	205	33 (16.10)	87 (42.44)	85 (41.46)	1.052	1.044	0.6108 to 1.812	0.9823
Case	188	29 (15.43)	80 (42.55)	79 (42.02)				

[a]Adapted odds ratio, Pro/Pro *vs* Arg/Pro and Arg/Arg; *P-value determined by χ^2 test.

The clinical and pathological features of *TP53**72 in the BC patients were analyzed according to genotype, and the results are shown in Table 3; significant differences were observed in the nuclear grade (P = 0.0084). We also analyzed the adapted histological grade, i.e., grade I versus II and III, and a significant difference in the distribution was found between the genotypes for this variable (P = 0.0265).

Table 3. Baseline patient clinicopathological characteristics and corresponding *TP53**72 polymorphism rates in the breast cancer group (N = 188).

Variables	Pro/Pro	Pro/Arg	Arg/Arg	P*	Variables	Pro/Pro	Pro/Arg	Arg/Arg	P*
Age, years					HER2 status				
<35	1 (10)	5 (50)	4 (40)	0.7463	Positive	7 (23.33)	12 (40)	11 (36.67)	0.2128
35-39	0 (0)	5 (71.43)	2 (28.57)		Negative	22 (14.19)	68 (43.87)	65 (41.94)	
40-49	10 (1612)	26 (41.94)	26 (41.94)		Missing	0 (0)	0 (0)	3 (100)	
50-59	11 (16.92)	23 (35.39)	31 (47.69)		Neoadjuvant chemotherapy response				
≥60	7 (15.91)	21 (47.73)	16 (36.36)		No	21 (15.22)	56 (40.58)	61 (44.20)	0.7350
Tumor stage					RP <50%	2 (9.52)	11 (52.38)	8 (38.10)	
T I	3 (13.64)	10 (45.45)	9 (40.91)	0.5569	RP >50%	6 (23.08)	11 (42.31)	9 (34.61)	
T II	12 (15)	28 (35)	40 (50)		Missing	0 (0)	2 (66.67)	1 (33.33)	
T III	13 (17.33)	36 (48)	26 (34.67)		Adjuvant chemotherapy				
T IV	0 (0)	5 (62.50)	3 (37.50)		Yes	25 (14.54)	75 (43.60)	72 (41.86)	0.6069
Missing	1 (33.33)	1 (33.33)	1 (33.33)		No	4 (28.57)	4 (28.57)	6 (42.86)	
Histological grade					Missing	0 (0)	1 (50)	1 (50)	
I	6 (35.29)	8 (47.06)	3 (17.65)	0.0799	Radiotherapy				
II	16 (13.22)	56 (46.28)	49 (40.50)		Yes	24 (16.78)	63 (44.06)	56 (39.16)	0.6562
III	7 (14.89)	15 (31.92)	25 (53.19)		No	5 (11.63)	16 (37.21)	22 (51.16)	
Missing	0 (0)	1 (33.33)	2 (66.67)		Missing	0 (0)	1 (50)	1 (50)	
Nuclear grade					Hormonal therapy				
I	4 (36.36)	4 (36.36)	3 (27.28)	0.0084	Yes	5 (21.74)	7 (30.43)	11 (47.83)	0.5217
II	16 (13.01)	63 (51.22)	44 (35.77)		No	24 (14.64)	73 (44.51)	67 (40.85)	
III	9 (17.31)	13 (25)	30 (57.69)		Missing	0 (0)	0 (0)	1 (100)	
Missing	0 (0)	0 (0)	2 (100)		Molecular subtype				
Lymph nodes committed					Luminal A	14 (15.39)	45 (49.45)	32 (35.16)	0.5019
0 ≤ 3	22 (17.60)	49 (39.20)	54 (43.20)	0.5934	Luminal B HER2-pos	3 (17.64)	7 (41.18)	7 (41.18)	
4 ≥ 25	6 (10.91)	28 (50.91)	21 (38.18)		Luminal B HER2-neg	3 (13.04)	9 (39.13)	11 (47.83)	
Missing	1 (12.50)	3 (37.50)	4 (50)		HER2-pos	4 (30.77)	5 (38.46)	4 (30.77)	
Estrogen receptor status					Basal-like	4 (11.43)	12 (34.28)	19 (54.29)	
Positive	20 (15.15)	62 (46.97)	50 (37.88)	0.4468	Missing	1 (11.11)	2 (22.22)	6 (66.67)	
Negative	9 (16.98)	18 (33.96)	26 (49.06)		Adapted histological grade				
Missing	0 (0)	1 (33.33)	2 (66.67)		I	6 (35.29)	8 (47.06)	3 (17.65)	0.0265
Progesterone receptor status					II and III	23 (13.69)	71 (42.26)	74 (44.05)	
Positive	17 (15.31)	52 (46.85)	42 (37.84)	0.5018					
Negative	12 (16.67)	26 (36.11)	34 (47.22)						
Missing	0 (0)	2 (40)	3 (60)						

*P value determined by χ^2 test.

DISCUSSION

TP53 mutations are associated with instability in cell development and cycle progression, and induction of apoptosis in malignant tumors (Hsieh and Lin, 2006). There is a high frequency of *TP53* alterations in human cancer. The *TP53* gene encodes the p53 protein, which, with its genetic variations, constitutes a complex family of several hundred proteins with heterogeneous properties (Jaiswal et al., 2011).

Our study corroborates the findings of Hsieh and Lin (2006); we did not detect the mutated somatic version of p53 at codons 11 or 248 in BC in Brazilian women. The mutation frequency at codon 248 was 17% according to Berns et al. (1998), and Powell et al. (2000) reported 10%. Moreover, Powell et al. (2000) reported that all types of mutation, with the exception of direct DNA contact mutations, are associated with worse survival in women with BC; DNA contact mutations accounted for about 25% of all mutations and two-thirds of these were in codons 248 and 273. Although codon 248 is considered a site of gene mutations, we did not find homozygous Gln (Gln/Gln) in Brazilian women with BC. Similarly, the *TP53* codon 11 mutation was not evident in this study compared with other studies. In addition, we detected homozygous Glu (Glu/Glu) and homozygous Arg (Arg/Arg) in *TP53**11 and *TP53**248 polymorphisms, respectively, in all samples.

Genetic variations at *TP53* codon 72 in BC have been discussed and studied frequently worldwide. In recent years, gene alterations that lead to a substitution of the amino acid Pro by Arg have been controversial. Consequently, we investigated this single nucleotide polymorphism (SNP) in mammary carcinoma. Proestling et al. (2012) showed that the p53 protein produced by the Arg-encoding allele appears to be a more potent transcription factor and tumor suppressor *in vivo* in human BC than the protein produced by the Pro-encoding allele. It has been suggested that the mechanism by which the codon 72 polymorphism increases apoptosis is the enhanced mitochondrial localization of p53 protein in cells with the Arg/Arg genotype; in contrast, the homozygous Pro (Pro/Pro) genotype induces higher levels of G1 arrest compared with the Arg/Arg genotype (Bišof et al., 2012).

Chen et al. (2013) studied Taiwanese women with smaller tumors, and found that there was no difference in genotype distribution between the control and case groups, even though a large number of patients with tumor size TI had the Arg/Arg genotype. Equally importantly, the differences are inherent in the relative prevalence of the polymorphism in different populations; it is interesting to find a discrepancy in the distributions of the *TP53* codon 72 polymorphisms between Asian and Caucasian populations. There were more Pro than Arg alleles, and a two-fold higher incidence of the Pro/Pro genotype among the Asian women. However, the Arg/Arg genotype is a risk factor for the development BC in Caucasian women. A comparison between control and case groups by Huang et al. (2003) revealed a significantly larger risk to Japanese women with the Pro/Pro genotype, strengthening the idea that racial, ethnic, and environmental differences play a critical role in BC. Moreover, a statistically significant linear correlation between frequency of the allele encoding Pro and latitude has been noted in several populations. This suggests that the two alleles may produce functionally distinct proteins, and that the allele encoding Pro might be selected or influenced according to environmental factors, such as exposure to high levels of ultraviolet light (Dumont et al., 2003). Interestingly, Leu et al. (2013) found that allele frequencies vary with geographic region; the Pro-encoding allele is more common in populations near the equator, while the Arg-encoding allele is more common in those living at a distance from the equator.

Comparative sequence analyses in non-human primates suggest that Pro is the ancestral

form, although Arg occurs at a high frequency (>50%) in some populations. A latitude gradient in variant frequency incited speculation that Pro might protect against the adverse consequences of sunlight or other environmental risk factors attributed to tumor development (Whibley et al., 2009).

Keshava et al. (2002) described the high prevalence of Arg in Caucasian women with BC from New York, although they did not find the same results in African-Americans. Previous studies have focused on European and Arab populations that showed a high incidence of Arg/Arg and the possibility that it represents a risk factor. In Brazil, the Arg/Arg polymorphism is correlated with increased susceptibility to malignant disease, as described by Damin et al. (2006). Contradictory to Damin et al.'s study, we found no such association with the *TP53**72 polymorphism in Brazilian women, notwithstanding the fact that the Arg/Arg genotype exhibited a prevalence of 42.02% and the Pro/Pro genotype that of 15.43% in cancer cases. The equivalent figures in the control group were 41.46 and 16.10%, respectively. The Arg/Arg genotype was predominant in both groups and there was no statistically significant difference between groups (P = 0.9823). The allelic frequencies showed that 0.63% of women without cancer and with BC have at least one Arg allele. To confirm our results, women with BC from Tunisia, Russia, India, Germany, the United Kingdom, Sweden, and Iran were studied and no significant association between the Arg/Arg genotype and the development of a tumor was found; this meta-analysis performed by Ma et al. (2011) revealed no evidence of any association between BC and the codon 72 polymorphism, even when the populations were grouped and submitted to stratified analysis.

BC is graded based on the scoring of three histologic features: tubule formation, mitotic count, and nuclear pleomorphism. This system is very important and works fairly robustly in classifying grade I and grade III invasive BC, but there is a high degree of variability in classifying grade II tumors (Ping et al., 2014). Our clinical pathological data indicate that only the nuclear grade presented a significant association with the genotype distribution (P = 0.0084), and the perceptual grades I, II, and III are described in Table 3. Nuclear grade II was most common and it was most frequently associated with the Pro/Arg genotype. There was a significant association between the Arg allele in the nuclear grades and differentiated pleomorphism and mammary tumors. The Pro/Pro genotype showed lower percentages in grades II and III. Martínez-Arribas et al. (2006) postulated that for women with tumors and pleomorphic cellular nuclei in grade III, there was an important association with poor prognosis parameters.

We also conducted an analysis of adapted histological grade, in which grades II and III were clustered owing to similarity of tissue features and compared with grade I. Comparing the histologic grades, the statistical analysis (Table 3) confirmed a significant association between genotype and cancer progression. Ping et al. (2014) reported that tumor grades showed the most prominent differences in *TP53* gene mutation frequency, and also that mutations in this gene were identified in 58% of grade III invasive breast carcinomas compared with only 4% in grade I lesions. In addition, there were no statistically significant differences in other variables in this study.

A previous study by Olivier et al. (2006) reported a correlation between *TP53* mutations and clinical pathological features, and a significant association with high rates of mortality.

Mostaid et al. (2014) evaluated codon 72 polymorphisms in several cancer types. They suggested that there was a significant relationship between the Pro/Pro genotype in codon 72 and an increased risk of tumorigenesis. Dastjerdi (2011) reported that the Arg/Arg genotype in colorectal cancer showed an association with an increased risk of tumor development in Iran. In contrast, a Brazilian population had a high prevalence of the Arg/Arg genotype and there was no correlation between the polymorphism and the risk of cancer in colorectal carcinoma (Lima et

al., 2006), which was corroborated by the results for head and neck squamous cell carcinoma (Mojtahedi et al., 2010). Once more, the population profile seems to be an important cause of discrepancies in the association between the polymorphism and the frequency of disease (Eltahir et al., 2012). The data reported in these studies from different regions of the world have convinced us that caution is required when interpreting observations about this polymorphism, bearing in mind the characteristics presented by each studied population.

In summary, our results indicate that polymorphisms at codons 11 and 248 of the *TP53* gene do not seem to be associated with predisposition to, and development of, BC in Brazilian women. In contrast, the polymorphism in codon 72 showed possible associations between nuclear grade and adapted histologic grade and BC. However, the allelic and genotypic comparisons of the polymorphism did not reveal statistically significant differences. It may be hypothesized, therefore, that the high prevalence of the Arg/Arg genotype in Brazil may be a regional factor, but may still contribute to the global distribution data and our knowledge of the behavior of BC. Further studies are warranted to elucidate the role of this polymorphism in breast carcinogenesis, and to widen our knowledge of this important disease, which affects millions of women worldwide.

Conflicts of interest

The authors declare no conflict of interest.

ACKNOWLEDGMENTS

Research supported by a CNPq grant.

REFERENCES

Akkiprik M, Sonmez O, Gulluoglu BM, Caglar HB, et al. (2009). Analysis of p53 gene polymorphisms and protein over-expression in patients with breast cancer. *Pathol. Oncol. Res.* 15: 359-368. http://dx.doi.org/10.1007/s12253-008-9129-6

Berns EM, van Staveren IL, Look MP, Smid M, et al. (1998). Mutations in residues of TP53 that directly contact DNA predict poor outcome in human primary breast cancer. *Br. J. Cancer* 77: 1130-1136. http://dx.doi.org/10.1038/bjc.1998.187

Bertheau P, Lehmann-Che J, Varna M, Dumay A, et al. (2013). p53 in breast cancer subtypes and new insights into response to chemotherapy. *Breast* 22 (Suppl 2): S27-S29. http://dx.doi.org/10.1016/j.breast.2013.07.005

Bišof V, Salihović MP, Narančić NS, Skarić-Jurić T, et al. (2012). The TP53 gene polymorphisms and survival of sporadic breast cancer patients. *Med. Oncol.* 29: 472-478. http://dx.doi.org/10.1007/s12032-011-9875-2

Camargo-Kosugi CM, D'Amora P, Kleine JP, Carvalho CV, et al. (2014). TP53 gene polymorphisms at codons 11, 72, and 248 and association with endometriosis in a Brazilian population. *Genet. Mol. Res.* 13: 6503-6511. http://dx.doi.org/10.4238/2014.August.26.1

Chen FM, Ou-Yang F, Yang SF, Tsai EM, et al. (2013). P53 codon 72 polymorphism in Taiwanese breast cancer patients. *Kaohsiung J. Med. Sci.* 29: 259-264. http://dx.doi.org/10.1016/j.kjms.2012.09.004

Damin AP, Frazzon AP, Damin DC, Roehe A, et al. (2006). Evidence for an association of TP53 codon 72 polymorphism with breast cancer risk. *Cancer Detect. Prev.* 30: 523-529. http://dx.doi.org/10.1016/j.cdp.2006.09.007

Dastjerdi MN (2011). TP53 codon 72 polymorphism and P53 protein expression in colorectal cancer specimens in Isfahan. *Acta Med. Iran.* 49: 71-77.

de Moura Gallo CV, Azevedo E Silva Mendonça G, de Moraes E, Olivier M, et al. (2005). TP53 mutations as biomarkers for cancer epidemiology in Latin America: current knowledge and perspectives. *Mutat. Res.* 589: 192-207. http://dx.doi.org/10.1016/j.mrrev.2005.01.002

Dumont P, Leu JI, Della Pietra AC, 3rd, George DL, et al. (2003). The codon 72 polymorphic variants of p53 have markedly different apoptotic potential. *Nat. Genet.* 33: 357-365. http://dx.doi.org/10.1038/ng1093

Eltahir HA, Adam AA, Yahia ZA, Ali NF, et al. (2012). p53 Codon 72 arginine/proline polymorphism and cancer in Sudan. *Mol. Biol. Rep.* 39: 10833-10836. http://dx.doi.org/10.1007/s11033-012-1978-0

Guimaraes DP and Hainaut P (2002). TP53: a key gene in human cancer. *Biochimie* 84: 83-93. http://dx.doi.org/10.1016/S0300-9084(01)01356-6

Hsieh YY and Lin CS (2006). P53 codon 11, 72, and 248 gene polymorphisms in endometriosis. *Int. J. Biol. Sci.* 2: 188-193. http://dx.doi.org/10.7150/ijbs.2.188

Huang XE, Hamajima N, Katsuda N, Matsuo K, et al. (2003). Association of p53 codon Arg72Pro and p73 G4C14-to-A4T14 at exon 2 genetic polymorphisms with the risk of Japanese breast cancer. *Breast Cancer* 10: 307-311. http://dx.doi.org/10.1007/BF02967650

Jaiswal PK, Goel A and Mittal RD (2011). Association of p53 codon 248 (exon7) with urinary bladder cancer risk in the North Indian population. *Biosci. Trends* 5: 205-210. http://dx.doi.org/10.5582/bst.2011.v5.5.205

Keshava C, Frye BL, Wolff MS, McCanlies EC, et al. (2002). Waf-1 (p21) and p53 polymorphisms in breast cancer. *Cancer Epidemiol. Biomarkers Prev.* 11: 127-130.

Leu JI, Murphy ME and George DL (2013). The p53 codon 72 polymorphism modifies the cellular response to inflammatory challenge in the liver. *J. Liver* 2: 117.

Levine AJ and Oren M (2009). The first 30 years of p53: growing ever more complex. *Nat. Rev. Cancer* 9: 749-758. http://dx.doi.org/10.1038/nrc2723

Lima JM, Serafim PV, Silva ID and Forones NM (2006). [Role of the genetic polymorphism of p53 (codon 72) gene in colorectal cancer]. *Arq. Gastroenterol.* 43: 8-13. http://dx.doi.org/10.1590/S0004-28032006000100005

Ma Y, Yang J, Liu Z, Zhang P, et al. (2011). No significant association between the TP53 codon 72 polymorphism and breast cancer risk: a meta-analysis of 21 studies involving 24,063 subjects. *Breast Cancer Res. Treat.* 125: 201-205. http://dx.doi.org/10.1007/s10549-010-0920-1

Martínez-Arribas F, Martín-Garabato E, Lafuente P, Tejerina A, et al. (2006). Proliferation measurement in breast cancer by two different methods. *Anticancer Res.* 26 (1A): 199-202.

Méplan C, Richard MJ and Hainaut P (2000). Metalloregulation of the tumor suppressor protein p53: zinc mediates the renaturation of p53 after exposure to metal chelators in vitro and in intact cells. *Oncogene* 19: 5227-5236. http://dx.doi.org/10.1038/sj.onc.1203907

Mojtahedi Z, Hashemi SB, Khademi B, Karimi M, et al. (2010). p53 codon 72 polymorphism association with head and neck squamous cell carcinoma. *Rev. Bras. Otorrinolaringol. (Engl. Ed)* 76: 316-320.

Mostaid MS, Ahmed MU, Islam MS, Bin Sayeed MS, et al. (2014). Lung cancer risk in relation to TP53 codon 47 and codon 72 polymorphism in Bangladeshi population. *Tumour Biol.* 35: 10309-10317. http://dx.doi.org/10.1007/s13277-014-2285-2

Olivier M, Langerød A, Carrieri P, Bergh J, et al. (2006). The clinical value of somatic TP53 gene mutations in 1,794 patients with breast cancer. *Clin. Cancer Res.* 12: 1157-1167. http://dx.doi.org/10.1158/1078-0432.CCR-05-1029

Pim D and Banks L (2004). p53 polymorphic variants at codon 72 exert different effects on cell cycle progression. *Int. J. Cancer* 108: 196-199. http://dx.doi.org/10.1002/ijc.11548

Ping Z, Siegal GP, Almeida JS, Schnitt SJ, et al. (2014). Mining genome sequencing data to identify the genomic features linked to breast cancer histopathology. *J. Pathol. Inform.* 5: 3. http://dx.doi.org/10.4103/2153-3539.126147

Powell B, Soong R, Iacopetta B, Seshadri R, et al. (2000). Prognostic significance of mutations to different structural and functional regions of the p53 gene in breast cancer. *Clin. Cancer Res.* 6: 443-451.

Proestling K, Hebar A, Pruckner N, Marton E, et al. (2012). The Pro allele of the p53 codon 72 polymorphism is associated with decreased intratumoral expression of BAX and p21, and increased breast cancer risk. *PLoS One* 7: e47325. http://dx.doi.org/10.1371/journal.pone.0047325

Stojnev S, Golubović M and Babović P (2010). TP53 gene mutations - from guardian of the genome to oncogene. *Acta Medica Medianae* 49: 59-63.

Whibley C, Pharoah PD and Hollstein M (2009). p53 polymorphisms: cancer implications. *Nat. Rev. Cancer* 9: 95-107. http://dx.doi.org/10.1038/nrc2584

Yersal O and Barutca S (2014). Biological subtypes of breast cancer: Prognostic and therapeutic implications. *World J. Clin. Oncol.* 5: 412-424. http://dx.doi.org/10.5306/wjco.v5.i3.412

RESEARCH ARTICLE

Antiproliferative and Cytotoxic Effect of Aqueous Extract from *Mussismilia braziliensis* Coral Mucus in Mouse Melanoma B16-F10 Cells

Jerônimo Pereira de França [1]*, Fernanda Luiza Andrade de Azevedo [1], Lucimar Pereira de França [1], Silvana Gaiba [1], Andrea Aparecida Fátima Souza Moraes [2], Vanina Monique Tucci-Viegas [1], Antonio de Miranda [2], Emiliano Nicolas Calderon [3] and Lydia Masako Ferreira [2].

[1]Departments of Biological Sciences and Agricultural and Environmental Sciences, Universidade Estadual de Santa Cruz, Brazil, [2]Departaments of Biophysics and Surgery, Universidade Federal de São Paulo, Brazil; [3]Departament of Invertebrates, Museu Nacional da Universidade Federal do Rio de Janeiro, Brazil.

* Author to whom correspondence should be addressed; E-Mail: jeronimopf@gmail.com; Tel.: +55-11-73-3680-5360; Fax: +55-11-73-3680-5360.

Abstract:

The cytotoxic effects and mechanisms of action of the aqueous extract isolated from the mucus of the Brazilian endemic coral *Mussismilia braziliensis* (cmAE) were compared to the ultraviolet-C (UVC) radiation-induced cytotoxicity in mouse melanoma B16-F10 cells. M. braziliensis cmAE inhibited B16-F10 cell growth (IC50 10 mg/mL) and induced cell death by apoptosis, as demonstrated by DNA fragmentation, formation of apoptotic bodies and membrane blebbing, similar to the effects induced by UVC radiation (LD85 6.4 mJ/cm^2). Moreover, treatment with cmAE caused a reduction in the mitochondrial activity of B16-F10 cells, inhibiting melanin synthesis even when cells were also exposed to UVC radiation. The cellular response to cmAE treatment, with or without exposure to UVC radiation, provoked altered expression of apoptotic proteins, markedly tumor suppressor protein 53 (p53) upregulation and cleaved caspase-3 activation. Our results showed that cmAE did not have antioxidant and/or photoprotective action in B16-F10 cells exposed to UVC radiation, but increased the cytotoxic activity in B16-F10 cells, inducing caspase-3 and p53-dependent apoptosis.

Keywords: Cancer – Apoptosis - inhibition of specific growth rate - Melanin synthesis - Ultraviolet C radiation

Introduction

Cutaneous melanoma is considered the most serious type of skin cancer. It is a highly lethal and very invasive neoplasm, accounting for less than 5 % of all skin cancer cases. Despite its low incidence, it is considered a problem for public health due to the significant raise in the number of cases, exceeding other malignancies growth rate (Jerant et al., 2000; Lasithiotakis et al., 2006; Jemal et al., 2009).

In the last few years there has been growing interest in marine products with biological activity. A large diversity of marine organisms has been extensively investigated, these organisms being secondary metabolite producers. These studies on the biotechnological potential of marine sources promising therapeutic agents are mentioned, with antibacterial, antiviral, antitumor and immunossupressive potential (Bhatnagar and Kim, 2010; Januar et al., 2010; Li and Vederas, 2009; Rashid et al., 2000; Blunt et al., 2004).

Marine organisms have developed evolutionary mechanisms for defense adaptation, such as toxins and other molecular compounds. Under such conditions, these compounds must overcome the diluent capacity of seawater to reach their target and to have the expected effect (Newman and Cragg, 2004; Bhatnagar and Kim, 2010; Hu et al., 2011).

Compounds isolated from octocorals (11-dehydrosinulariolide) were evaluated in A2058 cells which showed a dose-dependent inhibition of cellular proliferation, induction of apoptosis by the intrinsic pathway, cells in early and late apoptosis and increased expression of pro-apoptotic proteins such as caspase-3, caspase-9, Bax and also cytochrome C release into the cytosol, reduced expression of antiapoptotic proteins such as Bcl-2 and Bcl-xL (Su et al., 2012b). Bioactive isolates from Sinularia flexibilis showed moderate to weak cytotoxicity against four human tumor cell lineages, including human epithelial carcinoma cell line (HeLa), human laryngeal carcinoma cells (HEp-2) and breast cancer cell lines (MCF7 and MDA-MB-231) (Su et al., 2013).

The Sinularin compound was also evaluated for its antitumor effect in human melanoma cells (A2058) and Su et al (2012) suggest that natural marine compouds present important properties that may benefit the development of chemotherapeutic agents for melanoma (Su et al., 2012a).

It has been demonstrated that extracts from soft corals have potent cytotoxic activity and induce apoptosis, with morphological changes in cellular structure, chromatin condensation, nuclear DNA fragmentation and caspase-3 activation, all typical characteristics of programmed cell death. Octocorals methanolic extracts were tested for antineoplastic action and inhibited cell proliferation in tumor cell lines of central nervous system (SF-268), breast (MCF7) and lung (H460) (Januar et al., 2010).

Extracts from several coral species are rich sources of bioactive molecules with important pharmacological properties that may be useful for the development of antitumor and antimicrobial drugs (Fung and Ding, 1998; Iwashima et al., 2000; Li et al., 2005; Liang et al., 2008). Cembrane-type diterpenes from soft corals present antineoplastic action (Iwashima et al., 2000; Li et al., 2005; Cheng et al., 2008).

The scleractinian coral *Mussismilia braziliensis* (Verrill, 1868), Phylum Cnidaria, Class Anthozoa, Family Mussidae is a colonial marine invertebrate endemic to southern Bahia State, Brazil (Antônio-de-Souza, 2002). It has a massive limestone skeleton which produces mucus that covers all exposed surface. This mucus is made up of a complex mixture of components such as glycoprotein polymers, important physico-chemical characteristics of the mucus, providing lubrication and protection to underlying coral tissues (Leao and Kikuchi, 2005; Jaktar et al.,2010).

Material and Methods

Chemical and Reagents. The following drugs and reagents were used: 7β-Hydroxycholesterol, [3-(4,5-dimethylthiazol-2-yl)-2,5-diphenyltetrazolium] bromide (MTT), di(phenyl)-(2,4,6-trinitrophenyl)iminoazanium (DPPH), 7-aminoactinomycin D (7-AAD), ethylenediamine tetraacetic acid (EDTA), 4-(2-hydroxyethyl)-1-piperazineethanesulfonic acid (HEPES) buffer, ascorbic acid, citric acid, trolox, isopropyl alcohol,

penicillin, streptomycin, chloramphenicol, trypsin, RNase, paraformaldehyde, sodium hydroxide (NaOH), magnesium chloride ($MgCl_2$), ammonium chloride (NH4Cl), sodium azide, propidium iodide, dimethyl sulfoxide, saponin and Mueller Hinton Agar media from Sigma Chemical Co. (St. Louis, MO, USA). 4,6-diamidino-2-phenylindole, dihydrochloride (DAPI) and phalloidin conjugated to Alexa-Fluor 488 from Molecular Probe/Life (Eugene, OR, USA); antibodies against cleaved caspase-3 and activated p53 (SER 15) from Santa Cruz Biotechnology Inc. (CA, USA). Annexin-V-FLUOS staining kit from Roche Diagnostics (Mannheim, Germany). Mueller-Hinton broth from H-Media (Paris, France), Dulbecco Modified Eagle's Medium/Nutrient Mixture F12 DMEM/F12, phosphate buffered saline (PBS) and fetal bovine serum (FBS) from Vitrocell (Campinas, SP, Brazil). Resazurin, crystal violet, potassium chloride (KCl), sodium chloride (NaCl), dibasic sodium phosphate (Na_2HPO_4) and monobasic potassium phosphate (KH_2PO_4) from VETEC (Xerém, RJ, Brazil).

Cell Culture. The mouse melanoma B16-F10 cell line was purchased from Rio de Janeiro Cell Bank (BCRJ/UFRJ). The cells were maintained at 37 °C in an incubator with a humidified atmosphere of 5 % CO_2 and cultured in DMEM/F12 supplemented with 10 % heat-inactivated FBS, streptomycin (100 µg/mL) and penicillin (100 U/mL).

Aqueous Extracts Preparation Obtained from the Mussismilia braziliensis Coral Mucus. The Mussismilia braziliensis (Verrill 1868) coral mucus was collected from five healthy corals by lightly abrading the surface with a syringe tip (to trigger mucus production) and then aspirating the mucus. Corals were obtained at the south of Recife de Fora reef (16º25'9.64" S/038º59'17.37" W), in the waters of the coastal region of Santa Cruz de Cabrália, Porto Seguro, Bahia State, Brazil in April/2012. The specimens were identified by Dr. Emiliano Nicolas Calderon from the Departament of Invertebrates, Museu Nacional da Universidade Federal do Rio de Janeiro, Brazil, where a voucher specimen of M. braziliensis, have been deposited. The Mussismilia braziliensis coral mucus was lyophilized and then dissolved in PBS to obtain the aqueous extract.

Experimental Groups. Mouse melanoma B16-F10 cells were divided in 4 different groups: CG (Control Group), IG (Irradiated Group), TG (Group treated with aqueous extract of the Mussismilia braziliensis coral mucus, abbreviated as (cmAE) and TIG (Group treated with cmAE and then irradiated). In all groups, the B16-F10 cells were subcultured in six-well plates in complete medium (DMEM/F12, Fetal Bovine Serum – FBS and antibiotics) and cultivated for 24 h. Cells were then fasted for 24 h by incubation with medium without FBS in order to induce cell cycle arrest in the G0/G1 phase.

In CG, after 24 h of fasting, the serum-free culture medium was replaced with complete medium and cells were kept in a humidified incubator (5 % CO_2, 37 °C) for 48 h. The culture medium was then discarded and replaced by 1 mL sterile phosphate saline buffer – PBS (8.0 g de NaCl, 0.2 g KCl, 0.21 g Na_2HPO_4, 0.2 g KH_2PO_4) and kept for 30 min at room temperature (RT). PBS was then replaced with complete medium and cells were kept in a humidified incubator for further analysis.

For the IG, the serum-free culture medium was discarded and replaced by 1 mL sterile PBS. Cells were irradiated in PBS using a camera (UVC SpectroLinker TM XL-100) at 254 nm, with the following energy doses: 1, 2, 4, 6, 8 or 10 mJ/cm^2. After 30 min at RT, PBS was replaced with complete medium and cells were kept in a humidified incubator.

For the TG, after 24 h of fasting, the serum-free culture medium was discarded and cells were treated in complete medium containing 0.1, 1.0, 10 or 100 mg/mL cmAE and kept in a humidified incubator for 48 h. The culture medium was then discarded and replaced by 1 mL sterile PBS for 30 min (RT). Then, PBS was again replaced by complete medium containing 0.1, 1.0, 10 or 100 mg/mL cmAE and the cells were kept in a humidified incubator.

For the TIG, after 24 h of fasting, the serum-free culture medium was discarded and cells were treated with complete medium containing 0.1, 1.0, 10 or 100 mg/mL cmAE and kept in a humidified incubator for 48 h. The

culture medium was then discarded and replaced by 1 mL sterile PBS. Cells were irradiated in PBS using a camera (UVC SpectroLinker TM XL-100) at 254 nm, with the following energy doses: 1, 2, 4, 6, 8 or 10 mJ/cm^2. After 30 min at RT, PBS was replaced by complete medium containing 0.1, 1.0, 10 or 100 mg/mL cmAE and the cells were kept in a humidified incubator until further analysis.

Crystal Violet Assay: Growth Curve and Cell Survival. As a second method for determining the cytotoxicity of cmAE and/or UVC radiation (RUVC) on B16-F10 cells we used the crystal violet assay (Siddiqui et al., 2006), with modifications. Approximately 10^3 cells were subcultured by well in six-well plates in complete medium (CG). A cell growth curve was made with absorbance as ordinate and time as abscissa (9 points of cell counting over time) using the control group cells. For the other groups, the absorbance was read and the growth curve was used to obtain the corresponding cell number.

Subsequently, for each condition, the cells adhered to each well were counted, then the cells were washed with PBS and fixed in PBS containing paraformaldehyde (0.4 %) for 10 min. After washing with PBS the cells were incubated and slightly shaked at room temperature (RT) for 15 min with 50 µl staining solution (0.5 % crystal violet, 20 % methanol) which stains DNA. The dye was discarded and the cells were washed with PBS. The uptaken crystal violet was solubilized by addition of 200 µl methanol and 15 min incubation on a shaker. Finally, the amount of dye taken up by the monolayer was quantified by measuring the absorbance at 570 nm using a spectrophotometer plate reader (VERSAmax Tunable microplate reader, Molecular Devices, CA, USA) as proposed by Siddiqui et al., 2006.. The curve corresponding to the ratio of crystal violet absorbance (ABS) depends on the number of B16-F10 cells. Mathematically, this relationship is the linear regression coefficient (r2 = 0.9960) and the inverse of the slope is (1/slope = 5.26 x 10^8), N = 6.

Cell Viability Assay. The effects of cmAE treatment or radiation on cell viability were determined by MTT assay, which is based on the reduction of a tetrazolium salt by mitochondrial dehydrogenase in viable cells (Fernandes et al, 2014; Cunha et al 2014; Candida et al. 2014. For all experimental groups, cells were seeded in 96-well plates at a density of 1 × 10^4 cells/well and treated with ethidium monoazide (EMA) at a final concentration of 1, 5, 10 or 100 mg/mL. After 48 h, 50 µL of MTT stock solution (2 mg/mL) was added to each well to reach a total reaction volume of 250 µL, and the plates were incubated for an additional 4 h. Supernatants were aspirated, and the resulting formazan crystals were dissolved in 150 µL isopropyl alcohol. Absorbance was measured at 540 nm using a colorimetric MTT ELISA assay (VERSAmax Tunable microplate reader, Molecular Devices, CA, USA).

Melanin Content Measurement. For all groups, total melanin content was determined as previously described (Shin and Lee, 2013). Cells were then trypsinized and counted (as described in 4.1.5). Briefly, B16-F10 cells were harvested, washed with PBS, counted, lysed with 10 % dimethylsulfoxide at 80 ºC for 1 h, and melanins were solubilized in 1 N sodium hydroxide. Optical density of the clear supernatants was measured at 475 nm using an ELISA assay (VERSAmax Tunable microplate reader, Molecular Devices, CA, USA). Melanin content was expressed as absorbance per cell using a standard curve generated using synthetic melanin, linear regression coefficient (r2 = 0.9952) and the inverse of the slope (1/slope = 2.216 x 10^8), N = 6.

Determination of DPPH Radical Scavenging Capacity. The antioxidant activity of testing compounds was measured using the stable DPPH assay as modified by Wang et al. (Li et al., 2013). Proper concentrations of the samples were added to 100 µL of DPPH (60 µM) solution for a total of 200 µL with cmAE dissolved in methanol containing 0.1, 1.0, 10 or 100 mg/mL. Absorbance was recorded at 30 min using an ELISA assay (VERSAmax Tunable microplate reader, Molecular Devices, CA, USA). When DPPH reacted with an antioxidant compound that donates hydrogen, it was reduced, resulting in a decrease in the absorbance at 515 nm. Vitamin C or Trolox were used as a positive control. The

percentages of remaining DPPH were plotted against the sample to obtain the amount of antioxidant required to reduce the initial concentration of DPPH.

Apoptosis Assay. Flow cytometry technique assay as modified by Gaiba et al, 2012 and Moraes, 2012 was used to detect apoptosis in B16-F10 cells in all groups (Li et al., 2013; Bajbouj et al., 2012). After washing twice in PBS, 1×10^6 cells were stained with 100 µl annexin V staining solution, consisting of 20 µl FITC-conjugated annexin V reagent (20 µg/mL), 20 µl 7ADD (50 µg/mL), and 1000 µl of 1 M/L HEPES buffer, for 15 min at RT. Samples were examined by fluorescence-activated cell sorter (FACS) analysis, and the results were analyzed using Cell-Quest software (Becton Dickinson, San Jose, CA). Since positive annexin V staining indicates apoptotic and necrotic cells, 7ADD-positive cells were used to measure late apoptotic cells and necrotic cells whereas annexin V-positive and 7ADD-negative cells were counted as early apoptotic cells.

Flow Cytometric Analysis of Caspase-3 and p53. For the analysis of caspase-3 and p53 activation in B16-F10 cells, the cells were re-suspended in PBS containing 0.1 % sodium azide, homogenized and centrifuged at 1000 x g for 5 min. Cell pellets were fixed in 75 % ethanol at 4 °C overnight and washed in cold PBS with 50 mM NH4Cl. After washing, cells were permeabilized with PBS containing 0.1 % saponin and 10 % normal bovine serum for 30 min at 22 °C. Aliquots were incubated at 4 °C overnight with anti-caspase-3, or anti-activated p53, 1:800 dilution. The secondary antibodies conjugated with Alexa-Fluor 488 or 594 were diluted 1:1600 and incubated for 2 h at RT, protected from light. The samples were examined by fluorescence FACScan flow cytometer (Becton Dickinson, CA, USA) and the results were analyzed using Cell-Quest software. The procedure was performed as modified by Danova et al., 1990.

Flow Cytometric Analysis of DNA Content. Cells were seeded on a 6-well plate at a density of 1×10^5 cells per well. For all groups, after 48 h, cells were re-suspended in 50 µL of PBS at 4 ºC and fixed overnight in 75 % ethanol at 4 °C. Low molecular weight DNA fragments were extracted by 10 min incubation with extraction buffer solution (9 parts 50 mM Na_2HPO_4, 1 part 25 mM citric acid and 0.1 % triton x-100; pH 7.8). After centrifugation, the pellet cells were re-suspended and incubated in the dark at RT in 0.4 mL staining buffer (10 mM HEPES, 100 mM NaCl, 2 mM $MgCl_2$, 0.1 % triton x- 100; pH 6.8) with the addition of 250 µg RNAse and propidium iodide (50 µg/mL final concentration). Distribution of cell cycle phases with different DNA contents was determined using a flow cytometer FACS (Becton Dickinson, San Jose, CA, USA). Sub G1 cells in flow cytometric histograms were considered apoptotic cells. Analysis of cell cycle distribution and the percentage of cells in the G1, S, and G2/M phases of the cell cycle were determined using Cell-Quest software (Becton Dickinson, San Jose, CA, USA), assay as modified by Bajbouj et al., 2012.

Immunofluorescence Labeling. For all groups, B16-F10 cells were plated on glass coverslips, fixed in 0.4 % paraformaldehyde for 30 min at 4 °C, washed 3 times in PBS. Cells were then, permeabilized with 0.1 % saponin in PBS containing 10 % normal bovine serum for 30 min at 22 °C and stained with a combination of fluorescent dyes. Actin filaments F of cytoskeleton were immunostained with phalloidin conjugated with Alexa Fluor 488 (green). Phalloidin (1:500) incubation was performed in PBS containing 10 % normal bovine serum and 0.1 % saponin. Nuclei were counter-stained with blue fluorescent DNA stain DAPI (1:10000), and excited using a 750 nm multiphoton source (two simultaneous photon excitations at 375 nm). The images are a composite of 3 images acquired using filter sets appropriate for blue and red fluorescence, on a Zeiss confocal microscope (LSM 510, Germany) as adapted from Gaiba et al.,2012.

Antibacterial Activity Assay. Antibacterial activity was tested by means of a standard agar plate diffusion assay. Gram positive Staphylococcus aureus (CCBM 0324) and Enterococcus faecalis (CCBM 0279) bacterial strains and Gram negative Escherichia coli bacterial strains (obtained from the Culture Collection of Microorganisms of Bahia (CCMB), Laboratory of Microbiology, Universidade

Estadual de Santa Cruz, Ilhéus) were used. Precultured bacteria (grown in Mueller Hinton Agar media) were used to inoculate Mueller Hinton broth agar plates in a final concentration of 5×10^8 cells/L, standardized to a 0.5 McFarland scale. Four holes (1 cm diameter) were made into each agar plate and filled with 200 µL of unheated or heated samples in the case of cmAE. The inhibition zone for each sample was determined after overnight incubation of plates at 37 °C. After the incubation period, 30 µL of 0.01 % resazurin solution were added to each hole for the quantitative analysis of microbial growth for each sample dilution. As positive control we used chloramphenicol at a concentration of 10 mg/mL. Samples showing the highest bacterial growth inhibition were further diluted with deionized water (100 mg/mL to 0.78 mg/mL). Tests were repeated and minimal inhibitory concentrations were calculated (Minimum Inhibitory Concentration - MIC = the concentration in µg/mL that inhibits the growth of tested microorganism 1 mM from the rim of the hole). MIC as recommended by the Institute of Clinical and Laboratory Standards (CLSI, 2007) and adapted from Coban, 2012.

Statistical Analysis. Data are presented as mean ± SD of four independent experiments. Statistical analysis among groups was performed by one-way analysis of variance (ANOVA) followed by the Student–Newman–Keuls Multiple Range Test. GraphPad Prism v.3.0 software was used, $p < 0.05$ was considered to be statistically significant.

Results and Discussion

Antiproliferative and Cytotoxic Effects and mechanisms of action of the aqueous extract (cmAE) isolated from the mucus of the Brazilian endemic coral Mussismilia braziliensis in B16-F10 Cells. To determine the effects of M. braziliensis Coral Mucus aqueous extract (cmAE) in cell viability, B16-F10 cells were treated with various cmAE concentrations (1, 5, 10 and 100 mg/mL) for 48 h. MTT (3 - (4,5-dimethylthiazol-2-yl) -2,5 - diphenyltetrazolium a yellow tetrazole) is reduced to purple formazan in living cells. With the MTT test we assessed cell viability and proliferation following cmAE administration. Treatment with cmAE reduced B16-F10 cell proliferation in a time- and concentration-dependent manner. The most remarkable effects were observed at concentrations ranging from 5 to 100 mg/mL with a significant decrease in the total cell number ($p < 0.01$). A more efficient decrease in mitochondrial function was observed with doses ranging from 5 to 10 mg/mL, IC50 10 mg/mL, as shown in (Figure 1A).

Crystal violet staining was used to determine the number of viable cells. To evaluate the effect of various UVC radiation doses on cultured B16-F10 cells and identify the dose capable of promoting cell death in a similar way of the effect produced by cmAE, cells were irradiated using a 254 nm wavelength UVC camera (SpectroLinkerTM XL-100) with the following radiation doses: 1, 2, 4, 6, 8 and 10 mJ/cm^2 (Figure 1B). A single radiation dose of 6.4 mJ/cm^2 significantly decreased the total number of B16-F10 cells for the range from 2 to 10 mJ/cm^2 ($p < 0.05$), with a cell lethality of 85 % (LD85). Kowalczuk et al., 2001 observed a similar effect in G361 human melanoma cell line with a 6 mJ/cm^2 UVC radiation exposure. Our results suggest a recovery in cell growth from the 5th day of treatment in both cases. A more effective cytotoxic effect was observed with the combination of both treatments: cmAE administration and UVC radiation (TIG – Treated and Irradiated Group), which completely inhibited B16-F10 cell proliferation.

In (Figure 1C), an exponential cell growth was observed in the control group (CG), however, in the irradiated group (IG), cell count significantly decreased 24 h after exposure to 6.4 mJ/cm^2 UVC radiation ($p < 0.05$). MTT results are also confirmed for the treated group (TG) in (Figure 1C): cmAE treatment (10 mg/mL) significantly decreased cell viability ($p < 0.05$). Nevertheless, after 48 h, B16-F10 cell death significant increased in IG compared to TG. When comparing UVC radiation and cmAE treatment cytotoxicity (positive control), our results showed similar cytotoxicity for a continuous 10 mg/mL cmAE treatment and for a single UVC radiation dose of 6.4 mJ/cm^2 (LD85). We also observed a recovery in cell growth from the 5th day of treatment in both cases. Once again, a more effective

cytotoxic effect was observed with the combination of both treatments: cmAE administration and UVC radiation (treated and irradiated group - TIG), whith no proliferation recovery after 5 days.

Culture conditions and the in vitro growth patterns of B16-F10 cells in the control group (CG) were responsible for an adaptive response to the growth constraints imposed by high density and long permanence in culture, with monolayer and cluster formation in culture plates.

It is known that tumor cell growth in culture is continuous when nutrients are present in the medium even if there is no space left on the plate for growth. This continuous growth in two dimensions only is not self-regulated. However, depending on the stimulus, growth self-regulation may occur in B16-F10 melanoma cells in three phases. The first one is exponential for a few days, followed by a linear growth curve for approximately 100 days and then, reaching a critical diameter beyond which there is a dormant, quiescent phase (Folkman and Hochberg, 1973; Sutherland et al., 1971).

An exponential phase over time was observed for the control group, so as no stationary phase of growth (Figure 1C) which implies that the specific growth rate (μ) was constant during the nine days of culture (Figure 1D). In (Figure 1D) and (Figure 1E), the curve showing the total number (N) of B16-F10 viable cells was obtained using mathematic calculations to compare growth rates among different experimental groups, as described by other authors (Sullivan and Salmon, 1972; Laird, 1964):

$$\mathrm{N\,(t)} = \mathrm{N0\,(t)}\, e^{\mu t}$$

i.e., the Napierian logarithm of the total number of viable cells determines the specific growth rate:

$$\mu = \frac{\mathrm{Ln\,N\,(t)} - \mathrm{Ln\,N0\,(t)}}{t}$$

This equation determined the slope of the line or the specific growth rate (μ) in a defined time interval, in this case ranging from 5 to 9 days in all groups (Figure 1D). During that period, the groups treated with cmAE (TG) or irradiated (IG) maintained the same growth rate as the control group (CG), all of them significantly different from the group treated with cmAE and then irradiated (TIG), $p < 0.01$. In (Figure 1E), it is possible to observe the y-intercept, N0 (5) except for CG. This was estimated by interpolation using Graphpad Prism 3 software for the other groups. With these values we estimated the total number of B16-F10 cells at time t (0) (Figure 1F), which indicates the survival condition without treatment or exposure to radiation. This allows the theoretical determination of the amount of cells dying due to the treatment or due to UVC radiation, with all groups significantly different from CG.

Figure 1. Antiproliferative and cytotoxic effects of Coral Mucus aqueous extract (cmAE) in B16-F10 cells. MTT viability test showing the B16-F10 cells treated for 48 h with different concentrations of cmAE (1.0 - 100.0 mg/mL) (A) and after treatment with concentration up to 10 mg/mL significantly reduced the number of cells. B16-F10 cells were irradiated with the following radiation doses: 1, 2, 4, 6, 8 or 10 mJ/cm^2 (Figura IB). After 48 h, survival curve was examined using the crystal violet assay (B), also observed significantly decreased the total number of cell lines after radiation (IG), ($p < 0.05$). The total number of viable melanoma cell line (B16-F10) were counted on day 09 in all groups, were measured using the crystal violet technique (C). The slope of the line or the specific growth rate (μ) in a defined time interval (5 to 9 days) in all groups (D). The y-intercept, N0 (5) except for CG (E). Total number of B16-F10 cells at time t (0) (F). The MTT or crystal violet data shown are performed in triplicates. Results are means ± S.E.M from four independent experiments. (*statistically significant against the control for $p < 0.05$).

DNA lesions can be induced by chemical agents or radiation, which activate three cell cycle checkpoints in G1, S and G2; (Kousholt et al., 2012; Prudhomme, 2006a; Prudhomme, 2006). The cell division cycle consists of four distinct and interrelated phases: G1, S, G2 and M (mitosis). Cell cycle progression is regulated by cyclin-dependent kinases (CdK). CdK Inhibitor (CKI) can block kinase activity and promote cell cycle arrest stopping cell proliferation. To analyze the proportion of cells in different phases, cellular DNA content and cells with a low DNA content (fragmentation) before the G1 phase of the cell cycle were considered as hypodiploid cell ratio (sub-G1 phase) and were assessed by flow cytometry after 4h treatment with cmAE (10 mg/mL) and UVC radiation (6.4 mJ/cm^2), (Figure 2).

Figure 2. Effects of cmAE and UVC radiation on the Cell Cycle in B16-F10 cells. The effects of cmAE on cell cycle profile were examined by flow cytometric analysis. The B16-F10 melanoma cells with a lower DNA content than that of the G1 phase of the cell cycle was shown according to the sub-G1 fraction. B16-F10 melanoma cells exposed or not exposed to cmAE and UVC radiation, and 7AAD staining was used to analyze cell cycle distribution. All analyses 4h: after treatment. CG – Control Group (A); IG – Irradiated Group – UVC radiation at a single dose of D = 6.4 mJ/cm^2 (B); TG – Group treated with 10 mg/mL cmAE (C); TIG – Group treated with cmAE and irradiated (D); Quantitative analysis of percentage gated cells at Sub-G1 fraction; (F) Σ(S + G2M) phases in B16-F10 cells. In E, the sub-G1 fraction shows the B16-F10 melanoma cell of groups IG (B), TG (C) and TIG (D) significantly higher than CG (A), $p < 0.01$. There was also sub-G1 fraction an increase to significantly higher TIG compared to the IG group, $p < 0.01$. In (E), to the Σ(S + G2M) phases showing the B16-F10 melanoma cells of groups IG (B), significantly lower than the control group CG (A), $p < 0.05$. However, the Σ(S + G2M) phases to all groups treated with 10 mg/mL extract (TG and TIG) was significantly higher than the control group CG, $p < 0.05$.

Our results show that although cmAE induce cytotoxicity it was able to promote a significant increase in the amount of mitosis and cell synthesis, including the TIG group, where the number of mitosis and cells synthesis was lower by action of UVC radiation. The G1/S checkpoint is dependent on the p53 protein. DNA damage activates p53 and inhibits CdK leading to cell cycle arrest to prevent damaged DNA replication during the S phase. However, the p53 gene is mutated in 50 % of tumor cells, inducing G1/S checkpoint bypass in p53-mutated cells (Iwashima et al., 2000).

To avoid accumulation of mutations, cells respond to DNA lesions by halting cell cycle progression to allow time for DNA repair. CKIs, however, may affect tumor cells inducing the G2 checkpoint 1 (Chk1), essentially in p53-mutated cells due to DNA damaging agents. Therefore, combining a G2 checkpoint inhibitor (Chk1) with a DNA damaging agent selectively compel cancer cells to a premature and lethal mitosis due to accumulation of DNA lesions (Kousholt et al., 2012; Prudhomme, 2006a; Prudhomme, 2006).

To analyze the phosphorylated p53 protein accumulation by UVC radiation and/or cmAE in B16-F10 cells and were assessed by flow cytometry after 4h treatment with cmAE (10 mg/mL) and UVC radiation (6.4 mJ/cm^2), (Figure 3).

Figure 3. Flow cytometry analysis of phosphorylated p53 protein accumulation by UVC radiation and/or cmAE in B16-F10 cells. All analyses 4h: after treatment. CG – Control Group (A); IG – Irradiated Group – UVC radiation at a single dose of D = 6.4 mJ/cm^2 (B); TG – Group treated with 10 mg/mL cmAE (C); TIG – Group treated with cmAE and irradiated (D); A control performed with an irrelevant antibody is shown (A). The percentage of cells exhibiting phosphorylated p53 is indicated on each histogram. The numbers indicate the percentages of positive cells and fluorescence intensity. In (E), mean percentage of cleaved p53 for GC, GI, GT, and TIG experimental groups. Quantitative analysis of percentage of positive gated cells exhibiting phosphorylated p53 and there was IG (B) an increase to significantly higher compared to the CG (A) group, p <

0.01. Furthermore, the phosphorylated p53 protein to all groups treated with 10 mg/mL extract (TG and TIG) was significantly higher than the control group CG, $p < 0.05$ and $p < 0.01$, respectively. *Data were analyzed with one-way ANOVA followed by Newman Keuls test (significance level $p<0.05$) compared all groups to the control group (CG). Values represent the mean ± SEM of triplicate assays of one experiment representative of four similar results.

Nevertheless, after 4h, phosphorylated p53 protein accumulation in IG compared to TG. When comparing UVC radiation and cmAE treatment cytotoxicity, our results showed similar phosphorylated p53 protein accumulation for a continuous 10 mg/mL cmAE treatment and for a single UVC radiation dose of 6.4 mJ/cm^2, also with the combination of both treatments: cmAE administration and UVC radiation (treated and irradiated group - TIG). Our results suggest that the recovery of cell proliferation in TG and IG after the cytotoxic effects of cmAE or UVC radiation did not alter tumor growth rate because tumor cells are able to accumulate DNA damage without interfering with the cellular division machinery and/or mitosis and phosphorylated p53 protein accumulation in all groups studied.

In this context, in the last decade, there was a great interest in the G2 checkpoint in p53-mutant cells in which the G1 checkpoint is lacking. In these cells, only the G2 checkpoint could induce a delay in cell cycle progression to repair genetic material damage (Bartek and Lukas, 2003; Delia et al., 2003; Vermeulen et al., 2003; Xiao et al., 2003; Carrassa et al., 2004). Several molecules exhibiting inhibitory properties toward Chk1 have been previously described in the literature, such as bacterial metabolite UCN-01, naturally occurring compounds and synthetic compounds (Curman et al., 2001; Zhao et al., 2002; Kawabe, 2004; Prudhomme, 2006a), as well as marine sponge compounds (Curman et al., 2001). There are reports of bioactive metabolites from marine organisms (such as the gorgonian Euplexaura robusta) which showed moderate cytotoxicities against some tumor cell lines such as K562 and HeLa, and inhibitory activity against c-Met kinase (Zhang et al., 2012). Furthermore, it has been reported that secondary metabolites of soft corals belonging to the genus Capnella have weak tyrosine kinase p56lck (TK) inhibitory activity (Wright et al., 2003). There is an extensive interest in the discovery of Chk1 inhibitors as potential useful compounds, mostly from marine animals such as corals, to enhance the efficacy of antitumor agents that promote DNA damage. Thus, these molecules represent potential targets for antitumor therapy.

Coral Mucus of the aqueous extract (cmAE) no Showed Antioxidant Activity and Antimicrobial Activity. Marine organisms are exposed to UV radiation. There is strong evidence of UV-absorbing compounds in the mucus from corals acting as a protection against harmful UV radiation. In mucus composition there are several substances such as mycosporine-like aminoacids (MAA's) which vary from species to species, and its production is dependent on the level of environmental stress (Brown and Bythell, 2005; Rosic and Dove, 2011). It has been shown that the concentration of mycosporine-2-glycine, palythine and mycosporine-glycine increases after exposition to solar radiation (Brown and Bythell, 2005; Rosic and Dove, 2011). In corals, the mucus has several roles including possibly quenching of harmful oxygen radicals as described for mammalian mucosa (Brown and Bythell, 2005; Rosic and Dove, 2011). However, we did not observe antioxidant activity for the cmAE (Figure 4).

Figure 4. The antioxidant activity for the cmAE by DPPH assay. The absorbance was recorded at 30 min, when DPPH reacts with an antioxidant compound that donates hydrogen, it is reduced, resulting in a decrease in the absorbance at 515 nm. Acid Ascorbic was used as a positive control.

Vitamin C at the same concentration cmAE resulted in antioxidant activity of 88.6 %. To determine the uptake capacity of di(phenyl)-(2,4,6-trinitrophenyl)iminoazanium (DPPH) by the cmAE

dissolved in methanol containing 0 to 100 mg/mL. We assessed the antioxidant activity of the cmAE using the stable DPPH assay. Furthermore, we did not observe antibacterial activity for the cmAE (0.78 mg/mL to 100 mg/mL) was tested by agar plate diffusion assay and Minimal inhibitory concentration test against Gram positive Staphylococcus aureus and Enterococcus faecalis bacterial strains and Gram negative Escherichia coli (data not show).

Coral Mucus aqueous extract (cmAE) Reduced Melanin Levels in B16-F10 Cells. The protective role of melanin in the skin is generally against ultraviolet radiation damage. Pigmentation is a protective factor (Kowalczuk et al., 2001). Melanin plays a protective role against UV radiation in human skin by absorbing, scattering, photo-oxidizing, and scavenging free radicals. It also acts as a pseudo-dismutase minimizing the effects of reactive oxygen species and preventing damage to DNA, proteins, and cell membrane lipids (Pattak and Fitzpatrick, 1992). This study investigated the effects of the increase of intracellular melanin content in B16-F10 cells following exposure to UVC radiations (single dose of D = 6.4 mJ/cm^2) and treatment with cmAE (Figure 5).

Figure 5. Effect of intracellular content of melanin B16-F10 cells following exposure to UVC radiation a single dose of D = 6.4 mJ/cm^2 and treatment with 10 mg/mL of cmAE. Intracellular melanin content curve was examined using the content of melanin assay and crystal violet technique, also observed significantly decreased the melanin content of cell lines after treatment with 10 mg/mL cmAE (TG) and significantly increased the melanin content exposure of ultraviolet radiation B16-F10 (IG) compared with controls and in addition significantly reduced levels of melanin induced by UVC radiation to group treated with 10 mg/mL cmAE (TIG), $p < 0.01$. The intracellular melanin content of B16-F10 cells were counted on day 09 in all groups. The data shown are performed in triplicates. Results are means ± S.E.M from four independent experiments. (*statistically significant against the control for $p < 0.05$).

An exponential phase of melanin content increase over time was observed on CG and TG (treated with 10 mg/mL cmAE) (Figure 5). This indicates that the increase of melanin content was proportional to the specific growth rate (μ) and remained constant during the nine days of culture. Nevertheless, in TG the treatment with 10 mg/mL cmAE significantly inhibited the melanin content over time (3-9 days), $p < 0.05$. For the IG, approximately 4 days after exposing B16-F10 cells to UVC radiation we can observe a peak in the melanin content with a 300-fold increase compared to the CG content. In addition, melanin levels induced by UVC radiation significantly decreased in TG treated with 10 mg/mL ($p < 0.01$) and caused a ~24 h delay in the concentration peak of melanin. Our results suggest an antimelanogenic property of the cmAE, even though no antioxidant activity and antimicrobial activity were observed.

First of all, we investigated the effects of cmAE (10 mg/mL) and UVC radiation (6.4 mJ/cm^2) on morphological changes of B16-F10 cells after 48 h, under a confocal fluorescence microscope through DAPI and Phalloidin staining (Figure 6). Typical morphological changes have been identified such as membrane blebbing, cell shrinkage, chromatin condensation, nuclear fragmentation, and apoptotic bodies formation whereas CG cells did not show apoptotic morphological changes (Matsuo et al., 2011; Bajbouj et al., 2012).

Coral Mucus aqueous extract (cmAE) Promote Morphological Changes: Membrane Blebbing, Cell Shrinkage, Chromatin Condensation, Nuclear Fragmentation and the Formation of Apoptotic Bodies. Several in vitro and in vivo studies on skin cells have demonstrated that UV radiation can damage many molecules and structures (Matsuo et al., 2011; Bajbouj et al., 2012). Corroborating these results, our morphological analysis by confocal fluorescence microscopy of B16-F10 cells in CG showed characteristics of nuclear and cytoskeleton integrity. High cellularity was also observed (Figure 6). In contrast, cells exposed to UVC radiation at a single dose of D = 6.4 mJ/cm^2 and treated with 10 mg/mL cmAE (TIG – Figure 4A) presented changes in the

arrangement of actin filaments in the cellular cytoskeleton. Both IG and TG groups presented disruption of the actin filaments, with the formation of blebbing and nuclear fragmentation as a consequence of exposure to UVC radiation.

Figure 6. Confocal Fluorescence microscopy image of B16-F10 cells treated and untreated with coral mucus aqueous extract (cmAE) and UVC radiation. Overlap of images: location of the cell nuclei stained with DAPI (blue) and actin filaments making up the cytoskeleton labeled phalloidin conjugated to Alexa-Fluor 488 (green). CG: control group (A), IG: Irradiated group, UVC radiation a single dose of 6.4 mJ/cm^2 (B); TG: group treated with 10 mg/mL with cmAE and TIG (C): group treated with cmAE and then irradiated (D). DAPI staining was performed. Arrows indicate the cells with DNA fragmentation and membrane blebbing. Scale bars are 20 μm. These images are representative of 5 replicates.

Analysis of Apoptosis in B16-F10 Cells and activation of caspase-3. To clarify whether the inhibitory effect of cmAE on B16-F10 cell growth of is associated with apoptosis, we confirmed the apoptotic characterizations by several approaches such as morphological changes, DNA fragmentation and cell cycle considering hypodiploidic cells (sub-G1 phase) detected by 7-Amino-actinomycin D (7ADD) staining and fluorescence-activated cell sorter (FACS) flow cytometry technique assay, respectively (Figure 2). Another two important biochemical events during apoptosis were analyzed in treated cells: the exposure of phosphatidyl serine on cell surface (Figure 7) measured by the increase in Annexin-V positive cells and the activation of caspase-3, a key mediator of apoptosis (Bajbouj et al., 2012). To determine whether caspase-3 activity is involved in B16-F10 cells apoptosis induced by cmAE, immunofluorescence analysis was performed. Up-regulation of caspase-3 expression upon exposure to UVC radiation (LD85) and similar to IC50 concentration of extracts in B16-F10 was obtained in (Figure 8).

Figure 7. Flow cytometry analysis of apoptosis induced by UVC radiation and/or cmAE in B16-F10 cells. The numbers indicate the percentages of positive cells and fluorescence intensity. Contour diagrams (dot plot) (A, B, C and D) obtained by flow cytometry in B16-F10 cells, labeled with 7AAD (DNA marker) and Annexin - V (marker phosphatidylserine) for all analyses 4h:h after treatment. CG – Control Group (A); IG – Irradiated Group – UVC radiation at a single dose of D = 6.4 mJ/cm^2 (B); TG – Group treated with 10 mg/mL cmAE (C); TIG – Group treated with cmAE and irradiated (D); A control performed with an irrelevant antibody is shown (A). The lower left quadrants shows viable cells, which excluded 7AAD and not stained with Annexin-V. The upper right quadrants represent cells in late apoptosis or necrosis, with double staining for Annexin - V and 7AAD. The left upper quadrants cytograms these represent nonviable cells (7AAD uptake). The cytograms of the right lower quadrants show the apoptotic cells (Annexin -V labeled). In E, mean percentage of apoptotic or necrosis shows the B16-F10 melanoma cell of groups IG (B), TG (C) and TIG (D) significantly higher than CG (A), $p < 0.01$. Quantitative analysis of percentage of apoptotic and/or necrosis cells and there were IG (B) and TG an increase to significantly higher compared to the CG (A) group, $p < 0.01$. Furthermore, the percentage of apoptotic and/or necrosis cell an increase to significantly higher TIG compared to the IG group, $p < 0.05$.

Figure 8. Contour diagrams (dot plot) (E2, F2, C2 and D2) obtained activation of caspase-3 by UVC radiation and/or cmAE by flow cytometry for B16-F10 cells: E2) Control (CG); F2) Irradiated (IG) with the dose of UVC 6.4 mJ/cm^2; G2) treated with 10 mg/mL of cmAE (TG) and H2) treatment with 10 mg/mL with cmAE and exposed to UVC radiation, 6.4 mJ/cm^2 (TIG). A control performed with an irrelevant antibody is shown E2. The percentage of cells exhibiting active caspase-3 is indicated on each histogram. The numbers indicate the percentages of positive cells and fluorescence intensity. The numbers indicate the percentages of positive cells and fluorescence intensity. The results from one representative experiment of four experiments performed are shown. In (E), mean

percentage of cleaved caspase-3 for IG (B), TG (C) and TIG (D) significantly higher than CG (A), $p < 0.01$. Quantitative analysis of percentage of apoptotic and/or necrosis cells and there were IG (B) and TG an increase to significantly higher compared to the CG (A) group, $p < 0.01$. Furthermore, the percentage of activation of caspase-3 protein an increase to significantly higher TIG compared to the IG group, $p < 0.01$. *Data were analyzed with one-way ANOVA followed by Newman Keuls test (significance level $p<0.05$) compared all groups to the control group (CG). Values represent the mean ± SEM of triplicate assays of one experiment representative of four similar results.

The B16-F10 cell treatment with cmAE as well as with UVC radiation revealed high rates of apoptotic cells in all indicated concentrations. Our results indicated that cmAE treatment as well as UVC radiation induced cell death by apoptosis. This apoptosis process was accompanied by activation of caspase-3 expression after B16-F10 cells were treated with cmAE (Figure 8).

The cells exhibiting active caspase-3 effect in all groups compared to TG. Our results showed increased of active caspase-3 for a continuous 10 mg/mL cmAE treatment and for a single UVC radiation dose of 6.4 mJ/cm^2. Once again, more effective caspase-3 activation was observed with the combination of both treatments: cmAE administration and UVC radiation (treated and irradiated group - TIG). These experimental results suggest that up-regulation of caspase-3 expressions by the extracts cmAE may partially account for the cell apoptosis phenomenon in B16-F10 cells. Corroborating these results, Liang et al., 2008 demonstrated that extracts from soft corals Cladiella australis, Clavularia viridis and Klyxum simplex have potent cytotoxic activity and induce apoptosis, with morphological changes in cellular structure in carcinoma cells (SSC, SCC9 and SCC25), typical nuclear condensation, nuclear fragmentation and apoptotic bodies of cells and caspase-3 activation, all typical characteristics of programmed cell death. Flow cytometry indicated that extracts sensitized carcinoma cells in the G0/G1 and S-G2/M phases with a concomitant significantly increased sub-G1 fraction, indicating cell death by apoptosis.

In conclusion: The aqueous extract isolated from the mucus of the Brazilian endemic coral *Mussismilia braziliensis* (cmAE) inhibited B16-F10 cell growth (IC50 10 mg/mL) but did not alter tumor growth rate because tumor cells. Flow cytometry indicated that extracts sensitized B16-F10 cells in the G0/G1 and S-G2/M phases with a concomitant significantly increased sub-G1 fraction, indicating cell death by apoptosis. Moreover induced cell death by apoptosis, as demonstrated by DNA fragmentation, formation of apoptotic bodies and membrane blebbing, all typical characteristics of programmed cell death, similar to the effects induced by UVC radiation (LD85 6.4 mJ/cm^2). Moreover, treatment with cmAE caused a reduction in the mitochondrial activity of B16-F10 cells, inhibiting melanin synthesis even when cells were also exposed to UVC radiation. The cellular response to cmAE treatment, with or without exposure to UVC radiation, provoked altered expression of apoptotic proteins, markedly tumor suppressor protein 53 (p53) upregulation and cleaved caspase-3 activation. Our results showed that cmAE did not have antibacterial activity against Gram positive Staphylococcus aureus, Enterococcus faecalis bacterial strains and Gram negative Escherichia coli. Therefore, cmAE did not have antioxidant and/or photoprotective action in B16-F10 cells exposed to UVC radiation, but increased the cytotoxic activity in B16-F10 cells, inducing caspase-3 and p53-dependent apoptosis.

Various species of corals such as coral *Mussismilia braziliensis* are rich sources of secondary metabolites that may be useful for treatment of human diseases. These compounds may exhibit promising pharmacological properties in the development of anticancer drugs.

Acknowledgments

The authors are grateful to CAPES, CNPq and ETENE / FUNDECI - Banco do Nordeste do Brasil for the joint funding of this research project and to Ministério do Meio Ambiente [Ministry of Environment] (IBAMA License 55098858/2012), especially the Secretaria

Municipal de Meio Ambiente de Porto Seguro [Municipal Secretary of Environment, Porto Seguro] (License 62/2012). The authors wish to thank several of their colleagues working at Universidade Federal de São Paulo and Museu Nacional da Universidade Federal do Rio de Janeiro for their assistance in this project and to Projeto Coral Vivo for their collaboration. To Skin Cell Culture Laboratory, Plastic Surgery Division, Department of Surgery, UNIFESP. To Professor Dr. Helena Bonciani Nader responsible for the laboratory, Multiuser, Molecular Biology, UNIFESP and Professor Dr. Ismael Dale Cotrim Guerreiro da Silva, Laboratory of Molecular Gynecology, UNIFESP.

Conflicts of Interest

The authors declare no conflict of interest.

References

Antônio-de-Souza C (2002). Variação morfométrica de algumas espécies de corais Mussidae (Cnidaria, Atnhozoo) do Brasil. *Tropical Oceanography,* **30,** 14.

Bajbouj K, Schulze-Luehrmann J, Diermeier S, et al (2012). The anticancer effect of saffron in two p53 isogenic colorectal cancer cell lines. *BMC Complement Altern Med,* **12,** 69.

Bartek J, Lukas J (2003). Chk1 and Chk2 kinases in checkpoint control and cancer. *Cancer Cell*, **3,** 421-9.

Bhatnagar I, Kim SK (2010). Immense essence of excellence: marine microbial bioactive compounds. *Mar Drugs,* **8,** 2673-701.

Blunt JW, Copp BR, Munro MH, et al (2004). Marine natural products. *Nat Prod Rep,* **21,** 1-49.

Brown BE, Bythell JC (2005). Perspectives on mucus secretion in reef corals. *Mar Ecol Prog Ser,* **296,** 291-309.

Candida T, Franca JP, Chaves AL et al (2014). Evaluation of antitumoral and antimicrobial activity of Morinda lcitrifolia L. grown in Southeast Brazil *Acta Cir Bras,* **29,** 10-14.

Carrassa L, Broggini M, Erba E, et al (2004). Chk1, but not Chk2, is involved in the cellular response to DNA damaging agents: differential activity in cells expressing or not p53. *Cell Cycle,* **3,** 1177-81.

Cheng YB, Shen YC, Kuo YH, et al (2008). Cembrane diterpenoids from the taiwanese soft coral Sarcophyton stolidotum. *J Nat Prod,* **71,** 1141-5.

Coban AY (2012). Rapid determination of methicillin resistance among Staphylococcus aureus clinical isolates by colorimetric methods. *J Clin Microbiol,* **50,** 2191-3.

Cross CE, Halliwell B, Allen A (1984). Antioxidant protection: a function of tracheobronchial and gastrointestinal mucus. *Lancet,* **1,** 1328-30.

Cunha BL, Franca JP, Moraes AA et al (2014). Evaluation of antimicrobial and antitumoral activity of Garcinia mangostana L. (mangosteen) grown in Southeast Brazil. *Acta Cir Bras,* **29,** 21-28.

Curman D, Cinel B, Williams DE, et al (2001). Inhibition of the G2 DNA damage checkpoint and of protein kinases Chk1 and Chk2 by the marine sponge alkaloid debromohymenialdisine. *J Biol Chem,* **276,** 17914-9.

Danova M, Giordano M, Mazzini G, et al (1990). Expression of p53 protein during the cell cycle measured by flow cytometry in human leukemia. *Leuk Res,* **14,** 417-22.

Delia D, Fontanella E, Ferrario C, et al (2003). DNA damage-induced cell-cycle phase regulation of p53 and p21waf1 in normal and ATM-defective cells. *Oncogene,* **22,** 7866-9.

Fernandes AC, Franca JP, Gaiba S, et al (2014). Development of experimental in vitro burn model. *Acta Cir Bras,* **29,** 15-20.

Folkman J, Hochberg M (1973). Self-regulation of growth in three dimensions. *J Exp Med,* **138,** 745-53.

Fung FM, Ding JL (1998). A novel antitumour compound from the mucus of a coral, Galaxea fascicularis, inhibits topoisomerase I and II. *Toxicon,* **36,** 1053-8.

Gaiba S, Tucci-Viegas VM, Franca LP, et al (2012). Biological Effects Induced by Ultraviolet Radiation in Human Fibroblasts. *In Flow Cytometry - Recent Perspectives,* Ingrid Schmid, InTech, 439-56.

Hao Z, Duncan GS, Su YW, et al (2012). The E3 ubiquitin ligase Mule acts through the ATM-p53 axis to maintain B lymphocyte homeostasis. *J Exp Med,* **209,** 173-86.

Hu GP, Yuan J, Sun L, et al (2011). Statistical research on marine natural products based on data obtained between 1985 and 2008. *Mar Drugs,* **9,** 514-25.

Iwashima M, Matsumoto Y, Takahashi H, et al (2000). New marine cembrane-type diterpenoids from the Okinawan soft coral Clavularia koellikeri. *J Nat Prod,* **63,** 1647-52.
Januar HI, Chasanah E, Motti CA, et al (2010). Cytotoxic cembranes from Indonesian specimens of the soft coral Nephthea sp. *Mar Drugs,* **8,** 2142-52.
Jatkar AA, Brown BE, Bythell JC, et al (2010). Coral mucus: the properties of its constituent mucins. *Biomacromolecules,* **11,** 883-88.
Jemal A, Center MM, Ward E, et al (2009). Cancer occurrence. *Methods Mol Biol,* **471**, 3-29.
Jerant AF, Johnson JT, Sheridan CD, et al (2000). Early detection and treatment of skin cancer. *Am Fam Physician,* **62,** 357-68, 75-6, 81-2.
Kawabe T (2004). G2 checkpoint abrogators as anticancer drugs. *Mol Cancer Ther,* **3,** 513-9.
Kousholt AN, Fugger K, Hoffmann S, et al (2012). CtIP-dependent DNA resection is required for DNA damage checkpoint maintenance but not initiation. *J Cell Biol,* **197,** 869-76.
Kowalczuk C, Priestner M, Baller C, et al (2001). Effect of increased intracellular melanin concentration on survival of human melanoma cells exposed to different wavelengths of UV radiation. *Int J Radiat Biol,* **77,** 883-9.
Laird AK (1964). Dynamics of Tumor Growth. *Br J Cancer,* **13,** 490-502.
Lasithiotakis K, Leiter U, Kruger-Krasagakis S, et al (2006). Comparative analysis of incidence and clinical features of cutaneous malignant melanoma in Crete (Greece) and southern Germany (central Baden-Wurttemberg). *Br J Dermatol*, **154,** 1123-7.
Leao ZM, Kikuchi RK (2005). A relic coral fauna threatened by global changes and human activities, Eastern Brazil. *Mar Pollut Bull*, **51,** 599-611.
Li G, Zhang Y, Deng Z, et al (2005). Cytotoxic cembranoid diterpenes from a soft coral Sinularia gibberosa. *J Nat Prod,* **68,** 649-52.
Li JW, Vederas JC (2009). Drug discovery and natural products: end of an era or an endless frontier? *Science,* **325,** 161-5.
Li WJ, Lin YC, Wu PF, et al (2013). Biofunctional Constituents from Liriodendron tulipifera with Antioxidants and Anti-Melanogenic Properties. *Int J Mol Sci*, **14,** 1698-712.
Liang CH, Wang GH, Liaw CC, et al (2008). Extracts from Cladiella australis, Clavularia viridis and Klyxum simplex (soft corals) are capable of inhibiting the growth of human oral squamous cell carcinoma cells. *Mar Drugs,* **6,** 595-606.
Matsumura Y, Ananthaswamy HN (2004). Toxic effects of ultraviolet radiation on the skin. *Toxicol Appl Pharmacol*, **195,** 298-308.
Matsuo AL, Figueiredo CR, Arruda DC et al (2011).-Pinene isolated from Schinus terebinthifolius Raddi (Anacardiaceae) induces apoptosis and confers antimetastatic protection in a melanoma model. *Biochem Biophys Res Commun,* **411,** 449–54.
Moraes AA, Ferreira AT, Nogueira AP et al (2012). Gamma Radiation Induces p53-Mediated Cell Cycle Arrest in Bone Marrow Cells: InThech.
Newman DJ, Cragg GM (2004). Marine natural products and related compounds in clinical and advanced preclinical trials. *J Nat Prod*, **67,** 1216-38.
Pathak MA, Fitzpatrick TB (1992). The evolution of photochemotherapy with psoralens and UVA (PUVA): 2000 BC to 1992 AD. *J Photochem Photobiol B*, **14.** 3-22.
Prudhomme M (2006). Combining DNA damaging agents and checkpoint 1 inhibitors. *Curr Med Chem Anticancer Agents,* **4,** 435-38.
Prudhomme M (2006). Novel checkpoint 1 inhibitors. *Recent Pat Anticancer Drug Discov,* **1,** 55-68.
Rashid MA, Gustafson KR, Boyd MR (2000). HIV-inhibitory cembrane derivatives from a Philippines collection of the soft coral Lobophytum species. *J Nat Prod,* **63,** 531-3.
Rosic NN, Dove S (2011). Mycosporine-like amino acids from coral dinoflagellates. *Appl Environ Microbiol,* **77,** 8478-86.
Shin SH, Lee YM (2013). Glyceollins, a novel class of soybean phytoalexins, inhibit SCF-induced melanogenesis through attenuation of SCF/c-kit downstream signaling pathways. *Exp Mol Med*, **45,** e17.
Siddiqui EJ, Shabbir MA, Mikhailidis DP, et al (2006). The effect of serotonin and serotonin antagonists on bladder cancer cell proliferation. *BJU Int,* **97,** 634-9.
Su CC, Wong BS, Chin C, et al (2013). Oxygenated Cembranoids from the Soft Coral Sinularia flexibilis. *Int J Mol Sci,* **14,** 4317-25.
Su TR, Lin JJ, Chiu CC, et al (2012a). Proteomic investigation of anti-tumor activities exerted by sinularin against A2058 melanoma cells. *Electrophoresis,* **33,** 1139-52.

Su TR, Tsai FJ, Lin JJ, et al (2012b). Induction of apoptosis by 11-dehydrosinulariolide via mitochondrial dysregulation and ER stress pathways in human melanoma cells. *Mar Drugs*, **10,** 1883-98.
Sullivan PW, Salmon SE (1972). Kinetics of tumor growth and regression in IgG multiple myeloma. *J Clin Invest,* 51, 1697-708.
Sutherland RM, McCredie JA, Inch WR (1971). Growth of multicell spheroids in tissue culture as a model of nodular carcinomas. *J Natl Cancer Inst*, **46,** 113-20.
Vermeulen K, Van Bockstaele DR, Berneman ZN (2003). The cell cycle: a review of regulation, deregulation and therapeutic targets in cancer. *Cell Prolif*, **36,** 131-49.
Wright AD, Goclik E, Konig GM (2003). Oxygenated analogues of gorgosterol and ergosterol from the soft coral Capnella lacertiliensis. *J Nat Prod*, **66,** 157-60.
Xiao Z, Chen Z, Gunasekera AH, et al (2003). Chk1 mediates S and G2 arrests through Cdc25A degradation in response to DNA-damaging agents. *J Biol Chem*, **278,** 21767-73.
Zhang JR, Li PL, Tang XL, et al (2012). Cytotoxic tetraprenylated alkaloids from the South China Sea gorgonian Euplexaura robusta. *Chem Biodivers,* **9,** 2218-24.
Zhao B, Bower MJ, McDevitt PJ, et al (2002). Structural basis for Chk1 inhibition by UCN-01. *J Biol Chem,* **277,** 46609-15.

Development of experimental in vitro burn model[1]

Ana Carolina Morais Fernandes[I], Jerônimo Pereira de França[II], Silvana Gaiba[III], Antonio Carlos Aloise[IV], Andrea Fernandes de Oliveira[V], Andrea Aparecida de Fátima Souza Moraes[VI], Lucimar Pereira de França[II], Lydia Masako Ferreira[VII]

DOI: http://dx.doi.org/10.1590/S0102-86502014001400004

[I]MD. Resident, Burn Care Unit, Plastic Surgery Division, Universidade Federal de São Paulo, São Paulo, SP, Brazil. Technical procedures.
[II]PhD, Associate Professor, Department of Biological Sciences, Universidade Estadual de Santa Cruz, Ilhéus-BA, Brazil. Scientific and intellectual content of the study, interpretation of data and critical revision.
[III]PhD, Fellow Pos-PhD degree, Department of Biological Sciences, Universidade Estadual de Santa Cruz, Ilhéus-BA, Brazil. Technical procedures, acquisition and interpretation of data, manuscript writing.
[IV]PhD, Fellow Pos-PhD degree, Plastic Surgery Division, Universidade Federal de São Paulo, São Paulo, SP, Brazil. Interpretation of data and critical revision.
[V]PhD, Fellow PhD degree, Plastic Surgery Division, Universidade Federal de São Paulo, São Paulo, SP, Brazil. Interpretation of data and critical revision.
[VI]PhD, Department of Biological Sciences, Universidade Estadual de Santa Cruz, Ilhéus-BA, Brazil. Technical procedures.
[VII]Head and Full Professor, Plastic Surgery Division, UNIFESP, Researcher 1A-CNPq, Director Medicine III-CAPES, Sao Paulo-SP, Brazil. Interpretation of data and critical revision.

ABSTRACT

PURPOSE: To propose an experimental burn model in NIH-3T3 cell line.

METHODS: Induction of thermal injury in cultures of mouse fibroblast - NIH-3T3- cell line and determination of cell viability by MTT and imunofluorescence.

RESULTS: The heating of the Petri dish increased proportionally to the temperature of the base and the time of exposure to microwave. In this in vitro burn model, using the cell line NIH-3T3 was observed drastic cellular injury with significant changes in cell viability and activity. It showed drastically modified cell morphology with altered membrane, cytoskeleton and nucleus, and low cellularity compared to the control group.

CONCLUSION: The burn model in vitro using the cell line NIH-3T3 was reproductive and efficient. This burn model was possible to determine significant changes in cell activity and decreased viability, with drastic change in morphology, cell lysis and death.

Key words: Burn; fibroblast; cell line NIH-3T3; microwave; MTT; Confocal microscopy.

Introduction

Burns are responsible for many pathophysiological changes[1-3], represents a severe form of trauma[3,4]. Although there are many advances in knowledge of burn care, treatment is still suboptimal, because there is still lack of studies based on evidence[5].

In order to add knowledge about the pathophysiology and possible therapeutic agents in burns several experimental models can be applied: cell and tissue culture for studies of therapeutic agents mechanism of action and burned tissue substitutes; animal models to evaluate efficacy of therapeutic agents and in vivo study of biological phenomena - and thus allow clinical trials after verification of security aspects[6,7].

In experimental *in vivo* models it is difficult to characterize molecular changes by thermal burns at the cellular level in isolation, since there are many variables involved. Due to the systemic response by thermal injury, especially inflammatory and coagulation cascades, it is difficult to assess only the cellular effect produced by direct stimulation[8].

The objective of this study is to propose an experimental burn model of cultured fibroblasts.

Methods

Cell culture

Mouse fibroblast cell line NIH-3T3 was purchased from ATCC (American Type Culture Collection CRL-1658, Manassas, VA, USA). The cells were maintained at 37 °C in an incubator with a humidified atmosphere of 5 % CO_2 and 95 % O_2 and cultured in Dulbecco's modified eagle's medium (DMEM) with 10% fetal bovine serum (FBS) (Gibco, Grand Island, NY, USA), Gentamicin at 50 µg/mL (Gibco, Grand Island, NY, USA), Amphotericin B at 50 µg/mL (Biolab, São Paulo, SP, Brasil), (Figure 1).

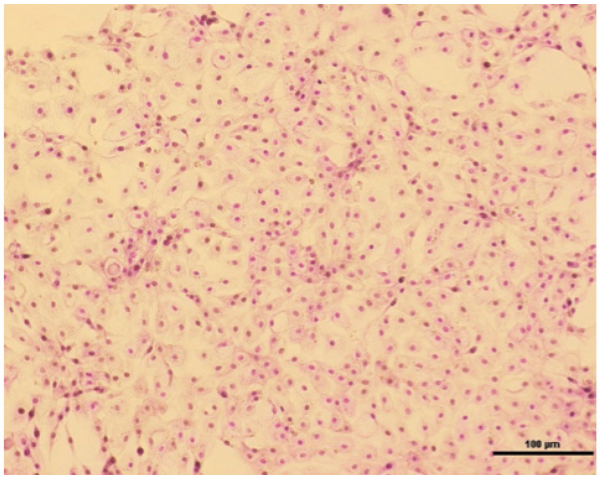

FIGURE 1 - Mouse fibroblast cell line NIH-3T3 culture on culture dish.

Burn in vitro model

Under sterile conditions inside a laminar flow the thermal injury was induced *in vitro* cells using a base of glass plate heated by a microwave oven (Brastemp BMA30A). The cell cultures (Culture dishes) were exposed to thermal injury (burn) by contact with the pre-heated base of glass at a specified temperature (Base inicial temperature – $T_{initial}$ base) in a microwave oven. The medium from the culture plates (Culture dishes) was aspirated and immediately them initial temperature (Dish inicial temperature – $T_{initial}$ dish) was determined. Then the bottom of the culture dish was placed in contact with the base of glass for 30 seconds (Figure 2). After induction of the burn, the final temperature of the base (T_{final} base) and final temperature of the dishes (T_{final} dish) were measured, and culture medium at 4 °C was added to decrease the temperature of the hot dish to stop the burning process.

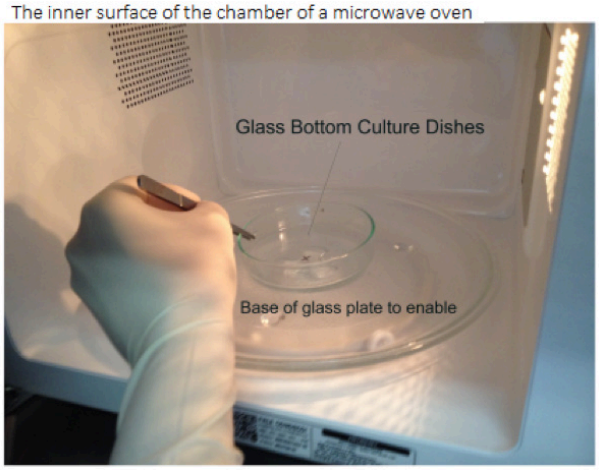

FIGURE 2 - Heating of the base of glass to enabe the heat transfer to the cell culture dishes.

Heating of the base of glass

The heating of the base of glass with thermal capacity (CV = 100.17cal/g.°C) was performed using a microwave oven with potency of 400W or 400J / s, as shown in Figure 3.

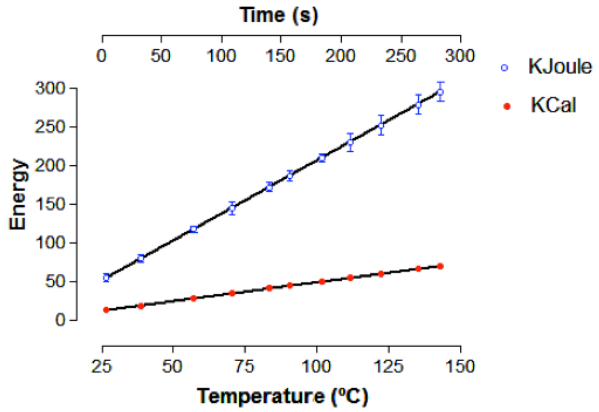

FIGURE 3 - Heat of the base of glass and heat transfer to the dishes with 3T3 line cell culture.

Figure 4 shows the changes in the temperature in the base of glass and the 3T3 cell culture dishes with thermal capacity Cvc = 8.5917 cal/g.°C, after a contact time of 30 seconds.

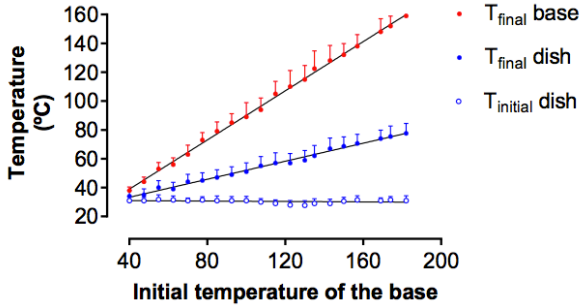

FIGURE 4 - Increase of the temperature of 3T3 culture dish following the transfer of heat from the base of glass to the culture dishes after a contact time of 30 seconds.

Effect of increased temperature on NIH-3T3 cell Viability

Cell viability assay

The effects of thermal injury on cell viability were determined by MTT assay, which is based on the reduction of a tetrazolium salt by mitochondrial dehydrogenase in viable cells. For all experimental groups cells were seeded, after tripsinization and resuspension in medium (DMEM) with Gentamicin at 50 µg/mL (Gibco, Grand Island, NY, USA) and Amphotericin B at 50 µg/mL, in 96-well plates at a density of 1×10^4 cells/well. Then 50 µL of MTT 10% (0.5mg/mL) was added to each well to reach a total reaction volume of 100 µL and the plates were incubated for 2h. Figure 5-A represents NIH-3T3 line cells containing formazan crystals after 2h incubation in MTT. Figure 5-B represents an expanded image where formazan crystals can be observed.

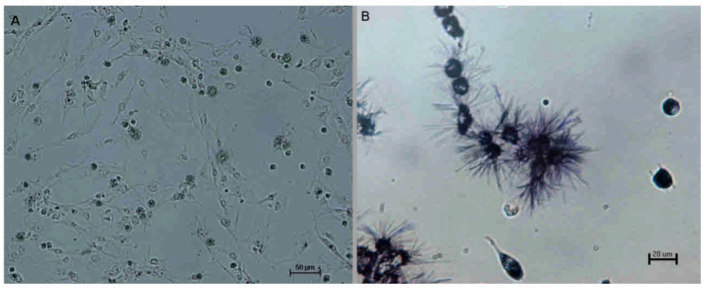

FIGURE 5 - **A**- NIH-3T3 cells 2h after incubation in MTT. **B**- Expanded image shows the formazan crystals.

The resulting formazan crystals were dissolved in 100 µL isopropyl alcohol. Absorbance was measured at 570 nm using a colorimetric MTT ELISA assay (VERSAmax Tunable microplate reader, Molecular Devices, CA, USA), (modified method of Zeng *et al.*[9]). All the experiments were thrice repeated and sample analyses were performed in quadruplicate.

Immunofluorescence labeling

The NIH-3T3 cells were plated on glass coverslips, fixed in 0.4 % paraformaldehyde for 30 min at 4 °C, washed 3 times in PBS. The cells were stained with CellMask™ Deep Red plasma membrane stain, *(1:1000),* Molecular Probe life technologies, *incubation was* performed in PBS containing 10 % normal bovine serum *for 40 min at 22 °C,* washed 3 times in PBS. *Cells were then, permeabilized with 0.1 % saponin in PBS containing 10 % normal bovine serum for 30 min at 22 °C and stained with a combination of fluorescent dyes. Actin filaments F of cytoskeleton were immunostained with phalloidin conjugated with Alexa Fluor 488 (green),* Molecular Probe life technologies. *Phalloidin (1:500) incubation was* performed in PBS containing 10 % normal bovine serum and 0.1 % saponin. Nuclei were counter-stained with blue fluorescent DNA stain DAPI (1:1000), Molecular Probe life technologies, *for 10 min at 22°C*. The images are a composite of 3 images acquired using filter sets appropriate for blue, green and red fluorescence, on a Confocal Laser Scanning Microscope Leica - TCS SP8 (Germany) as adapted from Gaiba et al. (2012).

Statistical analysis

Data are presented as mean ± SD of four independent experiments. Statistical analysis among groups was performed by one-way analysis of variance (ANOVA) followed by the Newman–Keuls Multiple Range Test. GraphPad Prism v.3.0 software was used, $p<0.05$ was considered to be statistically significant.

Results

The MTT test allowed the determination of two graphics curves (two phases), that show an inflection point for the delta temperature of 15 º C (Figure 6).

Morphological analysis of the control group by confocal microscopy (Figure 7).

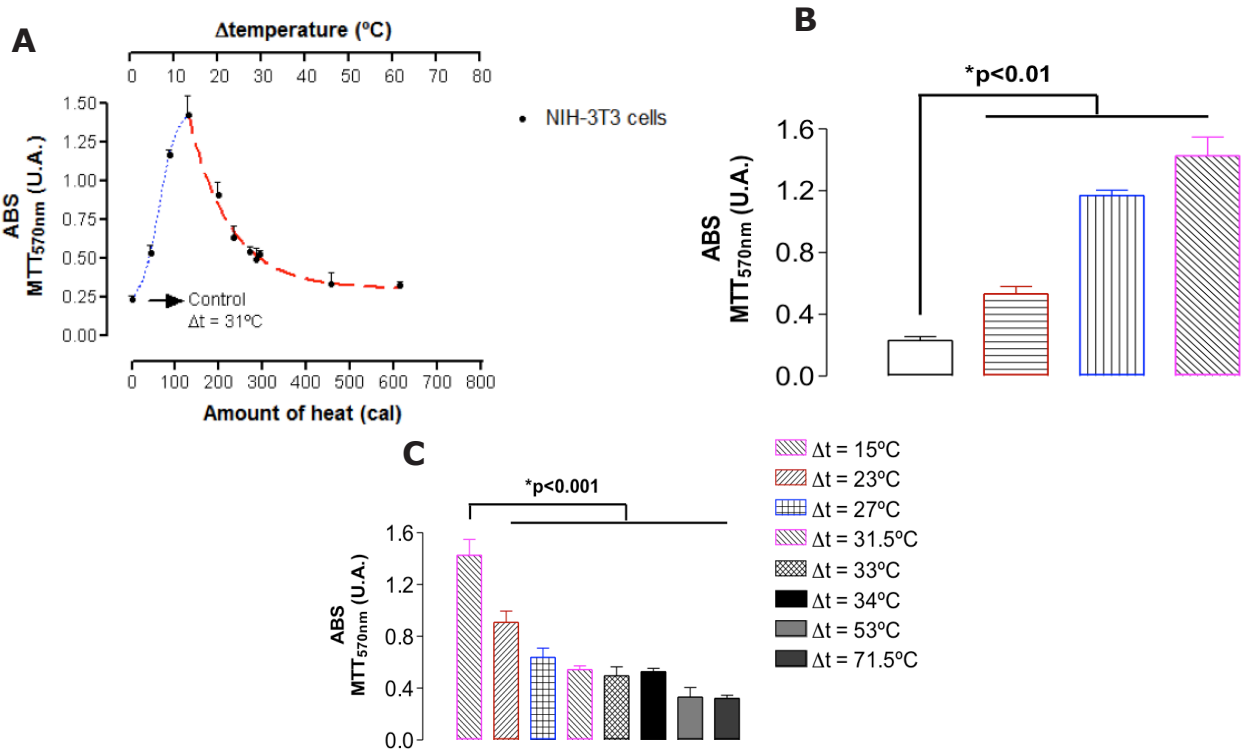

FIGURE 6 - The effects of thermal injury on cell viability determined by MTT assay. A- Represents the MTT assay that determinated two graphics curves (two phases) with an inflection point for the delta temperature of 15 º C. B- Blue line, represents the first phase (up) and the statistic difference of the experimental groups compared to the control group. C- Red line, represents the second phase (down) and the statistic difference of experimental groups compared to the inflection point.

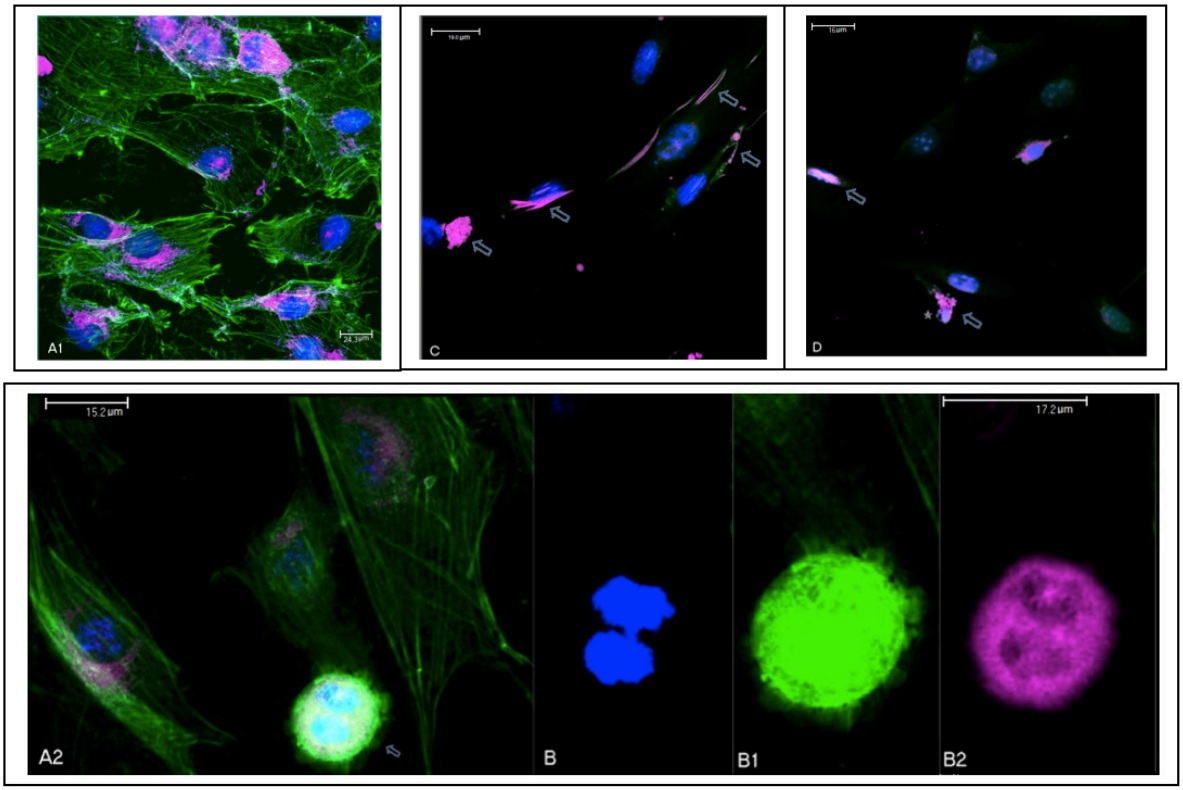

FIGURE 7 - Fluorescence microscopy image of NIH-3T3 cells control and after effects of thermal. Experimental Groups CG: (A1, A2) and microscopy with extended depth of field (B, B1 e B2) and after Heating of the base of glass plate to enabe to heat transfer to the glass botton culture dishes: (C e D). *The cells were stained with CellMask™ Deep Red plasma membrane stain* and location of the cell nuclei stained with DAPI (blue) and actin filaments making up the cytoskeleton labeled phalloidin conjugated to Alexa-Fluor 488 (green), overlap of images (A1, A2, C and D). DAPI staining was performed. Arrows (figure C and D) indicate the cells with DNA fragmentation and membrane blebbing. The star (figure A2) indicates pyknotic nuclei. Arrows (figure A2) indicate the cell division (mitosis) and microscopy with extended depth of field (B, B1 e B2). These images are representative of 5 replicates and 04 independent experiments.

Discussion

Burn process is difficult to study in vivo both in human and animal models. In vitro models have proved to be a valuable tool in the study of skin pathophysiology[10,11]. The exclusion of systemic variables makes the model feasible and repeatable and therefore provides a way to study the cellular and molecular alterations in the burn process[12].

In the literature there are not many in vitro burn experimental models, and none evaluated morphological changes or cell activity and viability.

The burn in vitro model using the NIH 3T3 cell line (Figure 1), under sterile conditions (Figure 2) was reproductive and efficient, allowing to analyze the effect of heat transfer to the base of glass-culture dishes (Figure 3). The process efficiency was achieved by the high thermal capacity of the material (glass) and mainly by the thermal capacity of the glass base that exceed 11x the thermal capacity of the culture plate, allowing the short time of 30 seconds in heat transfer without significant loss of thermal energy.

A high and constant power of the microwave oven is suitable for heating the glass plate, it is observed that the thermal energy (E) increased proportionally to the temperature and the exposure time to microwave (Figure 3). The linearity of the heating curves and the base of the culture plate after heat transfer from the base stated proportionality of the graphic curves corresponding to contact time (Figure 4). In this model it was possible to get in vitro burn lesion, promote cellular injuries with features and significant changes in cellular activity and viability observed by the MTT assay. The MTT assay, Figure 6, allowed the determination of two graphics curves (two phases) that show an inflection point for the delta temperature of 15 º C. These results suggest for the first phase (up) an increase in cellular activity as a linear function of temperature ($r^2 = 0.98$) to the point of inflection (T = 15°C) and then a second exponential decay phase of decrease ($r^2 = 0.98$) until saturation from delta temperature of 46 º C, with a significant decrease in cell viability by heat transfer.

Morphological analysis of cells in the control group showed high cellularity, irregular distribution of cells and formation of characteristic cluster growth of NIH-3T3 line cells; it was also observed extensive cellularity, maintained integrity of the cell nucleus and cytoskeleton and large numbers of cells in mitosis. However, exposed to different delta temperature it was observed drastic decrease in number of cells with large amount of fragmented cells, changes in the structure of the membrane and cytoskeleton (blebbing formation), presence of irregular and pyknotic nuclei and a reduction of number of cells in mitosis, as seen in Figure 7.

Conclusions

The in vitro burn model using the NIH-3T3 line cells was reproductive and efficient. In this model it was possible to get in vitro burns that promoted cellular injuries and significant changes in cellular activity and viability observed by the MTT assay. Also in this model burned cells showed a drastically modified morphology compared to the control group.

References

1. Ashburn MA. Burn pain: the management of procedure-related pain. J Burn Care Rehabil. 1995;16(3 Pt2):365-71.
2. Rosenkranz KM, Sheridan R. Management of the burned trauma patient: balancing conflicting priorities. Burns. 2002;28(7):665-9.
3. Summer GJ, Puntillo KA, Miaskowski C, Green PG, Levine JD. Burn injury pain: the continuing challenge. J Pain. 2007;8(7):533-48.
4. Hawkins A, Maclennan PA, McGwin Jr G, Cross JM, Rue LW, 3rd. The impact of combined trauma and burns on patient mortality. J Trauma. 2005;58(2):284-8.
5. Iurk LK, Oliveira AF, Gragnani A, Ferreira LM. Evidências no tratamento de queimaduras. Rev Bras Queimaduras. 2010;9(3):95-9.
6. Brigham PA, McLoughlin E. Burn incidence and medical care use in the United States: estimates, trends, and data sources. J Burn Care Rehabil. 1996;17(2):95-107.
7. Ferreira LM, Hochman B, Barbosa MV. Experimental models in research. Acta Cir Bras. 2005;20(Suppl 2):28-34.
8. Sobral CS, Gragnani A, Cao X, Morgan JR, Ferreira LM. Human keratinocytes cultured on collagen matrix used as an experimental burn model. J Burns Wounds. 2007;7:e6.
9. Zeng JZ, Zhang LK, Wang HX, Lu LQ, Ma LQ, Tang CS. Apelin protects heart against ischemia/reperfusion injury in rat. Peptides. 2009;30(6):1144-52.
10. Diegelman RF, McCoy BJ, Cohen IK. Growth kinetics and collagen synthesis by keloid fibroblasts in vitro. J Cell Physiol 1979; 98:341-6.
11. McCoy BJ, Cohen IK. Effect of cellular aging and density on cell growth and collagen synthesis in keloid and normal fibroblasts. In vitro. 1982;18:79-86.
12. Emanuelsson P, Kratz G. Characterization of a new in vitro burn wound model. Burns. 1997;23(1):32-6.

Acknowledgements

To Prof. Helena Bonciani Nader responsible for the laboratory, Multiuser, Molecular Biology, UNIFESP and Prof. Ismael Dale Cotrim Guerreiro da Silva, Laboratory of Molecular Gynecology, UNIFESP.

Correspondence:
Lydia Masako Ferreira
Disciplina de Cirurgia Plástica-UNIFESP
Rua Napoleão de Barros, 715/4º andar
04042-002 Sao Paulo - SP Brasil
Tel.: (55 11)5576-4118
Fax: (55 11)5571-6579
sandra.dcir@epm.br
jeronimopf@gmail.com

Financial source: National Council for Scientific and Technological Development (CNPq)

[I]Research performed at Skin Cell Culture Laboratory, Plastic Surgery Division, Department of Surgery, Federal University of Sao Paulo (UNIFESP), Brazil.

Evaluation of antimicrobial and antitumoral activity of Garcinia mangostana L. (mangosteen) grown in Southeast Brazil[1]

Bruna Lais Almeida Cunha[I], Jerônimo Pereira de França[II], Andrea Aparecida de Fátima Souza Moraes[III], Alba Lucilvânia Fonseca Chaves[II], Silvana Gaiba[IV], Renato Fontana[II], Celio Kersul do Sacramento[V], Lydia Masako Ferreira[VI], Lucimar Pereira de França[II]

DOI: http://dx.doi.org/10.1590/S0102-86502014001400005

[I]Graduate Student, Department of Biological Sciences, Universidade Estadual de Santa Cruz, Ilhéus-BA. Technical procedures.
[II]PhD, Associate Professor, Department of Biological Sciences, Universidade Estadual de Santa Cruz, Ilhéus-BA. Scientific and intellectual content of the study, interpretation of data and critical revision.
[III]PhD, Volunteer Faculty, Department of Biological Sciences, Universidade Estadual de Santa Cruz, Ilhéus-BA. Technical procedures, acquisition and interpretation of data.
[IV]PhD, Fellow Pos-PhD degree, Department of Biological Sciences, Universidade Estadual de Santa Cruz, Ilhéus-BA. Technical procedures, acquisition and interpretation of data, manuscript writing.
[V]PhD, Associate Professor, Departament of Agricultural and Environmental Sciences, Universidade Estadual de Santa Cruz, Ilhéus-BA. Interpretation of data and critical revision.
[VI]Head and Full Professor, Plastic Surgery Division, UNIFESP, Researcher 1A-CNPq, Director Medicine III-CAPES, Sao Paulo-SP, Brazil. Interpretation of data and critical revision.

ABSTRACT

PURPOSE: To characterize the anatomy of the fruit and leaf and the presence of phytocompounds. To evaluate the antitumor and antimicrobial activity of ethanolic extract of *Garcinia mangostana* L. (mangosteen) cultivated in southeastern Brazil.

METHODS: Anatomical characterization and histochemical reactions were performed for structural identification and the presence of phytocompounds. Preparation of ethanolic extract of the fruit, leaf and resin of mangosteen. Culture B16-F10 melanoma cells for treatment with mangosteen ethanolic extract to determine cell viability by MTT and genotoxic effect by comet assay. Evaluation by antimicrobial activity against *Staphylococcus aureus* and *Escherichia coli* by agar diffusion test and by determination of Minimum Inhibitory Concentration (MIC).

RESULTS: Our results showed many secretory canals in resin fruit and leaf; identifying lipids, starch, lignin and phenolic compounds. The leaf extract induced genotoxicity and apoptosis in B16-F10 cells, since the fragmentation of DNA in the comet assay. The ethanolic extract of mangosteen obtained in the resin, leaf and fruit showed antimicrobial activity against *Staphylococcus aureus* and *Escherichia coli* with a MIC at 0.1 mg/mL.

CONCLUSION: In conclusion, we have demonstrated both antimicrobial and antitumor activity of ethanol extract of mangosteen emphasizing its therapeutic potential in infectious diseases and in cancer, such as melanoma.

Key words: *Garcinia mangostana* L.; Drug Screening Assays, Antitumor; Anti-Infective Agents; Antimicrobial

Introduction

Cutaneous melanoma is considered the most serious type of skin cancer. It is a highly lethal and very invasive neoplasm, accounting for less than 5 % of all skin cancer cases. Despite its low incidence, it is considered a problem for public health due to the significant raise in the number of cases, exceeding other malignancies growth rate[1-3].

In the last few years there has been growing interest in natural products with biological activity, with relevance to anticancer activity. A large diversity of plants has been extensively investigated, these plants being secondary metabolite producers. These studies on the biotechnological potential of plants sources promising therapeutic agents are mentioned, with antibacterial, antiviral, antitumor and immunossupressive potential[3,4].

Garcinia mangostana L. (mangosteen) is a plant of Asian origin, belonging to the family Clusiaceae. It was introduced into Brazil in 1935 in Bahia, where it is still cultivated[5]. In some populations, especially in their countries of origin, the dried and ground mangosteen rind is used for medicinal purposes against dysentery and chronic diarrhea, besides being used as a homemade dye due to its color[6,7]. The biological activity of the mangosteen is subject of major scientific research, and its pericarp (rind) has been the main structure under study, demonstrating antioxidant[8], antimicrobial[9] and antidepressant activities[10]. Considering the therapeutic potential of the plant, this study aimed to characterize the morphological aspects of *Garcinia mangostana* L. cultivated in Southern Bahia and to evaluate its antimicrobial and antitumoral activity.

Methods

Plant materials and preparation of ethanolic extract

The leaf, fruit and resin of *Garcinia mangostana* L (mangosteen) collection was carried out in the city of Una, Southern region of Bahia, Brazil. Voucher specimens were deposited in the Herbarium of Department of Biological Sciences, University Estadual de Santa Cruz, Bahia, Brazil. The samples were washed with running tap water and separated before the fruit was chopped into pieces. They were oven-dried at 42°C for 5 days and ground to powder.

Plant materials used in this study were fresh fruits (seedless without core), leaf and resin of *Garcinia mangostana* L. The preparation of 70% ethanolic extract of dried plant was obtained by grinding and exposure to organic solvent for 8 days. A suspension of dried fruit (50 g) in water (150 mL) was extracted with ethanol (350 mL). Then, a rotary evaporator was used to remove the remaining alcohol and the aqueous layer and then followed by lyophilization to give water-soluble fractions.

Extraction of gamboge resin

The yellow exudate from the pericarp of the mangosteen fruit known as gamboge[11] resin was obtained after cooling and centrifuging the extract and removing alcohol, which resulted in the precipitation of resin and an aqueous supernatant purple color similar to the external appearance of mangosteen. To ensure the quality of separation of the sample, successive washes and centrifugations was taken until the characteristic yellow color prevailed and there were no other traces of dye.

Anatomical study of the mangosteen pericarp

For the anatomical description of the mangosteen pericarp, 10 μm thick sections were obtained with a rotatory microtome, and the mounted slides were stained with Astra blue and Safranin. The sections were analyzed in Photonic Microscopy (Axiostar model plus, ZEISS), x 200 magnification.

Histochemical of mangosteen pericarp and leaves

The mangosteen pericarp of the fruit and leaves were analyzed for compounds by histochemical reactions with Sudam III, Ferric chloride, Lugol and phloroglucinol acidified for identification of lipids phenolics, starch and lignin, respectively. The freehand cuts were performed with the help of razor (Gillette ®) and placed in contact with the reagent. The micrographs were obtained in Photonic Microscopy (Axiostar model plus, ZEISS), x200 magnification.

Antibacterial activity assay

Antibacterial activity was tested by means of a standard agar plate diffusion assay. Gram positive *Staphylococcus aureus* (CCBM 0324) and Gram negative *Escherichia coli* bacterial strains obtained from the Culture Collection of Microorganisms of Bahia (CCMB), Laboratory of Microbiology, University Estadual de Santa Cruz, Ilhéus, Bahia) were used. Tests were repeated and then calculated at Minimum Inhibitory Concentration (MIC). MIC as recommended by the Institute of Clinical and Laboratory Standards (CLSI, 2007) and adapted[9]. Evaluation of antitumor activity was done by determining the cell growth curve in the presence of the leaf and resin extract at concentrations of 0.1, 1 and 10mg/mL ethanolic extracts of mangosteen.

Antimicrobial test agar diffusion

The antimicrobial test agar diffusion technique was performed by the double layer well described by Groove and Randall[12] with adaptations. For the test we used a strain of *Staphylococcus aureus* obtained from the microbiology laboratory at the UESC. Initially prepared petri dishes containing 25 mL of Mueller-Hinto (MH) agar (HIMEDIA ®) for further use. Also prepared tubes containing 12.5 mL of MH agar, which were placed in a water bath (model 3618/4D, New Ethics ®) at 50ºC to prevent solidification until the time of the procedure. After growth on MH agar culture medium, 5 or 6 colonies were inoculated into 2.5 mL of MH broth, incubated for at 37°C for 6 h, to give a density of microorganisms equivalent to Mac Farland scale (0.5), analyzed in a spectrophotometer (V1600, for analysis ®) at 600 nm, which corresponds to 1,5 x10^8 cells/mL. To perform the procedure, the total volume of the inoculum was transferred to the test tube containing 12.5 mL of MH agar no solidified and immediately after mixing, was transferred to Petri dish previously prepared with agar base, left to stand in laminar flow to solidify. Then, there were perforations (holes) with straws sterile 6 mm, which were filled with 40 µL of mangosteen extract (100, 10 and 1 mg/mL), positive control (penicillin 1,200.000 IU) and negative control (DMSO). The plates remained at room temperature for 2 h in laminar flow, for the diffusion of the mangosteen extract. Subsequently, they were incubated at 37° C in a bacteriological incubator. The zones of growth inhibition were measured with a millimeter ruler in periods 24 and 48 h after mangosteen extract treatment.

Cell culture

The mouse melanoma B16-F10 cell line was purchased from Rio de Janeiro Cell Bank (BCRJ/UFRJ). The cells were maintained at 37 °C in an incubator with a humidified atmosphere of 5 % CO_2 and cultured in DMEM/F12 supplemented with 10 % heat-inactivated FBS, streptomycin (100 µg/mL) and penicillin (100 units/mL).

Cell viability assay

The effects of mangosteen extract treatment on cell viability were determined by MTT assay, which is based on the reduction of a tetrazolium salt by mitochondrial dehydrogenase in viable cells. For all experimental groups, cells were seeded in 96-well plates at a density of 1 × 10^4 cells/well and treated with mangosteen extract concentration 1 to 80 mg/mL for 48 h. After treatment, B16-F10 cells were briefly washed with PBS. A serum-free medium containing 50 µL of MTT stock solution (2 mg/mL) was added to each well to reach a total reaction volume of 250 µL, and the plates were incubated for an additional at 37° C for 4 h. Supernatants were aspirated, and the resulting formazan crystals were dissolved in 150 µL isopropyl alcohol. Absorbance of the product was measured at 540 nm using a colorimetric MTT ELISA assay (VERSAmax Tunable microplate reader, Molecular Devices, CA, USA). The absorbance of the negative control was considered as corresponding to a viability of 100%, and the values of treated cells were calculated as percentage of the control.

Comet assay

The alkaline comet assay was performed as described by Singh et al. (1988)[13] was adapted as follows. The melanoma cell line (B16-F10) was subcultured and seeded in culture bottles. After the process trypsinization, they were transferred to 15 mL Falcon tubes, centrifuged at 1500 rpm for 5 min. Then, the supernatant was discarded and a new aliquot of fresh DMEM/F12 medium was added. The cells were stored until the time of use. During the procedure, the cells were treated with different concentrations of the leaf extract of mangosteen (1,000, 100, and 10 mg/mL) and incubated for 1 hour in a humidified 37° C and 5% CO_2. After treatment, the cell suspension was subjected to centrifugation 1000 rpm at 4°C for 5 min. The supernatant was discarded and the pellet was resuspended (approximately 15 µL) by adding 95 µL low melting agarose at 37° C (0.75%), mixing gently. The samples were transferred to two sheets with agarose precoating normal melting point of 1.5 %. The slides were covered with coverslips, and then taken to the refrigerator for a period of 10 min, in sequence, the coverslips were removed carefully. The slides were then immersed in lysis solution (2.5 M NaCl, 100 mM EDTA, 10°mM TRIS, 1% Triton X-100 and 10 % DMSO, pH = 10.0) at 4°C for 12°h protected from light. After this time, immersed in the electrophoresis alkaline buffer (300 mM NaOH and 1 mM EDTA, pH> 13.0) at 4 °C for 20 min and thus subjected to electrophoresis for 15 min at 25 V and 300 mA. The slides were treated with neutralizing solution (0.4 M Tris-HCl, pH 7.5) for 15 min. Subsequently, we performed two washes with distilled water for 10°min. After neutralization, the slides were dried in an oven overnight at 37° C, fixed with a solution of 1 % acetic acid for 10 min. For coloring material was used solution of 0.05 % ammonium nitrate, 0.05 % silver nitrate, 0.075 % formaldehyde and 0.125 % tungstosílicico acid[14]. The slides were analyzed in photonic microscope (model Axiostar

plus, ZEISS) at 10X magnification. Images of 100 randomly selected cells (50 cells from each of two replicate slides). Cells were scored visually according to tail size (from undamaged – 0, to maximally damaged – 4). Visual scoring of comets is a valid evaluation method determined by international guidelines and recommendations for the comet assay[14,15].

Statistical analysis

Data are presented as mean ± SD of four independent experiments. Statistical analysis among groups was performed by one-way analysis of variance (ANOVA) followed by the Student–Newman–Keuls Multiple Range Test. GraphPad Prism v.3.0 software was used, $p < 0.05$ was considered to be statistically significant.

Results

Fruit and leaf anatomy and histochemistry

The analysis of paraffin-embedded sections and stained with Astra Blue and Safranin demonstrated the presence of large amounts of secretory ducts in the pericarp of fruit, primarily in the mesocarp (Figure 1 A, B).

In the evaluation of histochemical reactions were identified in secretory parenchyma of the central rib, whose contents exhibited the same appearance oxidation occurring in the pericarp (Figure 1 C) the region ducts.

The reaction with Lugol was positive for starch that can be observed in the parenchyma cells of the vascular tissue in the midrib of the leaf. The reaction to Sudam III showed not well defined, with characteristic reaction in the cuticle and uncertainty as to the content of the ducts as seen in fruit. At midrib was also observed the presence of calcium oxalate crystals.

Antimicrobial activity

The agar diffusion test was used for antimicrobial activity against *Staphylococcus aureus* and *Escherichia coli* strains of the ethanolic extract of resin (Figure 2A), leaves (Figure 2B) and pericarp (Figure 2C). For these extracts, the minimum inhibitory concentration (MIC) was also determined, Chart 1.

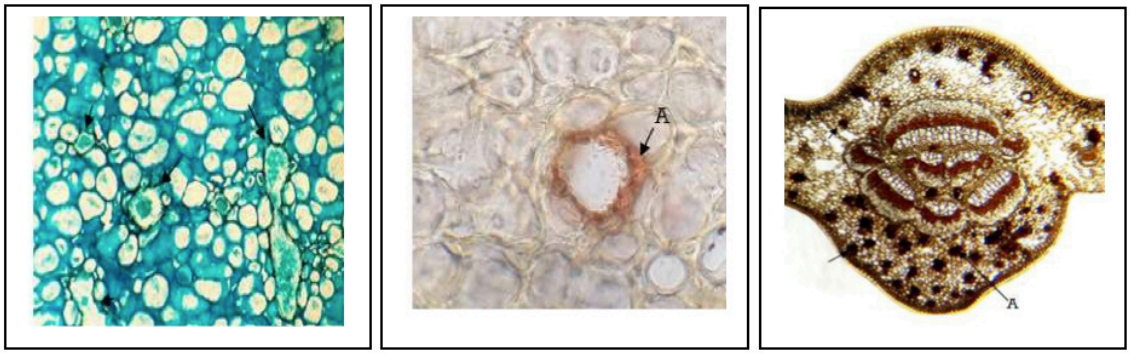

FIGURE 1 - (A) Cross-section of *Garcinia mangostana* L. (mangosteen) fruit showing several secretory ducts (arrows). **(B)** Positive reaction to Sudam III on the lining epithelial cells of secretory ducts. **(C)** Transverse section of the leaf midrib showing ferric chloride reaction.

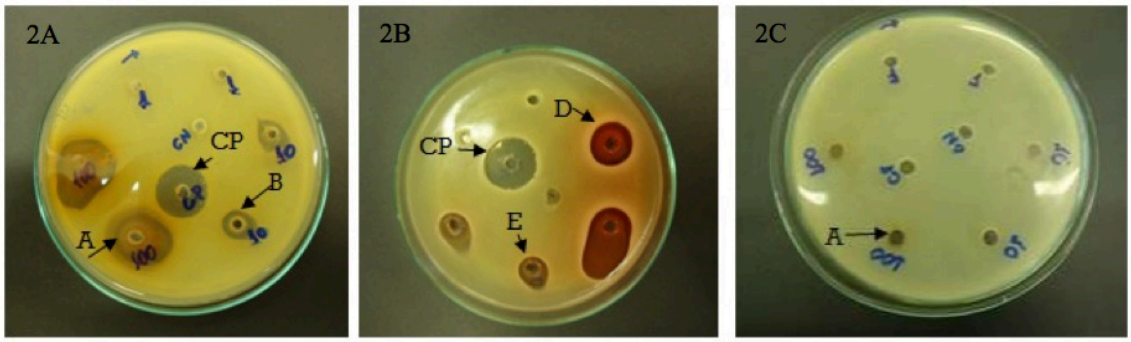

FIGURE 2 - A. Agar diffusion test in the mangosteen pericarp showing the inhibition of each well: 100°mg/mL (A); 10°mg/mL (B); positive control (PC). B. Agar diffusion test of mangosteen leaf showing the inhibition of each well: 100°mg/mL (D); 10°mg/mL (E); positive control (PC). C. Agar diffusion test of mangosteen resin showing the inhibition of each well: 100° mg/mL° (A); positive control (PC).

Agar diffusion test analysis

Chart 1. Agar diffusion test result - perforation technique (holeplate)

X	PERICARP			RESIN			LEAF			CP
Conc.	1 mg	10 mg	100 mg	1 mg	10 mg	100 mg	1 mg	10 mg	100 mg	
Halo (mm)	N	4 mm	10 mm	N	N	1 mm	N	3 mm	5mm	8mm

Cell viability analysis

Antiproliferative and cytotoxic effects of ethanolic extract of mangosteen in B16 - F10 cells. MTT viability test showing the B16-F10 cells treated with ethanolic extract of mangosteen (Figure 3).

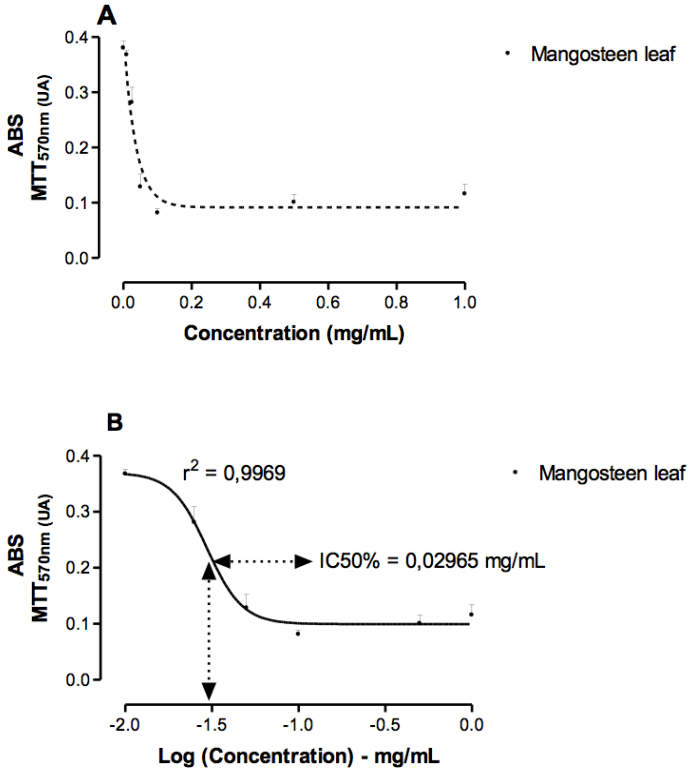

FIGURE 3 - Antiproliferative and cytotoxic effects of ethanolic extract of mangosteen in B16 - F10 cells. MTT viability test showing the B16-F10 cells treated for 48 h with different concentrations of extract (0 - 1 mg/mL) **(A)** and after treatment with extract concentration up to 5 mg/mL significantly reduced the number of cells ($p<0.05$). **(B)** IC50 =0.02965 mg/mL. The MTT data shown are performed in triplicates. Results are means ± S.E.M from four independent experiments (*statistically significant against the control for $p<0.05$).

Genotoxicity analysis by comet assay

The comet assay with ethanolic extract mangosteen leaf showed apoptosis induction in B16-F10, which was evidenced by DNA fragmentation and formation of apoptotic bodies mainly at the concentration of 1 mg/mL (Figure 4).

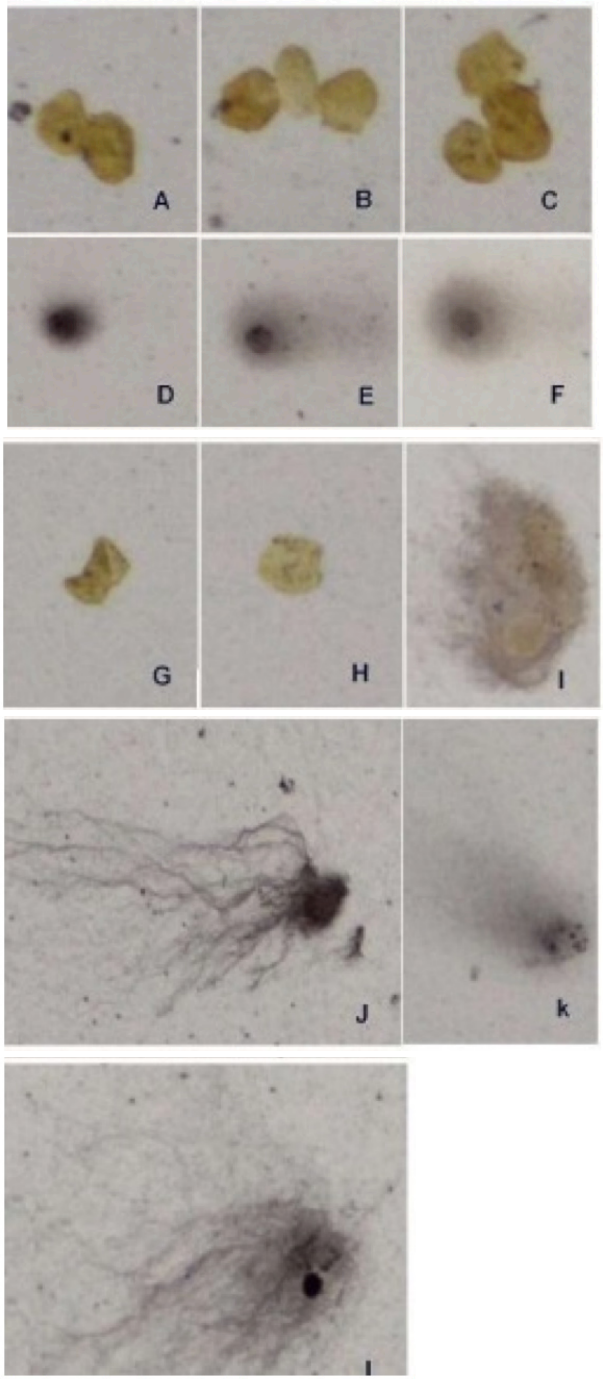

FIGURE 4 - **A**, **B**, **C**. Photomicrograph B16-F10 cells intact observed by microscopy optical, x400 magnification. **D**, **E**, **F**. Photomicrograph B16-F10 cells stimulated with Hydrogen Peroxide (positive control) with the scattering of fragments DNA of the cells. **G**, **H**, **I**. Photomicrograph cells B16-F10 stimulated 0.01 mg/mL of extract mangosteen leaf identifies a small degree of fragmentation and scattering of fragments DNA. **I**, **J**, **L**. Photomicrograph of cells B16-F10 stimulated 0.1 mg/ml of extract mangosteen leaf identifies the intense fragmentation and scattering of fragments DNA. Observe it extensive syrup comet consisting of DNA fragments. **K**. B16-F10 cells stimulated 1 mg/mL of extract mangosteen leaf identified intense fragmentation and scattering of DNA. Observer more points corresponding to the dark formation of apoptotic bodies.

Discussion

Malignant melanoma is a cancer with a high incidence, malignancy and poor prognosis. This cancer is highly metastatic and high mortality rate. Currently, there are no methods or effective drugs for treatment and thus new methods are necessarily expected[1,2].

Malignant melanoma cells exhibit enhanced survival and proliferation capabilities. One of the most important reasons for this is antiapoptosis capacity, which is the predominant problem for clinical tolerance of chemotherapy drugs. Therefore, the identification of an effective drug has been the focus of melanoma treatment[1,2]. Search for new chemopreventive and antitumor agents that are more effective but less toxic has kindled great interest in phytochemicals. Ethanolic extract *Garcinia mangostana* L. fruit is one such compound which was used in this study. *Garcinia mangostana* L is a herbal remedy with promising anticancer properties[10].

Asinelli *et al*.[16] in his work on the ontogeny of *Garcinia gardneriana* species found in southern Brazil, observed numerous secretory ducts and vascular bundles in the ovarian mesophyll, so that the diameter of the ducts increased from the periphery to the center noted that the changes anatomical suffered by this species during development is reported by other authors in species of Clusiaceae family. Souza[17] affirms that for fruits of ovarian origin of the flower, the mesocarp come from ovarian mesophyll, which underlies the results with reference to the earlier work, indicating the presence of ducts as a feature throughout this period of fruit development. Roth[18] confirms the Clusiaceae family as being characterized by the presence of peculiar secretory structures.

For histochemical reactions of the fruit, the pericarp was observed oxidation of this inside the secretory ducts in cuts-control content, interfering with the parameter for evaluating the results. Dorly *et al*.[19] identified as a yellow latex content of secretory ducts present in mangosteen. In young fruit there is a high concentration of tannins, triterpenoids and flavonoids in the pericarp ducts. Roth[18] points out that the brown color of immature fruit when cut is due to the oxidation of tannins.

As macroscopic aspect, the resin presents a yellowish color after transection of fresh fruit. Compounds xanthophylls are yellow[18]. Feng *et al*.[20] indicate the diversity of polipreniladosxanthonóides components that have been isolated from gamboge resin, which possibly explains the characteristic color of this substance. The epithelial cells lining the secretory ducts showed a positive reaction for Sudam III. These cells contain a high density of organelles such as plastids, mitochondria and vesicles of the Golgi complex[19]. The physiological characteristics of these cells may show a positive reaction to Sudam III.

When cross-sectional Garcinia mangostana sheet, it was observed with the naked eye similar to gamboge resin present in the pericarp exudate. In the evaluation of histochemical reactions were identified in secretory parenchyma of the central rib, whose contents exhibited the same appearance oxidation occurring in the pericarp the region ducts. Dorly *et al*.[19] confirmed the presence of secretory ducts gamboge resin parenchymal tissue in the midrib and in the intercellular space between the spongy mesophyll cells. This aspect oxidized caused uncertainty in the identification of a positive reaction, ferric chloride, since the characteristic color is similar in both.

The reaction was positive for the Lugol, can be observed in black-bluish in midrib, featuring positivity. The reaction to Sudam III showed not well defined, with characteristic reaction in the cuticle and uncertainty as to the content of the ducts as indicated in. At midrib was also observed in the presence of calcium oxalate crystals within cells.

Our results show that the rate of proliferation of B16-F10 cells is significantly inhibited by various concentrations of ethanolic extract *mangosteen*. fruit (0 - 1 mg/mL). Following treatment of B16-F10 cells with 10 mg/mL ethanolic extract of mangosteen fruit for 48 h, B16-F10 cells proliferation rate was only 45%.

To evaluate the genotoxic potential of the ethanolic extract *mangosteen*, we performed the comet assay. The comet assay technique use microgel for detecting DNA fragments. The larger number of double strand fragments is greater migration pattern (syrup) seen by Singh *et al*.[13] with better definition in alkaline conditions. The technique of Single Cell Gel Electrophoresis Assay (SCGE) shows the microscope imaging of scattering fragments of DNA became known by Comet Assay. This technique presents to the small number of cells, levels of sensitivity to DNA damage at low cost.

Moreover, the ethanolic extract mangosteen fruit exhibited a genotoxic effect on the B16-F10 cells. The extract of mangosteen induced apoptosis in B16-F10 cells, seen by DNA fragmentation in the comet assay, formation of apoptotic bodies mainly for the concentration of 1 mg/mL It was able to induce fragmentation in DNA and apoptosis the growth of tumor cells in experimental model systems, but little is known about its potential as an adjuvant chemotherapeutic agent[11,21]. Especially considering the antitumoral activity, this fruit can have a major role in the anticancer therapy[11,22].

The ethanolic extract of mangosteen fruit showed bacterial growth inhibition for *Staphylococcus aureus* compared to the positive control Minimum Inhibitory Concentration

(MIC), 1mg/mL determines the lowest concentration that is unanswered to inhibit bacterial growth. Thus, we investigated the bacterial susceptibility of gram-positive *Staphylococcus aureus* to the ethanolic extract of mangosteen. The choice of these microorganisms for the experiments is associated with the routine use of these strains for evaluation of antimicrobial activity. Moreover, these bacteria is human pathogen commonly isolated in Brazilian hospitals, representing 22.8% of isolates and often acquire resistance to antibiotics used[23].

Thus, the search for new antibacterial agents is important for infection control. Our results show that the ethanolic extract of mangosteen has antimicrobial activity, inhibiting the growth of gram-positive bacteria. The ethanolic extract of mangosteen showed MIC ranging 1 mg/mL and 10 mg/mL, showing greater effectiveness against Staphylococcus aureus strain where it exhibited a similar pattern to that caused by the antibiotic Ampicillin, positive control. These data corroborate others authors reported that the antimicrobial activity of the ethanolic extract of mangosteen, showing that its compounds may exhibit potent antibiotic activity against human pathogens[24].

The inhibitory of microbial growth may be attributed to the presence of phenolic compounds in the plant. There is evidence that the ethanolic extract of mangosteen can also submit antituberculosis action, inhibiting the growth of *Mycobacterium turbeculosis*[18]. Moreover, conducted studies demonstrating satisfactory for antihelmintic activity with aqueous and ethanolic extracts of mangosteen fruit. Although we found an inhibitory effect against pathogenic microorganisms, other studies should be performed to confirm and isolate the secondary metabolites that exhibit antimicrobial activity[19].

Conclusions

Garcinia mangostana L (mangosteen) fruit is widely used in alternative medicine for the treatment and prevention of tumors. Currently, there are many pre-clinical trials (animal model or in vitro). These studies have opened new perspectives for the understanding and medical use of this plant. Randomized clinical trials have to be performed to conclusive determination of their effects on human disease. The results obtained with the evaluation of the biological activity of the ethanolic extracts of the fruit, leaves and resin of mangosteen corroborate previous studies concerning its antimicrobial activity. Another observed activity was the potent genotoxic action of the leaf extract, after short exposure of the B16-F10 melanoma cell line. The presence of antimicrobial activity and genotoxic potential in leaves makes further research possible due to the abundance of leaves on the mangosteen tree. The phytocompounds from mangosteen may provide promising improvements in the therapeutic approach to infectious diseases and melanoma treatment.

References

1. Jerant AF, Johnson JT, Sheridan CD, Caffrey TJ. Early detection and treatment of skin cancer. Am Fam Physician. 2000;62(2):357-68, 375-6, 381-2.
2. Lasithiotakis KG, Petrakis IE, Garbe C. Cutaneous melanoma in the elderly: epidemiology, prognosis and treatment. Melanoma Res. 2010 Jun;20(3):163-70.
3. Jemal A, Siegel R, Xu J, Ward E. Cancer statistics, 2010. CA Cancer J Clin. 2010 Sep-Oct;60(5):277-300.
4. Rajamanickam S, Agarwal R. Natural products and colon cancer: current status and future prospects. Drug Dev Res. 2008 Nov 1;69(7):460-71.
5. Sacramento CK, Coelho EJ, Carvalho JEU de, Muller CH, Nascimento WMO do. Cultivo do mangostão no Brasil. Rev. Bras Fruticultura. 2007Abr;29 (1):195-203.
6. Almeyda N, Martin FW. Cultivation of neglected tropical fruits with promise: the mangosteen. Mayaguez: Agricultural Research Service. U.S. Department of Agriculture. 1976.
7. Muller CH. A cultura do mangostão. Brasília: EMBRAPA – SPI; 1995.
8. Jung HA, Su BN, Keller WJ, Mehta RG, Kinghorn AD.Antioxidant Xanthones from the pericarp of Garcinia mangostana. J Agric Food Chem.2006 Fev;54(6):2077-82.
9. Nguyen PT, Marquis RE. Antimicrobial actions of asur-mangostin against oral streptococci. Can J Microbiol. 2011 Mar;57(3):217-25.
10. Gnerre C, Thull U, Gaillard P, Testa B, Fernandez E, Silva F, Pinto M, Pinto MM, Wolfender JL, Hostettmann K, Cruciani, G. Natural and synthetic xanthones as monoamine oxidase inhibitors: biological assay and 3D-DSAR. Helvitica Chimica Acta.2001;84:552-70.
11. Lee SB, Chen CM. United States Patent. Compounds isolated from Gamboge resin having activity in inhibiting the growth of tumor/ cancer cells and pharmaceutical compositions comprising the same. Nº. US 7,138,428, Nov. 21, 2006.
12. Grove DC, Randall WA. Assay methods of antibiotics, a laboratory manual. New York: Medical Encyclopedia, 1995. (Antibiotics monographs, 2).
13. Singh NP, McCoy MT, Tice RR, Schneider EL. A simple technique for quantitation of low levels of DNA damage in individual cells. Exp Cell Res. 1988 Mar;175(1):184-91.
14. Hartmann A, Speit G. The contribution of cytotoxicity to DNA-effects in the single cell gel test (comet assay). Toxicol Lett. 1997;90:183-8.
15. Burlinson B, Tice RR, Speit G, Agurell E, Brendler-Schwaab SY, Collins AR, Escobar P, Honma M, Kumaravel TS, Nakajima M, Sasaki YF, Thybaud V, Uno Y, Vasquez M, Hartmann A; In Vivo Comet Assay Workgroup, part of the Fourth International Workgroup on Genotoxicity Testing. Fourth International Workgroup on Genotoxicity testing: results of the in vivo Comet assay workgroup. Mutat Res. 2007;627:31–5.
16. Asinelli MEC, Souza MC, Mourão KSM. Fruit ontogeny of Garcinia gardineriana (Planch & Triana) Zappi (Clusiaceae). Acta Botanica Bras. 2011 Jan/Mar;25(1):43-52.
17. Souza LA. Morfologia e Anatomia vegetal: célula, tecidos, órgãos e plântulas. Ponta Grossa: UEPG; 2003.
18. Roth I. Fruits of angiosperms. Gebr.Borntraeger; 1977.

Evaluation of antitumoral and antimicrobial activity of Morinda citrifolia L. grown in Southeast Brazil[I]

Thamyris Candida[I], Jerônimo Pereira de França[II], Alba Lucilvânia Fonseca Chaves[II], Fernanda Andrade Rodrigues Lopes[III], Silvana Gaiba[IV], Celio Kersul do Sacramento[V], Lydia Masako Ferreira[VI], Lucimar Pereira de França[II]

DOI: http://dx.doi.org/10.1590/S0102-86502014001400003

[I]Graduate Student, Department of Biological Sciences, Universidade Estadual de Santa Cruz, Ilhéus-BA, Brazil. Technical procedures.
[II]PhD, Associate Professor, Department of Biological Sciences, Universidade Estadual de Santa Cruz, Ilhéus-BA, Brazil. Scientific and intellectual content of the study, interpretation of data and critical revision.
[III]PhD, Nurse Graduate, Department of Biological Sciences, Universidade Estadual de Santa Cruz, Ilhéus-BA, Brazil. Scientific and intellectual content of the study, interpretation of data and critical revision.
[IV]PhD, Fellow Pos-PhD degree, Department of Biological Sciences, Universidade Estadual de Santa Cruz, Ilhéus-BA, Brazil. Technical procedures, acquisition and interpretation of data, manuscript writing.
[V]PhD, Associate Professor, Department of Agricultural and Environmental Sciences, Universidade Estadual de Santa Cruz, Ilhéus-BA, Brazil. Interpretation of data and critical revision.
[VI]Head and Full Professor, Plastic Surgery Division, UNIFESP, Researcher 1A-CNPq, Director Medicine III-CAPES, Sao Paulo-SP, Brazil. Interpretation of data and critical revision.

ABSTRACT

PURPOSE: To evaluate the antitumor and antimicrobial activity of ethanolic extract of *Morinda citrifolia* L. fruit cultivated in southeastern Brazil.

METHODS: Preparation ethanolic extract of the fruit of *Morinda citrifolia* L. Culture of melanoma cells B16-F10 for treatment with ethanolic extract of Morinda citrifolia L. fruit to determine cell viability by MTT and determination temporal effect of ethanolic extract fruit on the cell growth B16-F10 for 8 days. Evaluation of antimicrobial activity of ethanolic extract fruit against *Staphylococcus aureus* and *Escherichia coli* by determination of Minimum Inhibitory Concentration (MIC).

RESULTS: The ethanolic extract of *Morinda citrifolia* L. fruit (10mg/mL) decreased cellular activity and inhibited 45% the rate of cell proliferation of B16-F10 melanoma treated during period studied. The ethanolic extract of *Morinda citrifolia* L. fruit demonstrated antimicrobial activity inhibiting the growth of both microorganisms studied. *Staphylococcus aureus* was less resistant to ethanolic extract of *Morinda citrifolia* L. fruit than *Escherichia coli,* 1 mg/mL and 10 mg/mL, respectively.

CONCLUSION: What these results indicate that the ethanolic extract of the fruit of *Morinda citrifolia* L. showed antitumor activity with inhibition of viability and growth of B16-F10 cells and also showed antibacterial activity as induced inhibition of growth of *Staphylococcus aureus* and *Escherichia coli.*

Key words: *Morinda citrifolia* L.; *Morinda*; Drug Screening Assays Antitumor; Anti-Infective Agents; Antimicrobial.

Introduction

Cutaneous melanoma is considered the most serious type of skin cancer. It is a highly lethal and very invasive neoplasm, accounting for less than 5 % of all skin cancer cases. Despite its low incidence, it is considered a problem for public health due to the significant raise in the number of cases, exceeding other malignancies growth rate[1-3].

In the last few years there has been growing interest in natural products with biological activity, with relevance to anticancer activity. A large diversity of plants has been extensively investigated, these plants being secondary metabolite producers. These studies on the biotechnological potential of plants sources promising therapeutic agents are mentioned, with antibacterial, antiviral, antitumor and immunossupressive potential[3,4].

Morinda citrifolia L, known as Noni, belongs to the Rubiaceae family native to Southeast Asia and secularly used in Polynesian traditional medicine. Noni juice is widely used in complementary medicine due to its probable antioxidant, anti-inflammatory and antitumor effects against diseases such as cancer, atherosclerosis, diabetes and ulcer[5,6].

Products derived from *Morinda citrifolia* L. fruit have been commercialized in the USA since the 1990s and are distributed all over the world. A large number of beneficial effects have been claimed for Noni. However, clinical data are essentially lacking. To what e ffxtent the findings from experimental pharmacological studies are of potential clinical relevance is not clear at present[7].

Many pharmacological studies of *Morinda citrifolia* L juice and isolated compounds from the fruit has been published. These compounds including iridoids, flavonoids, lignans, coumarins and anthraquinones[7,8]. The purposes of this study were to evaluate antioxidant, antitumoral and antimicrobial activity of ethanolic extract from *Morinda citrifolia* L. fruit grown in Southeast Brazil.

Methods

Plant materials and preparation of ethanolic extract

The fruits of *Morinda citrifolia* L. were collect in the campus of the State University of Santa Cruz, Bahia, Brazil. Voucher specimens were deposited in the Herbarium of Department of Biological Sciences, State University of Santa Cruz, Bahia, Brazil. The samples were washed with running tap water and separated before being chopped into pieces. They were oven-dried at 42 °C for 5 days and ground to powder.

Plant materials used in this study were fresh fruits (seedless without core) of *Morinda citrifolia* L.. The preparation of 70% ethanolic extract of dried fruit (50 g) was obtained by grinding and exposure to organic solvent. A suspension of dried fruit (50 g) in water (150 mL) was extracted with ethanol (350 mL) for 8 days. The aqueous layer was evaporated and then followed by lyophilization to give a water-soluble fraction.

Cell Culture

The mouse melanoma B16-F10 cell line was purchased from Rio de Janeiro Cell Bank (BCRJ/UFRJ). The cells were maintained at 37 °C in an incubator with a humidified atmosphere of 5 % CO_2 and cultured in DMEM/F12 supplemented with 10 % heat-inactivated FBS, streptomycin (100 µg/mL) and penicillin (100 units/mL).

Effect of ethanolic extract of Morinda citrifolia L on B16-F10 cell growth inhibition

B16-F10 cells at 80% confluence, the cells were harvested with trypsin, and serum-free medium was used to obtained a single-cell suspension. The cells were then seeded in 06-well plates at a density of 200,000 cells/well. After 24 h, the wells were replaced with fresh medium, including FBS. Next, the wells were treated with 10mg/mL ethanolic extract of *Morinda citrifolia* L. and the cell numbers were counted following 1-8 days. A control group was prepared simultaneously and a growth curve was generated.

Cell Viability Assay

The effects of Noni extract treatment on cell viability were determined by MTT assay, which is based on the reduction of a tetrazolium salt by mitochondrial dehydrogenase in viable cells. For all experimental groups, cells were seeded in 96-well plates at a density of 1 × 104 cells/well and treated with Noni extract at a final concentration of 1 to 80mg/mL . After 48 h, 50 µL of MTT stock solution (2 mg/mL) was added to each well to reach a total reaction volume of 250 µL, and the plates were incubated for an additional 4 h. Supernatants were aspirated, and the resulting formazan crystals were dissolved in 150 µL isopropyl alcohol. Absorbance was measured at 540 nm using a colorimetric MTT ELISA assay (VERSAmax Tunable microplate reader, Molecular Devices, CA, USA).

Antibacterial activity assay

Antibacterial activity was tested by means of a standard agar plate diffusion assay. Gram positive Staphylococcus aureus (CCBM 0324) and Gram negative Escherichia coli bacterial

strains (obtained from the Culture Collection of Microorganisms of Bahia (CCMB), Laboratory of Microbiology, University Estadual de Santa Cruz, Ilhéus) were used. Tests were repeated and was calculated at Minimum Inhibitory Concentration (MIC). MIC as recommended by the Institute of Clinical and Laboratory Standards (CLSI, 2007) and adapted[9]. Evaluation of antitumor activity was done by determining the cell growth curve in the presence of 10mg/mL ethanolic extracts of *Morinda citrifolia* L.

Statistical Analysis

Data are presented as mean ± SD of four independent experiments. Statistical analysis among groups was performed by one-way analysis of variance (ANOVA) followed by the Student–Newman–Keuls Multiple Range Test. GraphPad Prism v.3.0 software was used, $p < 0.05$ was considered to be statistically significant.

Results

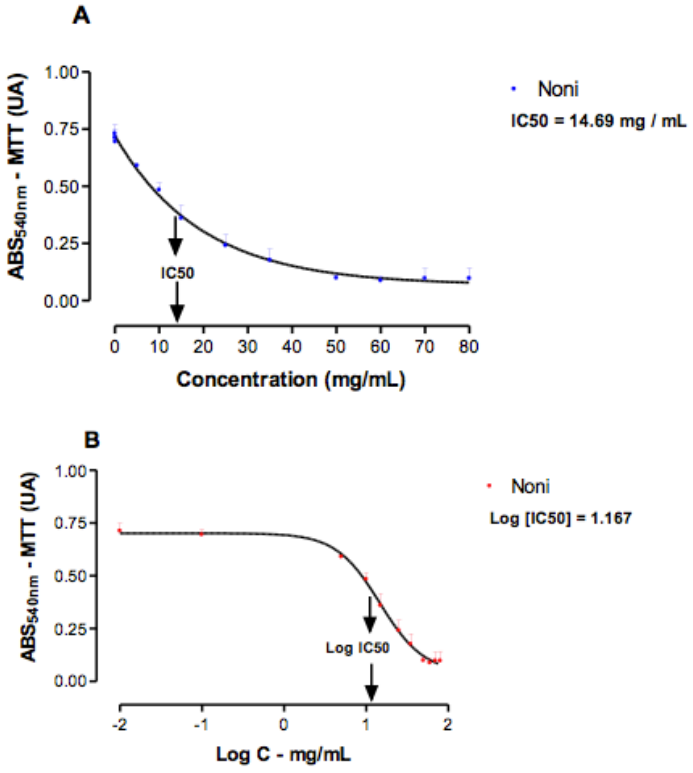

FIGURE 1 - Antiproliferative and cytotoxic effects of ethanolic extract of *Morinda citrifolia* L in B16-F10 cells. MTT viability test showing the B16-F10 cells treated for 48 h with different concentrations of extract (0 - 80 mg/mL) (A) and after treatment with extract concentration up to 5 mg/mL significantly reduced the number of cells ($p < 0.05$). (B) –Log [IC50]=1.167. The MTT data shown are performed in triplicates. Results are means ± S.E.M from four independent experiments. (*statistically significant against the control for $P < 0.05$).

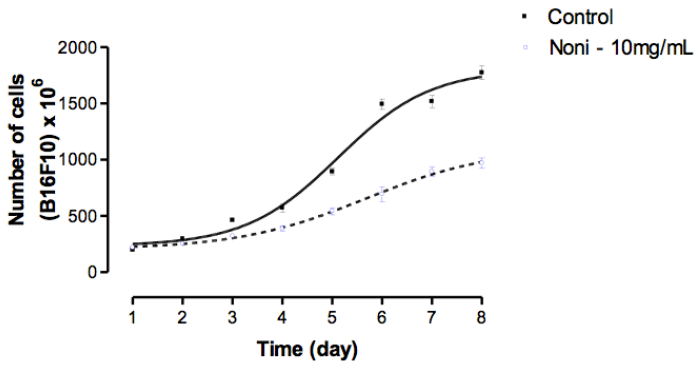

FIGURE 2 - Inhibitory activity of 10mg/mL ethanolic extract of *Morinda citrifolia* L on B16-F10 cell growth. The upper line of the graph presents the control group without ethanolic extract of *Morinda citrifolia* L treatment and the bottom line presents the group treated with ethanolic extract. At the end of each time-period, the cells were trypsinized to produce a single cell suspension and the cell number was counted. Data are presented as the mean ± standard error of the mean.

CHART 1 - Minimum Inhibitory Concentration (MIC) results; + = inhibitory concentration.

Strains	Concentration		
	10mg/mL	1mg/mL	0.1mg/mL
Staphylococcus aureus	-	+	-
Escherichia coli	+	-	-

Discussion

Malignant melanoma is a cancer with a high incidence, malignancy and poor prognosis. This cancer is highly metastatic and high mortality rate. Currently, there are no methods or effective drugs for treatment and thus new methods are necessarily expected[1,2].

Malignant melanoma cells exhibit enhanced survival and proliferation capabilities. One of the most important reasons for this is antiapoptosis capacity, which is the predominant problem for clinical tolerance of chemotherapy drugs. Therefore, the identification of an effective drug has been the focus of melanoma treatment[1,2]. Search for new chemopreventive and antitumor agents that are more effective but less toxic has kindled great interest in phytochemicals. Ethanolic extract *Morinda Citrifolia* L. fruit is one such compound which was used in this study. Morinda citrifolia L is a herbal remedy with promising anticancer properties[10].

Our results show that the rate of proliferation of B16-F10 cells is significantly inhibited by various concentrations of ethanolic extract *Morinda Citrifolia* L. fruit (0 - 80 mg/mL) (Figure 1).

Following treatment of B16-F10 cells with 10 mg/mL ethanolic extract of fruit *Morinda citrifolia* L. for 8 days, the cell proliferation rate was only 45% (Figure 2). Moreover, the time-dependent assay confirmed ethanolic extract *Morinda citrifolia* L. fruit exhibited a longlasting suppressive effect on the B16-F10 cells.

It has shown to inhibit the growth of tumor cells in experimental model systems, but little is known about its potential as an adjuvant chemotherapeutic agent[11-14].

The ethanolic extract of *Morinda citrifolia* L. fruit showed bacterial growth inhibition for *Staphylococcus aureus* and *Escherichia coli* compared to the positive control (Chart 1) Minimum Inhibitory Concentration (MIC), 1mg/mL determines the lowest concentration that is unanswered to inhibit bacterial growth. Thus, we investigated the bacterial susceptibility of gram-positive (*Staphylococcus aureus*) and Gram-negative (*Escherichia coli*) to the ethanolic extract. The choice of these microorganisms for the experiments is associated with the routine use of these strains for evaluation of antimicrobial activity. Moreover, these bacteria are human pathogens commonly isolated in Brazilian hospitals, representing 22.8% and 13.8% of isolates, respectively and often acquire resistance to antibiotics used (15)[14].

Thus, the search for new antibacterial agents is important for infection control. Our results show that the ethanolic extract of *Morinda citrifolia* L. has antimicrobial activity, inhibiting the growth of both gram-positive as gram-negative bacteria. The extract showed MIC ranging 1 mg /mL and 10 mg/mL, showing greater effectiveness against Staphylococcus aureus strains (Chart 1) where it exhibited a similar pattern to that caused by the antibiotic inhibition Ampicillin. For strain of Escherichia coli MIC was 10 mg/mL (Chart 1). These data corroborate others authors reported that the antimicrobial activity of the extract of *Morinda citrifolia* L, showing that its compounds may exhibit potent antibiotic activity against human pathogens such as *Staphylococcus aureus, Bacillus subtilis, Escherichia coli, Pseudomonas aeruginosa, Salmonella and Shigella*[16,17].

The inhibitory of microbial growth may be attributed to the presence of phenolic compounds in the plant. There is evidence that the Noni extract can also submit antituberculosis action, inhibiting the growth of *Mycobacterium turbeculosis*[18]. Moreover, conducted studies demonstrating satisfactory for antihelmintic activity with aqueous and ethanol extracts of *Morinda citrifolia* L. fruit. Although we found an inhibitory effect against pathogenic microorganisms, other studies should be performed to confirm and isolate the secondary metabolites that exhibit antimicrobial activity[19].

Morinda citrifolia L fruit is widely used in alternative medicine for the treatment and prevention of tumors. Currently, there are many pre-clinical trials (animal model or in vitro). These studies have opened new perspectives for the understanding and medical use of this plant. Randomized clinical trials have to be performed to conclusive determination of their effects on human disease. Especially considering the antitumoral activity, this fruit can have a major role in the anticancer therapy[10].

Conclusions

The ethanolic extract *Morinda citrifolia* L. fruit induce cell growth inhibition on *Staphylococcus aureus* and *Escherichia coli* and cell growth inhibition on B16-F10 cells. Considering the acquire resistance to antibiotics used and chemoresistance exhibited by melanoma towards conventional chemotherapy drugs, this novel compound may provide promising improvements in the therapeutic approach to infectious diseases and melanoma treatment.

References

1. Jerant AF, Johnson JT, Sheridan CD, Caffrey TJ. Early detection and treatment of skin cancer. Am Family Physician. 2000;62(2):357-68.
2. Lasithiotakis KG, Petrakis IE, Garbe C. Cutaneous melanoma in the elderly: epidemiology, prognosis and treatment. Melanoma Res. 2010 Jun;20(3):163-70.
3. Jemal A, Siegel R, Xu J, Ward E. Cancer statistics, 2010. CA Cancer J Clin. 2010 Sep-Oct;60(5):277-300.
4. Rajamanickam S, Agarwal R. Natural products and colon cancer: current status and future prospects. Drug Dev Res. 2008 Nov 1;69(7):460-71.
5. Wang MY, West BJ, Jensen CJ, Nowicki D, Su C, Palu AK, Anderson G. Morinda citrifolia (Noni): a literature review and recent advances in Noni research. Acta Pharmacol Sin. 2002 Dec;23(12):1127-41.
6. Chan-Blanco Y, Vaillant F, Perez AM, Reynes M, Brillouet J, Brat P. The fruit Noni (Morinda citrifolia L.). J Foot Comp Anal. 2006;19:645-54.
7. Potterat O, Hamburger M. Morinda citrifolia (Noni) fruit--phytochemistry, pharmacology, safety. Planta Med. 2007 Mar;73(3):191-9.
8. Mohamed MF, Frye RF. Effects of Herbal Supplements on Drug Glucuronidation. Review of Clinical, Animal, and In Vitro Studies. Planta Med 2011;77:311–21.
9. Coban AY. Rapid determination of methicillin resistance among Staphylococcus aureus clinical isolates by colorimetric methods. J Clin Microbiol. 2012;50(7):2191-3.
10. Baiju M, Mathews PP, Skariah KS, Ambika K. Morinda Citrifolia - Noni: A brief review of its anti cancer activity. Health Sci. 2012;1(3):JS004B.
11. Kamei H, Koide T, Kojima T, Hashimoto Y, Hasegawa M. Inhibition of cell growth in culture by quinones. Cancer Biother Radiopharm. 1998 Jun;13(3):185-8.
12. Hiramatsu T, Imoto M, Koyano T, Umezawa K. Induction of normal phenotypes in ras-transformed cells by damnacanthal from *Morinda citrifolia*. Cancer Lett. 1993 Sep 30;73(2-3):161-6.
13. Liu G, Bode A, Ma WY, Sang S, Ho CT, Dong Z. Two novel glycosides from the fruits of *Morinda citrifolia* (Noni) inhibit AP-1 transactivation and cell transformation in the mouse epidermal JB6 cell line. Cancer Res. 2001 Aug 1;61(15):5749-56.
14. Taşkin EI, Akgün-Dar K, Kapucu A, Osanç E, Doğruman H, Eraltan

H, Ulukaya E. Apoptosis-inducing effects of Morinda citrifolia L. and doxorubicin on the Ehrlich ascites tumor in Balb-c mice. Cell Biochem Funct. 2009 Dec;27(8):542-6., 27, 542-6.

15. Sader HS, Mendes RE, Gales AC, Jones RN, Pfaller MA, Zoccoli C, Sampaio J. Perfil de sensibilidade a antimicrobianos de bactérias isoladas do trato respiratório baixo de pacientes com pneumonia internados em hospitais brasileiros - Resultados do Programa SENTRY, 1997 e 1998. J Bras Pneumol. 2001;27(2):59-67.
16. Mohtar M, Shaari K, Ali NAM, Ali AM. Antimicrobial activity of selected Malaysian plants against micro-organisms related to skin infection. J Tropical Forest Products. 1998;4:(2):199-206.
17. Jayasinghe UL, Jayasooriya CP, Bandara BM, Ekanayake SP, Merlini L, Assante G. Antimicrobial activity of some Sri Lankan Rubiaceae and Meliaceae. Fitoterapia. 2002 Aug;73(5):424-7.
18. Serafini MR, Santos RC, Guimarães AG, Dos Santos JP, da Conceicão Santos AD, Alves IA, Gelain DP, de Lima Nogueira PC, Quintans-Júnior LJ, Bonjardim LR, de Souza Araújo AA. *Morinda citrifolia* Linn leaf extract possesses antioxidant activities and reduces nociceptive behavior and leukocyte migration. J Med Food. 2011 Oct;14(10):1159-66.
19. Brito DR, Fernandes RM, Fernandes MZ, Ferreira MD, Rolim FR, da Silva Filho ML. Anthelmintic activity of aqueous and ethanolic extracts of *Morinda citrifolia* fruit on Ascaridia galli. Rev Bras Parasitol Vet. 2009 Oct-Dec;18(4):32-6.

Acknowledgements

To Skin Cell Culture Laboratory, Plastic Surgery Division, Department of Surgery, UNIFESP.

Correspondence:
Lucimar Pereira de França
Departamento de Ciências Biológicas
Universidade Estadual de Santa Cruz-UESC
Rod. Jorge Amado, Km 16
45662-900 Ilhéus - Bahia Brasil
Tel./Fax: (55 73)3680-5360
lucimarfrancap@gmail.com
jeronimopf@gmail.com

National Council for Scientific and Technological Development (CNPq), Bahia Research Foundation (FAPESB) and ETENE/FUNDECI- Banco do Nordeste do Brasil

[I]Research performed at Biophysic Cellular and Molecular Laboratory, State University of Santa Cruz (UESC), Brazil.

19. Dorly S, Rodoedhypoerwanto J. secretory duct structure and phytochemistry compounds of yellow latex in mangosteen fruit. HAYATI J Biosciences. 2008;15(3):99-104.
20. Feng F, Liu WY, Chen YS, Guo QL, You QD. Five novel prenylatedxanthones from Resina Garciniae. J Asian Nat Prod Res. 2007 Sep-Dec;9(6-8):735-41.
21. Matsumoto K, Akao Y, Kobayashi E, Ohguchi K, Ito T, Tanaka T, Nozawa Y. Induction of apoptosis by xanthones from mangosteen in human leukemia cell lines. J Nat. Prod. 2003 Jul;66(8):1124-7.
22. Akao y, Nakagawa Y, Nozawa Y. Anti-cancer effects of xanthones from pericarps of mangosteen. Int J Mol Sci. 2008 Mar;9 (3):335-70.
23. Sader HS, Mendes RE, Gales AC, Jones RN, Pfaller MA, Zoccoli C, Sampaio J. Perfil de sensibilidade a antimicrobianos de bactérias isoladas do trato respiratório baixo de pacientes com pneumonia internados em hospitais brasileiros - Resultados do Programa SENTRY, 1997 e 1998. J Bras Pneumol. 2001;27(2):59-67.
24. Jung HA, Su BN, Keller WJ, Mehta RG, Kinghorn AD. Antioxidant Xanthones from the pericarp of Garcinia mangostana. J Agric Food Chem. 2006 Fev;54(6):2077-82.

Acknowledgements

To the Skin Cell Culture Laboratory, Plastic Surgery Division, Department of Surgery, UNIFESP.

Correspondence:
Lucimar Pereira de França
Departamento de Ciências Biológicas
Laboratório de Biofísica Celular e Molecular
Universidade Estadual de Santa Cruz-UESC
Rodovia Jorge Amado, Km 16
45662-900 Ilhéus - Bahia Brazil
Tel./Fax: (55 73)3680-5360
lucimarfrancap@gmail.com
jeronimopf@gmail.com

National Council for Scientific and Technological Development (CNPq), Bahia Research Foundation (FAPESB) and ETENE/FUNDECI- Banco do Nordeste do Brasil

[1]Research performed at Laboratory of Molecular and Cellular Biophysics, State University of Santa Cruz (UESC), Brazil.

Cent. Eur. J. Biol. • 9(7) • 2014 • 717-726
DOI: 10.2478/s11535-014-0301-6

VERSITA

Central European Journal of **Biology**

The action of CGRP and SP on cultured skin fibroblasts

Review Article

Bernardo Hochman[1]*, Vanina M Tucci-Viegas[1,2], Paola KP Monteiro[1], Jerônimo P França[3], Silvana Gaiba[1,3], Lydia M Ferreira[1]

[1]*Plastic Surgery Division, Department of Surgery, Postgraduate Program in Translational Surgery, Universidade Federal de São Paulo (Unifesp), 04024-002 - São Paulo/SP, Brazil*

[2]*Department of Agricultural and Environmental Sciences, Universidade Estadual de Santa Cruz (UESC), 45662-900 - Ilhéus/BA, Brazil*

[3]*Department of Biological Sciences, Universidade Estadual de Santa Cruz (UESC), 45662-900 - Ilhéus/BA, Brazil*

Received 12 October 2013; Accepted 22 December 2013

Abstract: Background/purpose: Calcitonin gene-related peptide (CGRP) is the most abundant neuropeptide in the skin, followed by substance P (SP), vasoactive intestinal peptide (VIP), and other neuropeptides in smaller amounts. The proliferative effect of neuropeptides on fibroblasts may affect wound healing and may be associated with hyperproliferative skin and mesenchymal disorders. Understanding the neuropeptidergic action on fibroblasts may provide relevant information to a deeper comprehension of the healing process. This study reviews the action of the main neuropeptides, CGRP and SP, on cultured human skin fibroblasts. Methods: A systematic literature search was conducted on Medline and Web of Science databases on December 21, 2013. Results: A total of 74 articles were retrieved using the proposed search strategies and 3 were found in the references section of the selected articles. Thirteen of the retrieved articles studied the action of CGRP and SP on cultured human skin fibroblasts, 12 of which related to SP and 1 related to both CGRP and SP. Conclusion: Only one study was retrieved about the action of both CGRP and SP on cultured human skin fibroblasts. Further studies are necessary to investigate CGRP on skin fibroblasts and its role in the fibroplasia phase of wound healing.

Keywords: *Calcitonin gene-related peptide • Substance P • Fibroblasts • Wound healing • Skin*

1. Key points:

- Neurogenic inflammation promotes the release of cytokines and growth factors, inducing extracellular matrix synthesis by fibroblasts in the healing phase. Neurogenic inflammation has a direct modulator effect on the subsequent phases of the healing process, especially on the proliferative phase.
- Neuropeptides, especially CGRP and SP, probably have a specific and active participation in the process of fibrosis, and directly act in the proliferative phase of wound healing.
- CGRP is the most abundant neuropeptide in the skin, followed by SP, VIP, and other neuropeptides in smaller amounts.
- The aim of this study was to review the action of the main neuropeptides, CGRP and SP, on cultured human skin fibroblasts.
- VIP and CGRP, alone or in combination with SP, stimulate the proliferation of murine and human keratinocytes; however, the functional role of VIP and CGRP in skin fibroblasts is not well defined.
- SP is one of the most potent vasodilators; it releases nitric oxide from endothelial cells. This effect is 100 times more potent than that of histamine at similar concentrations. SP produces erythema and edema in a dose-dependent manner, but unlike CGRP, it induces plasma extravasation.
- Unlike CGRP, SP induces human mast cell degranulation with release of histamine.
- SP also induces proliferation of human dermal fibroblasts and human and murine keratinocytes and stimulates neovascularization *in vivo* and proliferation of endothelial and smooth muscle cells.
- SP and CGRP are frequently present in the same nerve fiber. SP release may induce the co-release

* *E-mail: bernardo@queloide.com.br*

of CGRP, which in turn may enhance the action of SP, although CGRP may have long-lasting effects. The release of SP or CGRP may induce an increase in the levels of SP receptors.

- The fact that human skin fibroblasts express neuropeptides receptors suggests that they may respond to SP and other neuropeptides. For instance, exogenous SP was shown to induce autocrine production of SP by human skin fibroblasts.
- Human skin fibroblasts express mRNA for RAMP1, indicating that these cells have low-expression of (but still express) CGRP receptors.
- The ability of SP to induce synthesis and proliferation of human dermal fibroblasts and keratinocytes is well known. SP was shown to increase human fibroblasts proliferation in a concentration-dependent manner. The addition of SP to cultured human dermal fibroblasts also increased the motility of fibroblasts in a concentration–dependent manner.
- SP exerts chemoattractant effects on human skin fibroblasts, triggering a concentration-dependent migratory response, and NK-1R was shown to be responsible for this effect. The ability of SP to promote chemotaxis in human fibroblasts is another proinflammatory activity of this neuropeptide, extending to the fibroplasia phase of wound healing.
- Fibroblasts and keratinocytes can express NK-1R at both protein and transcriptional levels, and this expression is upregulated by SP indicating that these cells and neuropeptide may be involved in the regulation of skin immune responses.
- Cutaneous nociceptive nerve endings are needed in wound healing. The proliferative effect of neuropeptides on fibroblasts may cause disturbances of wound healing, which may be associated with hyperproliferative skin disorders (*e.g.,* keloids) and mesenchymal disorders (*e.g.*, scleroderma).
- The understanding of the neuropeptidergic action on fibroblasts may provide relevant information to a deeper comprehension of the healing process.
- Despite being the most abundant neuropeptide in the skin, only one study was found describing the effects of CGRP in combination with SP and alpha-MSH on cultured human skin fibroblasts and keratinocytes, investigating the IL-8/IL-8R system. The rationale was based on the fact that IL-8 plays an important role in cutaneous inflammation, and that SP, CGRP, and alpha-MSH also regulate cytokine production. SP and CGRP in concentrations of 10^{-8}M had no effect on the expression of IL-8 and IL-8R in human dermal fibroblasts.
- Further studies are necessary to investigate the action of CGRP on skin fibroblasts and its role in the fibroplasia phase of wound healing.

2. Introduction

Neurogenic inflammation is caused by the presence of local neuropeptides, which are special neurotransmitters synthesized mainly in sensory neurons of the dorsal root ganglion [1-3] and released by exocytosis from peptidergic cutaneous C-fibers (unmyelinated afferents or polymodal C-nociceptors), and in smaller amounts by thinly myelinated A-delta fibers [4-6].

Neuropeptides, also called neurotrophins or neurohormones, are released in much smaller amounts than common small-molecule neurotransmitters, such as catecholamines. However, neuropeptides are usually 1000 times more potent than neurotransmitters and act on their target cells by paracrine, juxtacrine or endocrine signaling [7]. While common neurotransmitters act as a pool in a rapid, massive transient manner on target cells, the neuropeptide action is slow and has prolonged effects that may last for days, months or years. Therefore, neuropeptides promote long-lasting changes in the mechanism of cellular metabolism by activating or deactivating specific genes [7].

Calcitonin gene-related peptide (CGRP) is the most abundant neuropeptide in the skin followed by substance P (SP), vasoactive intestinal peptide (VIP), and other neuropeptides in smaller amounts [8]. Usually, nerve endings deep in the dermis contain increased quantities of CGRP, SP, VIP and Neurokinin A (NKA), while those that penetrate the epidermis contain only SP, VIP and NKA [9,10]. The cutaneous concentration of neuropeptides changes according to the anatomic location. CGRP is a 37-amino acid peptide expressed by neurons and endocrine cells in different tissues [11]. Two isoforms of the CGRP peptide have been described: alpha-CGRP, which is formed by the alternative mRNA splicing of the calcitonin gene located on chromosome 11; and beta-CGRP, which is encoded by a different, but closely related gene [11-17]. Alpha-CGRP and beta-CGRP differ from each other by three amino acids in humans and by one amino acid in rats [13,15], and exhibit overlapping biological actions [16].

CGRP acts intensively on sweat glands and perivascular nerves [9,18]. The specific receptors, CGRP 1 and CGRP 2 receptors, coupled to the adenylate cyclase system bind to G-proteins [9]. CGRP is the most potent vasodilator known and its vasodilator effect on the skin (which is constant in the arterioles of all studied species) is caused by direct action on the muscle vascular bed.

Therefore, this effect is independent of endothelial cells and does not involve protein extravasation [8,19,20]. Even at concentrations 1000 times that needed to induce vasodilation, CGRP cannot stimulate pruritus or pain in human skin. Also, CGRP has a limited or absent capacity to release histamine from mast cells, although it may induce mast cell degranulation and tumor necrosis factor-alpha (TNF-alpha) release [21]. On the other hand, the trophic effects of CGRP occur at much lower concentrations than that needed to induce vasodilation. CGPR contributes to edema formation induced by interleukins (IL) 1 and 8 (IL-1 and IL-8), increases the expression and synthesis of IL-8 in endothelial cells, is a chemotactic for neutrophils and stimulates the proliferation of keratinocytes in mice [22]. CGRP was shown to accelerate and increase cytokine-dependent IL-6 production in Swiss 3T3 fibroblast culture [23].

SP is an important member of the tachykinin family. It is an 11-amino acid peptide, which was named "substance P" because it was first obtained as a "powder" [24]. SP and NKA belong to the phylogenetically ancient tachykinin peptide family. Tachykinins are defined structurally by the common C-terminal amino acid sequence Phe-Xaa-Gly-Leu-Met-NH_2 (Xaa = Phe, Tyr, Val, or Ile) [25]. The mammalian tachykinins are encoded on three different genes, named preprotachykinin (TAC) 1, TAC3 and TAC4 according to the Human Genome Organization (HUGO) [26]. TAC1, the first gene that was cloned from bovine brain, encodes SP. Also, a discrete genomic segment of TAC1 encodes NKA by alternative RNA splicing of the same gene to yield alpha-TAC1 and beta-TAC1 [27]. SP has a similar distribution to CGRP with respect to its targets. SP receptors, neurokinin (NK)-1R, NK-2R and NK-3R, coupled with a G-protein have been described in mast cells, polymorphonuclear leukocytes, monocytes, macrophages, thymus-derived (T) lymphocytes (or T cells), and bone marrow-derived (B) lymphocytes (or B cells) [9,28]. SP is one of the most potent vasodilators; it releases nitric oxide from endothelial cells. This effect is 100 times more potent than that of histamine at similar concentrations. SP produces erythema and edema in a dose-dependent manner, but unlike CGRP, it induces plasma extravasation [29]. In addition, SP is chemotactic for T cells, enhances the proliferation and action of T and B cells, induces the expression of IL-1 and IL-6 by T cells, increases the production of immunoglobulins, the activity of natural killer cells and macrophages, and the production of IL-1 and IL-6 by T cells, TNF-alpha and prostaglandin E 2b (PGE 2b) mediated by NK-1R. However, unlike CGRP, SP induces human mast cell degranulation with release of histamine [9,28]. SP also induces proliferation of human dermal fibroblasts [30] and human and murine keratinocytes [31,32] and stimulates neovascularization *in vivo* and proliferation of endothelial and smooth muscle cells [9,28,33]. The neuropeptides VIP and CGRP, alone or in combination with SP, stimulate the proliferation of murine [30] and human [34,35] keratinocytes; however, the functional role of VIP and CGRP in skin fibroblasts is not well defined [36]. CGRP has been shown to elicit 3T3 and IMR-90 (Human foetal lung) fibroblasts migration in culture, with a chemotactic and chemokinetic response [37].

The presence of the main neuropeptides CGRP and SP in the skin, as well as of those others occurring in cutaneous nerve endings, is directly controlled by the availability of neural growth factor (NGF). NGF is a peptide synthesized and secreted by keratinocytes, dermal fibroblasts, and Schwann cells [38,39]. The inverse also occurs, that is, neurogenic inflammation or the presence of SP and CGRP may induce an increase in the NGF concentration in the skin, indicating the existence of a mutual trophic communication whose importance is still under study, especially regarding tissue repair [40]. SP and CGRP are frequently present in the same nerve fiber. SP release may induce the co-release of CGRP, which in turn may enhance the action of SP, although CGRP may have long-lasting effects. Moreover, the release of SP or CGRP may induce an increase in the levels of SP receptors (NK-1R) [32,41,42].

Since 1990's, cutaneous neurogenic inflammation has been studied more extensively [9]. Sympathetically dependent neurogenic inflammation triggers a strong arteriolar vasodilation effect that modulates the amount of inflammatory mediators (such as histamine, arachidonic acid, bradykinin, and prostaglandins, typical of the inflammatory phase that will follow) and the global recruitment of immune-inflammatory cells, which together activate the inflammatory phase of wound healing [1,2,43,44]. As a direct consequence, the neurogenic inflammation promotes the release of cytokines and growth factors, inducing extracellular matrix synthesis by fibroblasts in the healing phase. The neurogenic inflammation has a direct modulatory effect on the subsequent phases of the healing process, especially on the proliferative phase [45-47].

Neuropeptides, especially CGRP and SP, have a specific and active participation in the fibrosis process, directly acting in the proliferative phase of wound healing for the production of extracellular matrix [1,2,4,42]. Dermal fibroblasts have receptors for these neuropeptides, but their role in these cells is not as well-known as in the neurogenic inflammation phase. The expression of CGRP and adrenomedullin (ADM) receptors in human

dermal fibroblasts and keratinocytes has been described, but a more profound analysis of the differentiated action of these neuropeptides in these cells is yet to be done [36]. The ability of SP to induce synthesis and proliferation of human dermal fibroblasts and keratinocytes is well known [30,31]. However, the fact that these cells express neuropeptides receptors suggests that they may respond to SP and other neuropeptides [32]. The neuropeptides VIP and CGRP, alone or in combination with SP, stimulate the proliferation of murine [30] and human [34,35] keratinocytes, but the functional role of CGRP in skin fibroblasts is not well defined [36].

Cutaneous nociceptive nerve endings are necessary in wound healing. The proliferative effect of neuropeptides on fibroblasts may cause disturbances of wound healing, which may be associated with hyperproliferative skin disorders (e.g., keloids) and mesenchymal disorders (e.g., scleroderma) [36,48,49]. The understanding of the neuropeptidergic action on fibroblasts may provide relevant information to a deeper comprehension of the healing process. The subject of our study, neuropeptides in experimental *in vitro* studies, wouldn't allow a proper systematic review due to the intrinsic nature of the articles and of the subject itself. However, a review using a systematization of the literature search strategy could bring significant contribution to the understanding of the action of the major neuropeptides in the proliferative phase of wound healing, after the neurogenic inflammation phase. Besides that, this search strategy systematization allows the review to include all articles exclusively relevant to the subject and, since the search strategy is presented, it also allows the review to be updated at any time. Therefore, the aim of this study was to review the action of the main neuropeptides, CGRP and SP, on cultured human skin fibroblasts.

3. Methods

A systematic literature search was conducted on Medline (PubMed) and Web of Science (Thomson Reuters) databases on December 21, 2013. The search strategies were as follows:

(a) PubMed – search 1:

Search ("Calcitonin Gene-Related Peptide"[Mesh] OR "Substance P"[Mesh]) AND "Fibroblasts"[Mesh] AND "Skin"[Mesh] AND "Cells, Cultured"[Mesh]

(b) PubMed – search 2:

Search ("Calcitonin Gene-Related Peptide" OR "Substance P") AND "Fibroblasts" AND "Skin" AND "Cells, Cultured"

(c) Web of Science:

TS= (Fibroblast* AND (Calcitonin-Gene Related Peptide OR Substance P) AND (Skin) AND (Cultured Cell*))

No qualifier or limit was used in the search. Publications found simultaneously in both databases were counted only once. The articles were categorized according to the model used (human or animal), and neuropeptide(s) studied. For the selected articles, we also checked the References section as some important articles couldn't be retrieved by the search criteria. The conclusions of the studies were summarized and review articles were excluded from the study. Articles in which the content was not related to the objectives of the present study were also excluded.

4. Results

A total of 74 articles were retrieved using the proposed search strategies of which 14 articles were retrieved from Medline (PubMed search 1), 21 from Medline (PubMed search 2) with a total of 24 different articles from both Pubmed searches (1 and 2), and 50 articles retrieved from Web of Science. However, 13 articles were common to both databases, so that 61 different articles were retrieved. Also, 5 review articles and 46 articles presenting topics not related to the objectives of this study were excluded from the sample. Ten articles were previously selected using the search engines, which studied the action of the main neuropeptides on cultured human skin fibroblasts. For these articles (and for all articles selected thereafter), we also checked the References section, as some relevant articles seemed to have escaped the search criteria. Three new articles were retrieved this way, for a total of 13 articles concerning the action of CGRP and/or SP on cultured human skin fibroblasts, of which 12 were related to SP and 1 was related to both CGRP and SP. A summary of the content of these articles is shown in Table 1 [30,50-61]. A schematic drawing is proposed showing the molecular mechanisms of CGRP and SP in human skin fibroblasts and is shown in Figure 1.

5. Discussion

A study has investigated the effects of CGRP, SP and alpha-melanocyte-stimulating hormone (alpha-MSH) on the IL-8/IL-8R system in a cultured human keratinocyte cell line and dermal fibroblasts [50]. The rationale was based on the fact that IL-8 plays an important role in the cutaneous inflammation and SP, CGRP, and alpha-MSH

	Retrived Articles	Neuropeptides	Action on skin fibroblasts
1	Nilsson *et al*., 1985 [30]	SP	SP stimulate DNA synthesis in cultured human skin fibroblasts, and this stimulation is inhibited by the SP-antagonist spantide.
2	Kiss *et al*., 1999 [50]	CGRP and SP	SP and CGRP in concentrations of 10^{-8} M had no effect on the expression of Interleukin 8 (IL-8) and Interleukin 8 Receptor (IL-8R) in human dermal fibroblasts.
3	Kähler *et al*., 1993 [51]	SP	SP potently stimulated fibroblast growth in the presence of acetylsalicylic acid after growth arrest by 48 h serum starvation. SP stimulated fibroblast growth in a manner typical of competence factors. Arachidonic acid metabolites were involved in the cell cycle-dependent mitogenic action of SP on human skin fibroblasts.
4	Kähler *et al*., 1993 [52]	SP	SP had a potent chemotactic effect, attracting human dermal fibroblasts in a concentration-dependent manner.
5	Parenti *et al*., 1996 [53]	SP	The addition of SP to cultured human dermal fibroblasts increased the motility of fibroblasts in a concentration–dependent manner with a 50% increase in migration at a concentration of 10^{-8} M.
6	Bae *et al*., 2002 [54]	SP	Exogenous SP induced autocrine production of SP by human skin fibroblasts.
7	Liu *et al*., 2006 [55]	SP	SP and gamma interferon (IFN-gamma) upregulated the expression of Neurokinin 1 Receptor (NK-1R) in human dermal fibroblasts, as well as in HaCaT (a human epidermal keratinocyte cell line) cells.
8	Kähler *et al*., 1996 [56]	SP	The combination of SP with Epidermal Growth Factor (EGF) synergistically stimulated the proliferation of human dermal fibroblasts and release of PGE 2.
9	Hu *et al*., 2002 [57]	SP	SP increased the proliferation of human fibroblasts in a concentration-dependent manner.
10	Morbidelli *et al*., 1993 [58]	SP	Synthetic selective NK-1R antagonists of human skin fibroblasts induced a significant displacement to the right of the dose-response curves induced by SP and the selective NK-1R agonist. The selective NK-2R antagonist did not modify the proliferative response to the tachykinins used. The growth-promoting effect of Basic Fibroblast Growth Factor (bFGF) was not changed by any of the tachykinin antagonists tested.
11	Xie *et al*., 2011 [59]	SP	Fibroblastic CD10 expression may down-regulate skin inflammation by degrading SP or reducing its level in the dermal microenvironment. Targeted disruption of CD10 by siRNA augmented SP production from Fbs
12	Liu *et al*., 2007 [60]	SP	SP induced the production of IFN-gamma, IL-1beta, IL-8 and Monocyte Chemotactic Protein (MCP)-1 in HaCaT cells and human dermal fibroblasts. Matrine 5-100 μg/mL inhibited SP-induced IL-1beta, IL-8 and (MCP)-1 production in HaCaT cells and human dermal fibroblasts, with no effect on IFN-gamma production in both cells. SP had no effect on IL-6 secretion in HaCaT cells and human dermal fibroblasts. Fibroblasts did not constitutively secrete Tumor Necrosis Factor-gamma (TNF-gamma). Neither SP nor matrine induced the secretion of this cytokine.
13	Liu *et al*., 2008 [61]	SP	SP induced the production of IFN-gamma, IL-1beta and IL-8 in HaCaT cells and human dermal fibroblasts. Cetirizine 1-100 micromol x L(-1) inhibited SP-induced IL-1beta and IL-8 production in HaCaT cells and human dermal fibroblasts, with no effect on IFN-gamma production in both cells. SP had no effect on IL-6 secretion in HaCaT cells and human dermal fibroblasts.

Table 1. Summary of the action of the neuropeptides CGRP and SP on skin fibroblasts.

also regulate cytokine production. The authors reported that alpha-MSH induced a time-dependent expression of IL-8 mRNA in fibroblasts, while SP and CGRP did not act on dermal fibroblasts at a concentration of 10^{-8} M L^{-1}. On the other hand, SP and CGRP upregulated the expression of IL-8 mRNA in keratinocytes, but had no effect on the production of IL-8; alpha-MSH had no effect on either IL-8 or IL-8/IL-8R system in these cells [50].

Neuropeptides exert a variety of modulatory effects on inflammatory cellular responses. In order to investigate other activities of neuropeptides in the inflammatory processes, a study has assessed the ability of SP to stimulate chemotaxis in human fibroblasts [51]. Kähler *et al*. [52] reported that SP was a potent chemoattractant for human fibroblasts *in vitro*, triggering a concentration-dependent migratory response. When testing the chemoattractant properties of SP fragments, only the C-terminal fragment analog induced migratory responses [52]. It was suggested that chemotactic responsiveness is encoded by the C-terminus of the SP, which is known to be active in NK receptors. The ability of substance P to promote chemotaxis in human fibroblasts, which extends to the fibroplasia phase of wound healing, is another proinflammatory activity of this neuropeptide [52].

Other study has addressed cell migration and the distance human dermal fibroblasts move after the addition of SP to the culture medium [53]. The authors observed an increase in the motility of fibroblasts

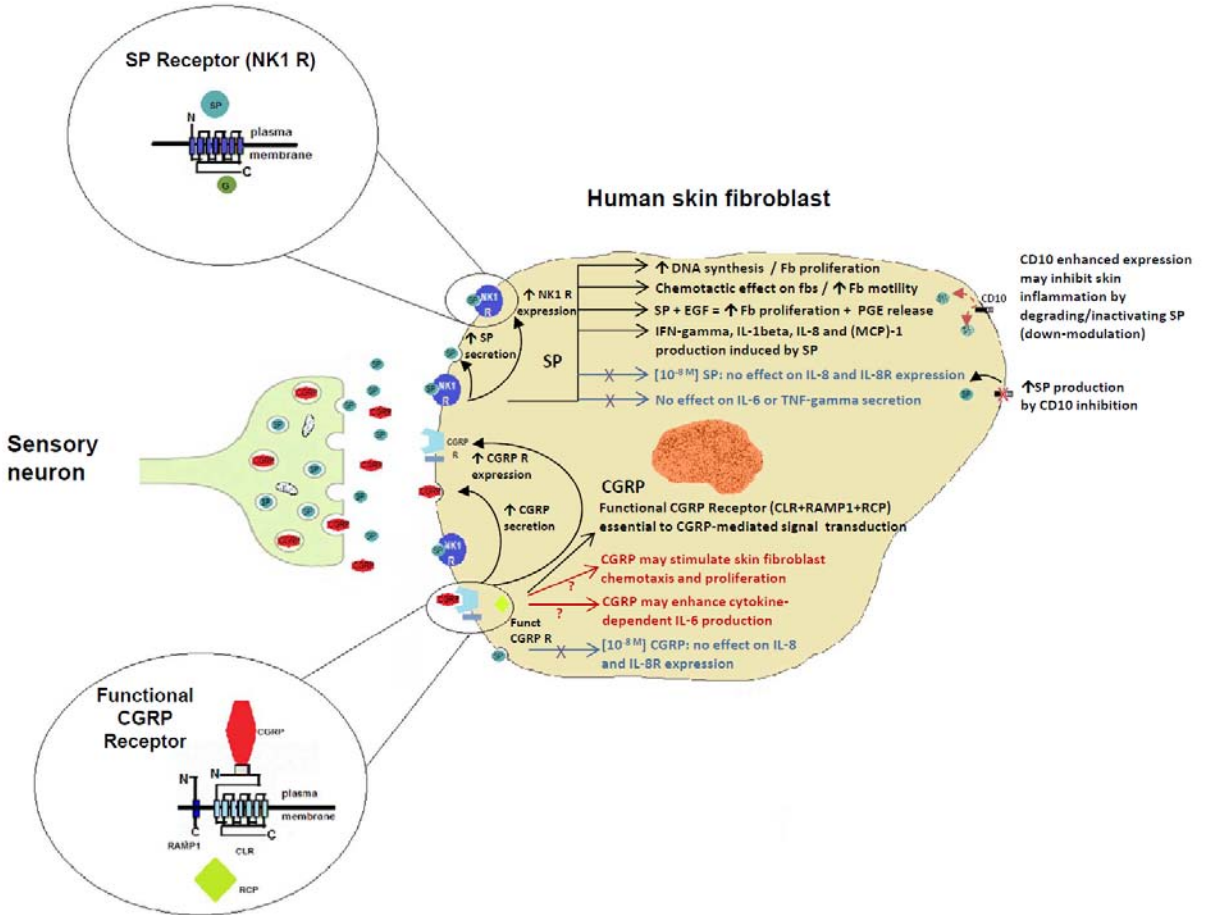

Figure 1. Schematic drawing showing the molecular mechanisms of CGRP and SP in human skin fibroblasts. Fb: Fibroblast; SP: Substance P; CGRP: Calcitonin Gene-Related Peptide; CD10: Cluster of Differentiation 10; EGF : Epidermal Growth Factor ; IL-1beta: Interleukin 1 beta; IL-6: Interleukin 6; IL-8: Interleukin 8; IL-8R: Interleukin 8 Receptor; IFN-gamma: Gamma Interferon; (MCP)-1: Monocyte Chemotactic Protein 1; PGE: Prostaglandin E; TNF-gamma: Tumor Necrosis Factor-gamma; NK-1 R: Neurokinin 1 Receptor (SP Receptor); CLR : Calcitonin-Like Receptor; RAMP1: Receptor-Activity-Modifying Protein 1; RCP : Receptor Component Protein. Blue arrows: no effect. Red arrows: possible effect.

in a concentration-dependent manner. An SP concentration of 10^{-8} M lead to a 50% increase in fibroblast migration. SP is a potent effector of fibroblast migration, and NK-1R is responsible for this effect. These observations reinforce the importance of the specific role of NK-1R in mediating the trophic function of SP at the level of skin fibroblasts [53].

Neutral endopeptidase (NEP) is a cell-surface enzyme that degrades SP. NEP mRNA was detected in fibroblasts, keratinocytes and endothelial cells in the skin and wound tissue, which makes this enzyme a possible factor in the attenuation of proinflammatory and mitogenic action of these neuropeptides [62].

A study on the mechanisms that regulate the autocrine induction of SP by cultured human fibroblasts has shown for the first time that SP mRNA, NEP mRNA, and SP may be induced by normal skin fibroblasts in response to exogenous SP [54].

SP can be a possible factor in the pathogenesis of cutaneous allergic inflammation. An investigation of the expression of NK-1R for SP in cultured human dermal fibroblasts and epidermal keratinocytes has reported that fibroblasts and keratinocytes can express NK-1R at both protein and transcriptional levels, and that this expression is upregulated by SP, gamma-interferon (IFN-gamma) and spantide I [55]. This suggests that fibroblasts and keratinocytes may be involved in the regulation of skin immune responses, and that NK-1R may play an important role in the pathogenesis of cutaneous allergic inflammation [55].

SP stimulates the growth and proliferation of human dermal fibroblasts through arachidonic acid metabolites. Other investigations have reported that when cell growth was interrupted due to serum deprivation for more than 48 h, SP was not able to stimulate fibroblast proliferation [51]. SP, fibroblast growth factor (FGF) and epidermal

growth factor (EGF) are mitogenic for fibroblasts [51]. Another investigation has tested the effects of a submaximal concentration of SP (10^{-9} M) combined with either FGF or EGF on fibroblast proliferation and release of arachidonic acid metabolites. The authors observed that the combination of SP with EGF synergistically stimulated the proliferation of fibroblasts and release of PGE 2, while the addition of SP to cultures containing FGF had no effect on cell growth. Therefore, the interactions of SP with FGF and EGF differently affect the mitogenic response based on the release of arachidonic acid metabolites [56].

SP also affects the proliferation of skin fibroblasts [52]. A study on the role of SP in the formation of hypertrophic scars has reported that SP increased *in vitro* proliferation of skin fibroblasts in a dose-dependent manner, with maximum rate for an SP concentration of 25 ng mL^{-1} [58]. Moreover, after 48 h in culture with SP (25 ng mL^{-1}), fibroblasts expressed more mRNA for transforming growth factor (TGF)-beta 1 than those that were not exposed to the neuropeptide, suggesting that SP may play an important role in the phenotypic changes of fibroblasts during skin healing. A disturbance in the expression of these changes may result in the formation of hypertrophic scars and possibly keloids [57].

The effects of synthetic selective tachykinin receptor antagonists on the growth of cultured human skin fibroblasts have been evaluated [58]. Selective antagonists for the NK-1R and NK-2R were tested against SP, against a selective NK-1R agonist, and against basic fibroblast growth factor (bFGF). All selective NK-1R antagonists tested at the concentration of 10^{-5} M L^{-1} induced a significant displacement to the right of the dose-response curves induced by SP and by the selective NK-1R agonist. The selective NK-2R antagonist did not change the proliferative response to the tachykinins used. The growth-promoting effect of bFGF was not affected by any of the antagonists tested. These results indicate that the synthetic receptor-selective antagonists may become an important tool to the study of *in vitro* biological effects of tachykinin on cultured cells [58].

CGRP and ADM couple to the same type of transmembrane receptor, the calcitonin-like receptor (CLR). The selective specificity of CLR for these peptides depends on which members of a family of single-transmembrane-domain proteins, called receptor-activity-modifying proteins (RAMPs), are expressed (i.e., RAMP1, RAMP2 or RAMP3) [63]. The simultaneous expression of CLR and RAMP is essential for the expression of functional receptors. Studies on transfection of different cell types have confirmed this hypothesis [63-65].

COS-7 fibroblasts (African green monkey kidney COS-7 cells) do not express significant levels of endogenous RAMPs [66], but have been commonly used as a transfection model. Transfection of rat CLR, when co-expressed with mRAMP1 in COS-7 cells, results in the expression of a functional CGRP receptor [64].

The rat myogenic cell line L6 is considered a fibroblast cell line and has receptors for CGRP in its endogenous form. The cell line L6 expresses mRNA for RAMP1 and RAMP2; Rat-2 fibroblasts express mRNA only for RAMP2 [67] without receptor for CGRP. Withers *et al*. [67] reported that Swiss 3T3 fibroblasts have high-affinity receptors for ADM, but no CGRP receptor. On the other hand, Evans *et al*. [69] detected functional CGRP receptors by cAMP assays in NIH3T3 cells.

Human skin fibroblasts express mRNA for RAMP1, indicating that human skin fibroblasts have low-expression of (but still express) CGRP receptor [36].

Evans *et al*. [69], working with NIH3T3 and COS-7 fibroblasts, proposed that a functional CGRP receptor complex requires at least three proteins: the CGRP receptor itself, composed by CLR and RAMP1 (the chaperone protein to route CLR to the cell surface), and a receptor component protein (RCP) to couple the complex CLR + RAMP1 to the cellular signal transduction pathway.

In conclusion, although CGRP is the most abundant neuropeptide in the skin, only one study was found in the literature describing the action of CGRP in combination with SP on cultured human skin fibroblasts. SP is a neuropeptide that has been shown to exert proliferative and chemoattractant effects on human skin fibroblasts, and to be linked to cutaneous immune reactions. Human skin fibroblasts have low-expression of CGRP receptor. Therefore, further studies are necessary to investigate the action of CGRP on skin fibroblasts and its role in the fibroplasia phase of wound healing.

Acknowledgements

The authors wish to thank Gabriela Soares Silva Brito, BSc, MSc (Unifesp) and Felipe Contoli Isoldi, MD (Unifesp) for their contribution to this study.

References

[1] Holzer P. Neurogenic vasodilatation and plasma leakage in the skin. Gen Pharmacol. 1998; 30:5-11.

[2] Rossi R, Johansson O. Cutaneous innervation and the role of neuronal peptides in cutaneous inflammation: a minireview. Eur J Dermatol. 1998; 8:299-306.

[3] Watson RE, Supowit SC, Zhao H, Katki KA, Dipette DJ. Role of sensory nervous system vasoactive peptides in hypertension. Braz J Med Biol Res. 2002; 35:1033-45.

[4] Petersen LJ, Church MK, Skov PS. Histamine is released in the wheal but not the flare following challenge of human skin in vivo: a microdialysis study. Clin Exp Allergy. 1997; 27:284-95.

[5] Weidner C, Klede M, Rukwied R, Lischetzki G, Neisius U, Skov PS, Petersen LJ, Schmelz M. Acute effects of substance P and calcitonin gene-related peptide in human skin--a microdialysis study. J Invest Dermatol. 2000; 115:1015-20.

[6] Toyoda M, Morohashi M. New aspects in acne inflammation. Dermatology. 2003; 206:17-23.

[7] Steinhoff M, Ständer S, Seeliger S, Ansel JC, Schmelz M, Luger T. Modern aspects of cutaneous neurogenic inflammation. Arch Dermatol. 2003; 139:1479-88.

[8] Esteves Junior I, Ferreira LM, Liebano RE. Peptídeo relacionado ao gene da calcitonina por iontoforese na viabilidade de retalho cutâneo randômico em ratos [Calcitonin gene-related peptide by iontophoresis on the viability of the randon skin flaps in rats]. Acta Cir Bras. 2004; 19:626-9.

[9] Lotti T, Hautmann G, Panconesi E. Neuropeptides in skin. J Am Acad Dermatol. 1995; 33:482-96.

[10] Hagner S, Haberberger RV, Overkamp D, Hoffmann R, Voigt KH, McGregor GP. Expression and distribution of calcitonin receptor-like receptor in human hairy skin. Peptides. 2002; 23:109-16.

[11] Amara SG, Jonas V, Rosenfeld MG, Ong ES, Evans RM. Alternative RNA processing in calcitonin gene expression generates mRNAs encoding different polypeptide products. Nature. 1982; 298:240-4.

[12] Rosenfeld MG, Mermod JJ, Amara SG, Swanson LW, Sawchenko PE, Rivier J, Vale WW, Evans RM . Production of a novel neuropeptide encoded by the calcitonin gene via tissue-specific RNA processing. Nature. 1983; 304:129-35.

[13] Amara SG, Evans RM, Rosenfeld MG. Calcitonin/calcitonin gene-related peptide transcription unit: tissue-specific expression involves selective use of alternative polyadenylation sites. Mol Cell Biol. 1984; 4:2151-60.

[14] Goodman EC, Iversen LL. Calcitonin gene-related peptide: novel neuropeptide. Life Sci. 1986; 38:2169-2178.

[15] Breimer LH, MacIntyre I, Zaidi M. Peptides from the calcitonin genes: molecular genetics, structure and function. Biochem J. 1988; 255:377-90.

[16] Brain SD, Grant AD. Vascular actions of calcitonin gene-related peptide and adrenomedullin. Physiol Rev. 2004; 84:903-34.

[17] Peters EM, Ericson ME, Hosoi J, Seiffert K, Hordinsky MK, Ansel JC, Paus R, Scholzen TE. Neuropeptide control mechanisms in cutaneous biology: physiological and clinical significance. J Invest Dermatol. 2006; 126:1937-47.

[18] Kakizoe E, Kobayashi Y, Gonda T, Shimoura K, Hattori K, Okunishi H. Synergistic interactions between neuropeptide and histamine on the capillary permeability in rat skin: evaluation by reflectance spectrophotometry. Microvasc Res. 1997; 54:27-34.

[19] Slominski A, Wortsman J. Neuroendocrinology of the skin. Endocr Rev. 2000; 21:457-87.

[20] Sleijffers A, Herreilers M, van Loveren H, Garssen J. Ultraviolet B radiation induces upregulation of calcitonin gene-related peptide levels in human Finn chamber skin samples. J Photochem Photobiol B. 2003; 69:149-52.

[21] Seiffert K, Granstein RD. Neuropeptides and neuroendocrine hormones in ultraviolet radiation-induced immunosuppression. Methods. 2002; 28:97-103.

[22] Seike M, Ikeda M, Morimoto A, Matsumoto M, Kodama H. Increased synthesis of calcitonin gene-related peptide stimulates keratinocyte proliferation in murine UVB-irradiated skin. J Dermatol Sci. 2002; 28:135-43.

[23] Sakuta H, Inaba K, Muramatsu S. Calcitonin gene-related peptide enhances cytokine-induced IL-6 production by fibroblasts. Cell Immunol. 1995; 165(1):20-5.

[24] V Euler US, Gaddum JH. An unidentified depressor substance in certain tissue extracts. J Physiol. 1931;72(1):74-87.

[25] Johansson A, Holmgren S, Conlon JM. The primary structures and myotropic activities of two tachykinins isolated from the African clawed frog, Xenopus laevis. Regul Pept. 2002; 108:113-21.

[26] Patacchini R, Lecci A, Holzer P, Maggi CA. Newly discovered tachykinins raise new questions

about their peripheral roles and the tachykinin nomenclature. Trends Pharmacol Sci. 2004; 25:1-3.
[27] Nawa H, Kotani H, Nakanishi S. Tissue-specific generation of two preprotachykinin mRNAs from one gene by alternative RNA splicing. Nature. 1984; 312:729-734.
[28] Schmelz M, Petersen LJ. Neurogenic inflammation in human and rodent skin. News Physiol Sci. 2001; 16:33-7.
[29] Cappugi P, Tsampau D, Lotti T. Substance P provokes cutaneous erythema and edema through a histamine-independent pathway. Int J Dermatol. 1992; 31:206-9.
[30] Nilsson J, von Euler AM, Dalsgaard CJ. Stimulation of connective tissue cell growth by substance P and substance K. Nature. 1985; 315:61-3.
[31] Tanaka T, Danno K, Ikai K, Imamura S. Effects of substance P and substance K on the growth of cultured keratinocytes. J Invest Dermatol. 1988; 90:399-401.
[32] Scholzen T, Armstrong CA, Bunnett NW, Luger TA, Olerud JE, Ansel JC. Neuropeptides in the skin: interactions between the neuroendocrine and the skin immune systems. Exp Dermatol. 1998; 7:81-96.
[33] Okabe T, Hide M, Koro O, Yamamoto S. Substance P induces tumor necrosis factor-alpha release from human skin via mitogen-activated protein kinase. Eur J Pharmacol. 2000; 398:309-15.
[34] Takahashi K, Nakanishi S, Imamura S. Direct effects of cutaneous neuropeptides on adenylyl cyclase activity and proliferation in a keratinocyte cell line: stimulation of cyclic AMP formation by CGRP and VIP/PHM, and inhibition by NPY through G protein-coupled receptors. J Invest Dermatol. 1993; 101:646-51.
[35] Kakurai M, Fujita N, Kiyosawa T, Inoue T, Ishibashi S, Furukawa Y, Demitsu T, Nakagawa H. Vasoactive intestinal peptide and cytokines enhance stem cell factor production from epidermal keratinocytes DJM-1. J Invest Dermatol. 2002; 119:1183-8.
[36] Albertin G, Carraro G, Parnigotto PP, Conconi MT, Ziolkowska A, Malendowicz LK, Nussdorfer GG. Human skin keratinocytes and fibroblasts express adrenomedullin and its receptors, and adrenomedullin enhances their growth in vitro by stimulating proliferation and inhibiting apoptosis. Int J Mol Med. 2003; 11:635-9.
[37] Yule KA, White SR. Migration of 3T3 and lung fibroblasts in response to calcitonin gene-related peptide and bombesin. Exp Lung Res. 1999; 25(3):261-73.
[38] Donnerer J, Schuligoi R, Stein C. Increased content and transport of substance P and calcitonin gene-related peptide in sensory nerves innervating inflamed tissue: evidence for a regulatory function of nerve growth factor in vivo. Neuroscience. 1992; 49:693-8.
[39] Amann R, Sirinathsinghji DJ, Donnerer J, Liebmann I, Schuligoi R. Stimulation by nerve growth factor of neuropeptide synthesis in the adult rat in vivo: bilateral response to unilateral intraplantar injections. Neurosci Lett. 1996; 203:171-4.
[40] Amann R, Egger T, Schuligoi R. The tachykinin NK(1) receptor antagonist SR140333 prevents the increase of nerve growth factor in rat paw skin induced by substance P or neurogenic inflammation. Neuroscience. 2000; 100:611-5.
[41] Wallengren J. Vasoactive peptides in the skin. J Investig Dermatol Symp Proc. 1997; 2:49-55.
[42] Wu H, Guan C, Qin X, Xiang Y, Qi M, Luo Z, Zhang C. Upregulation of substance P receptor expression by calcitonin gene-related peptide, a possible cooperative action of two neuropeptides involved in airway inflammation. Pulm Pharmacol Ther. 2007; 20:513-24.
[43] Baluk P. Neurogenic inflammation in skin and airways. J Investig Dermatol Symp Proc. 1997; 2:76-81.
[44] Sauerstein K, Klede M, Hilliges M, Schmelz M. Electrically evoked neuropeptide release and neurogenic inflammation differ between rat and human skin. J Physiol. 2000; 529:803-10.
[45] Akaishi S, Ogawa R, Hyakusoku H. Keloid and hypertrophic scar: neurogenic inflammation hypotheses. Med Hypotheses. 2008; 71:32-8.
[46] Hochman B, Nahas FX, Sobral CS, Arias V, Locali RF, Juliano Y, Ferreira LM. Nerve fibres: a possible role in keloid pathogenesis. Br J Dermatol. 2008; 158:651-2.
[47] Ferreira LM, Gragnani A, Furtado F, Hochman B. Control of the skin scarring response. An Acad Bras Cienc. 2009; 81:623-9.
[48] Stelnicki EJ, Doolabh V, Lee S, Levis C, Baumann FG, Longaker MT, Mackinnon S. Nerve dependency in scarless fetal wound healing. Plast Reconstr Surg. 2000; 105:140-7.
[49] Tucci-Viegas VM, Hochman B, Franca JP, Ferreira LM. Keloid explant culture: a model for keloid fibroblasts isolation and cultivation based on the biological differences of its specific regions. Int Wound J. 2010; 7:339-48.
[50] Kiss M, Kemény L, Gyulai R, Michel G, Husz S, Kovács R, Dobozy A, Ruzicka T. Effects of the neuropeptides substance P, calcitonin gene-

related peptide and alpha-melanocyte-stimulating hormone on the IL-8/IL-8 receptor system in a cultured human keratinocyte cell line and dermal fibroblasts. Inflammation. 1999; 23:557-67.

[51] Kähler CM, Herold M, Wiedermann CJ. Substance P: a competence factor for human fibroblast proliferation that induces the release of growth-regulatory arachidonic acid metabolites. J Cell Physiol. 1993; 156:579-87.

[52] Kähler CM, Sitte BA, Reinisch N, Wiedermann CJ. Stimulation of the chemotactic migration of human fibroblasts by substance P. Eur J Pharmacol. 1993; 249:281-286.

[53] Parenti A, Amerini S, Ledda F, Maggi CA, Ziche M. The tachykinin NK1 receptor mediates the migration-promoting effect of substance P on human skin fibroblasts in culture. Naunyn Schmiedebergs Arch Pharmacol. 1996; 353:475-81.

[54] Bae SJ, Matsunaga Y, Takenaka M, Tanaka Y, Hamazaki Y, Shimizu K, Katayama I. Substance P induced preprotachykinin-a mRNA, neutral endopeptidase mRNA and substance P in cultured normal fibroblasts. Int Arch Allergy Immunol. 2002; 127:316-21.

[55] Liu JY, Hu JH, Zhu QG, Li FQ, Sun HJ. Substance P receptor expression in human skin keratinocytes and fibroblasts. Br J Dermatol. 2006; 155:657-62.

[56] Kähler CM, Herold M, Reinisch N, Wiedermann CJ. Interaction of substance P with epidermal growth factor and fibroblast growth factor in cyclooxygenase-dependent proliferation of human skin fibroblasts. J Cell Physiol. 1996; 166:601-8.

[57] Hu D, Chen B, Zhu X, Tao K, Tang C, Wang J. Substance P up-regulates the TGF-beta 1 mRNA expression of human dermal fibroblasts in vitro. Zhonghua Zheng Xing Wai Ke Za Zhi. 2002; 18:234-6.

[58] Morbidelli L, Maggi CA, Ziche M. Effect of selective tachykinin receptor antagonists on the growth of human skin fibroblasts. Neuropeptides. 1993; 24:335-41.

[59] Xie L, Takahara M, Nakahara T, Oba J, Uchi H, Takeuchi S, Moroi Y, Furue M. CD10-bearing fibroblasts may inhibit skin inflammation by down-modulating substance P. Arch Dermatol Res. 2011;303(1):49-55.

[60] Liu JY, Hu JH, Zhu QG, Li FQ, Wang J, Sun HJ. Effect of matrine on the expression of substance P receptor and inflammatory cytokines production in human skin keratinocytes and fibroblasts. Int Immunopharmacol. 2007; 7(6):816-23.

[61] Liu JY, Zhao YZ, Peng C, Li FQ, Zhu QG, Hu JH. Effect of cetirizine hydrochloride on the expression of substance P receptor and cytokines production in human epidermal keratinocytes and dermal fibroblasts. Yao Xue Xue Bao. 2008;43(4):383-7.

[62] Olerud JE, Usui ML, Seckin D, Chiu DS, Haycox CL, Song IS, Ansel JC, Bunnett NW. Neutral endopeptidase expression and distribution in human skin and wounds. J Invest Dermatol. 1999; 112:873-81.

[63] McLatchie LM, Fraser NJ, Main MJ, Wise A, Brown J, Thompson N, Solari R, Lee MG, Foord SM. RAMPs regulate the transport and ligand specificity of the calcitonin-receptor-like receptor. Nature. 1998; 393:333-9.

[64] Husmann K, Sexton PM, Fischer JA, Born W. Mouse receptor-activity-modifying proteins 1, -2 and -3: amino acid sequence, expression and function. Mol Cell Endocrinol. 2000; 162:35-43.

[65] Chakravarty P, Suthar TP, Coppock HA, Nicholl CG, Bloom SR, Legon S, Smith DM. CGRP and adrenomedullin binding correlates with transcript levels for calcitonin receptor-like receptor (CRLR) and receptor activity modifying proteins (RAMPs) in rat tissues. Br J Pharmacol. 2000; 130:189-95.

[66] Bailey RJ, Hay DL. Pharmacology of the human CGRP1 receptor in Cos 7 cells. Peptides. 2006; 27:1367-75.

[67] Choksi T, Hay DL, Legon S, Poyner DR, Hagner S, Bloom SR, Smith DM. Comparison of the expression of calcitonin receptor-like receptor (CRLR) and receptor activity modifying proteins (RAMPs) with CGRP and adrenomedullin binding in cell lines. Br J Pharmacol. 2002; 136:784-92.

[68] Withers DJ, Coppock HA, Seufferlein T, Smith DM, Bloom SR, Rozengurt E. Adrenomedullin stimulates DNA synthesis and cell proliferation via elevation of cAMP in Swiss 3T3 cells. FEBS Lett. 1996; 378:83-7.

[69] Evans BN, Rosenblatt MI, Mnayer LO, Oliver KR, Dickerson IM. CGRP-RCP, a novel protein required for signal transduction at calcitonin gene-related peptide and adrenomedullin receptors. J Biol Chem. 2000; 275(40):31438-43.